ESPOO 2005 VTT RESEARCH NOTES 2301

Kari Sipilä, Esa Pursiheimo, Tuula Savola,
Carl-Johan Fogelholm, Ilkka Keppo &
Pekka Ahtila

Small-Scale Biomass CHP Plant and District Heating

VTT TIEDOTTEITA – RESEARCH NOTES 2301

Small-Scale Biomass CHP Plant and District Heating

Kari Sipilä & Esa Pursiheimo
VTT Processes

Tuula Savola & Carl-Johan Fogelholm
Energy Engineering and Environmental Protection
Helsinki University of Technology

Ilkka Keppo & Pekka Ahtila
Energy Economics and Power Plant Engineering
Helsinki University of Technology

ISBN 951–38–6722–6 (soft back ed.)
ISSN 1235–0605 (soft back ed.)

ISBN 951–38–6723–4 (URL: http://www.vtt.fi/inf/pdf/)
ISSN 1455–0865 (URL: http://www.vtt.fi/inf/pdf/)

JULKAISIJA – UTGIVARE – PUBLISHER

VTT, Vuorimiehentie 5, PL 2000, 02044 VTT
puh. vaihde 020 722 111, faksi 020 722 4374

VTT, Bergsmansvägen 5, PB 2000, 02044 VTT
tel. växel 020 722 111, fax 020 722 4374

VTT Technical Research Centre of Finland, Vuorimiehentie 5, P.O.Box 2000, FI–02044 VTT, Finland
phone internat. +358 20 722 111, fax +358 20 722 4374

VTT Prosessit, Lämpömiehenkuja 3, PL 1606, 02044 VTT
puh. vaihde 020 722 111, faksi 020 722 6538

VTT Processer, Värmemansgränden 3, PB 1606, 02044 VTT
tel. växel 020 722 111, fax 020 722 6538

VTT Processes, Lämpömiehenkuja 3, P.O.Box 1606, FI–02044 VTT, Finland
phone internat. +358 20 722 111, fax +358 20 722 6538

Technical editing Anni Kääriäinen

Valopaino Oy, Helsinki 2005

Sipilä, Kari, Pursiheimo, Esa, Savola, Tuula, Keppo, Ilkka, Fogelholm, Carl-Johan & Ahtila, Pekka. Small-Scale Biomass CHP Plant and District Heating. Espoo 2005. VTT Tiedotteita – Research Notes 2301. 129 p. + app. 7 p.

Keywords combined heat and power generation, biomass, district heating plants, small-scale co-generation, steam Rankine cycle, organic Rankine cycle, optimisation, modelling, simulation

Abstract

CHP potential in Finland has been evaluated to be 80 MW of electricity and 214 MW of heat with 6000 hours of annual peak load time based on the district heat production in biofuelled CHP plants in the year 2000. Part of this capacity is already built when this report has been written. The total amount of possible CHP units is 51. 90% of the CHP would be smaller than 10 MW in thermal effect. Most of the potential CHP plants (53%) would be 1–5 MW in thermal effect.

The profitability of an investment in a small biofuel-fired CHP plant was also studied. An optimisation model was constructed describing production, distribution and consumption of heat. The energy production in CHP plants is based on simulations done for three different size plants, thus giving a wider perspective on the behaviour of such a plant. The results indicate, that the economically feasible scale for biofuel-fired CHP plants remains relatively large; when a biofuel-fired boiler is among the options for heat production, no investment is made in the smallest of three CHP plants. Specific investment costs for the two larger plants could be only slightly higher until no investment in them would be made either. This means, that if these plants were scaled down, their specific investment cost should not rise considerably. A rise of 3 percent in the discount rate causes again the same effect. Taking into account that the future electricity prices are not deterministic in the real world and therefore a higher rate of return is required, the competitiveness of the biofuel-fired boiler increases even more.

Possibilities to increase the power production and the power-to-heat ratio of 1–20 MW_e CHP plants using biomass fuels were studied with simulation and optimisation tools. The basis for the simulations and optimisations was the data collected from Finnish and Swedish small-scale CHP plants between 2002 and 2004. Four existing CHP plants from Finland and Sweden were selected to represent a BAT technology in the different sizes of CHP processes. The results showed that the addition of a feed water preheater, a steam reheater, and a two-stage district heat exchanger is profitable with the current electricity price of 30 €/MWh. This increases the power-to-heat ratios from 0.23–0.50 to 0.45–0.50 depending on the case plant. The considered integration of a gas engine needs electricity prices over 42–45 €/MWh but increases the power-to-heat ratios to 0.59–0.78. The addition of a fuel dryer was connected to the integration of gas engine and gas

turbine, as this provided extra heat to the flue gases that could be used for fuel drying. When the simulation and the optimisation results are compared, higher profits are gained with the process change combinations suggested by the optimisation model than with the separate process changes evaluated one-by-one with the simulation models. Thus, the optimisation model shows its capability to handle the trade-offs between power production, efficiency, costs, and complexity of the process.

ORC process plant is evaluated as one possibility for small-scale biofuelled CHP power plant. The organic substance to be used is Diphenyl-DiphenylEther, which is a mixture of two substances. There are three thermodynamical areas: liquid, moist steam and dry steam. Based on the organic substance properties the property functions have been developed for calculation software. 15 functions are required to define the interdependencies of the different variables for ORC medium in the simulation model. Simulation is first modelled for a BAT technology ORC plant (Admont) and secondly to explore possibilities of improvements by adding some new properties to the basic plant model. Possibilities to improve the basic process are to make the process starting point (pressure and temperature) higher after the boiler, to change the temperature of the preheated air and to use double circle organic process. Simulation results indicate that the most simple structure is the best choice for an ORC plant subjected to power-to-heat ratio. Only the combustion pre-heater has a positive effect on electricity efficiency when compared to the basic ORC plant, although pre-heater does not affect electricity production at all but it improves boiler efficiency. Any changes in the organic cycle, superheating or double cycle structure, only decrease the power-to-heat ratio. It seems that turbine expansion from the saturated steam temperature is optimal for the ORC plant. Since one of the reasons behind choosing organic substance for working medium is avoiding moist steam in the turbine, it is not reasonable to examine whether starting turbine expansion from the moist steam area were worthwhile. A big question for profitability of double ORC process is the detailed extra investment cost.

Preface

This is the final report of a three-years research project ”Small-scale biomass CHP plants and district heating”. The project was coordinated by the Finnish District Heat Association (SKY, –31.12.2004) and Finnish Energy Industries (1.1.2005–) and funded by the National Technology Agency (Tekes) with several Finnish companies. The aim of the project was to find out improved solutions for small-scale biomass CHP production.

The scope of the study was chosen to include present biomass CHP technologies with electric power output between 1–20 MW_e. A narrow review of emerging technologies is also included that have not yet reached commercial and technical maturity. However, a detailed analysis of gasification technologies was excluded from this study.

This project was carried out by Technical Research Centre of Finland (VTT) and Helsinki University of Technology (HUT). Mr Kari Sipilä from VTT Processes was the project manager. Ms Tuula Savola led by Prof. Carl-Johan Fogelholm from the Helsinki University of Technology, Laboratory of Energy Engineering and Environmental Protection made simulation analysis and optimisations of the steam CHP processes. The results of this sub-task are presented in the Licentiate’s thesis ”Simulation and optimisation of power production in biomass-fuelled small-scale CHP plants” by Tuula Savola. The Sections 1.2, 2.1.1, 2.3, 4 and the Appendix A in this report are extracted from the thesis. Mr. Ilkka Keppo led by Prof. Pekka Ahtila from the Helsinki University of Technology, Laboratory of Energy Economics and Power Plant Engineering made calculations and wrote the economical analysis of CHP plants (Section 3). Mr. Esa Pursiheimo from VTT Processes made description of ORC-media properties, process calculation and analysis of an ORC CHP plant (Section 5).

A state-of-the-art report Kirjavainen et al., 2004, ”Small-scale biomass CHP technologies: Situation in Finland, Denmark and Sweden” (OPET Report 12) was written as a part of this project The purpose of the report was to identify the best available technologies (BAT) for small-scale biomass CHP plants currently used.

In addition, this project produced the following publications:

Salomón, M., Savola, T., Kirjavainen, M., Martin, A. R. & Fogelholm, C.-J. 2002. Distributed Combined Heat and Power Generation with Small-Scale Biomass Plants – State of the Art Review. Second International Symposium on Distributed Generation: Power Generation and Market Aspects. October 2–4, 2002. Stockholm, Sweden.

Savola, T., Salomón, M. & Fridh, J. 2003. Efficient technologies for small-scale CHP processes using biofuels. Euroheat & Power English Edition II (2003), pp. 24–29.

Savola, T. & Keppo, I. 2005. Off-design simulation and mathematical modeling of small-scale CHP plants at part loads. Applied Thermal Engineering 25(8-9), pp. 1219–1232.

Savola, T. & Fogelholm, C.-J. 2005. Increased power-to-heat ratio of small-scale CHP plants using biomass fuels and natural gas. Energy Conversion and Management. (Submitted.)

Savola, T. & Fogelholm, C.-J. 2005. MINLP optimisation model for increased power production in small-scale CHP plants. Applied Thermal Engineering. (Submitted.)

Keppo, I. & Savola, T. 2005. Economic appraisal of small biofuel-fired CHP plants. Energy Conversion and Management. (Submitted.)

Contents

1. Introduction

1.1 Combined heat and power (CHP) production

Combined heat and power (CHP) production is simultaneous generation of usable heat and electricity in a single process. In traditional CHP production the heat from steam condensing after the steam turbine is used for heating, e.g. in district heating or cooling networks, instead of dissipating it with the cooling water into the environment. In the case of industrial CHP plants the steam can be also extracted in higher pressures from the turbine and used as process heat. The fuel consumption can be decreased approximately 25–35% with CHP production compared to the power and heat generation in separate processes (Cogen Europe et al., 2001). Thus the CO_2 emissions per produced heat and power are reduced and the total efficiency of the generation increases.

New interesting and promising technologies like gasification for gas motors, stirling engines, fuel cells and organic Rankine cycle (ORC) are being developed, but most of them have not yet reached the technical and commercial maturity. Anyway many pilot projects have been carried out.

The fuel variation used in the CHP production is fairly large. Natural gas, coal, light fuel oils including diesel oil, solid and gaseous biomasses, and waste fuels have all been used for CHP production. Currently, the processes that are most often used in the CHP production with natural gas are a gas turbine and a recovery boiler process, an internal combustion engine process including heat recovery, and a gas turbine process with a combined steam cycle. The CHP plants using biomass fuels are often steam Rankine cycle processes with fluidised bed boilers or grate furnaces, while coal is usually fired in pulverised coal-fired boilers. In addition to these processes, in the future there will be potential for special CHP technologies developed for micro-scale (under 500 kW_e) processes.

In the EU only 10% (74 GW_e) of the electricity is generated in CHP plants, most of which are industrial plants (Cogen Europe et al., 2001). Thus, there exists potential to increase the efficiency of fossil fuel utilisation and to reduce fossil CO_2 emissions with more extensive CHP production. The European Directive of Cogeneration (Directive 2004/8/CE) was approved in the beginning of 2004 and it promotes the CHP production as a means to increase the power plant efficiencies and to reduce the CO_2 emissions in the EU. There is potential to increase the electricity generation from CHP production in the EU to 18% by the year 2010 and to 22% by the year 2020. This means increasing the installed CHP capacity to 135 GW_e by 2010 and to 195 GW_e by 2020. Especially for Central and Eastern Europe there has been estimated to be possibilities to increase the CHP production by 50% from 22 GW_e to 38 GW_e (Cogen Europe et al., 2001).

In Finland about 30% of the electricity and 75% of district heating is currently produced with CHP (Finergy, 2002). In 2002 there were 58 places in Finland, which have CHP production connected to DH network. The total capacity was 4310 MW electricity and 6790 MW heat. Helsinki, the capital of Finland, has the biggest CHP capacity of 1017 MW in electricity and 1300 MW in heat. Many of the large-scale power plants have already been converted to CHP plants, so the possibilities to increase the amount of CHP in Finland is in converting smaller regional heating plants to CHP production. There are some 40 small-scale CHP plants with electric power less than 20 MW_e connected to district heating networks in Finland. Ten of these plants utilise oil or coal as fuel while the others use either natural gas, biomass or peat. During the last 10 years, no new coal or oil fired plants have been built while 10 new biomass plants and several gas fired units have started operation. Most of the small CHP plants using biomass use also peat as fuel. In some plants, peat is the main fuel and the share of biomass is less than 30%. These plants are often using domestic biofuels that may be available in nearby regions and that are considered to be neutral on CO_2 emissions.

The forward temperature of district heating water has considerable effect on several economic and technical parameters within the district heating system. Combined heat and power production benefits from low temperature levels, because more electricity can be produced. On the other hand the forward temperature has also a lowering effect on the return temperature and would enable preheating of water with cheap energy. Also the price of electricity is a risk for CHP investment decision making. One goal is to determine, which plants are used with minimum outgoing DH water temperature and which circumstances are essential for economic operation.

1.2 Challenges of biomass-fuelled small-scale CHP production

Biomass fuels are attracting much interest as renewable and CO_2 neutral fuel alternatives. With CHP production they offer large potential to reduce the use of fossil fuels. To utilise the biofuel resources effectively, the distances of fuel transportation should be minimised and the CHP production should be situated as near the fuel source as possible. In CHP production also the end use of heat sets requirements for the plant location, as the CHP plants should either be connected to a district heating or cooling network or situated near an industrial site.

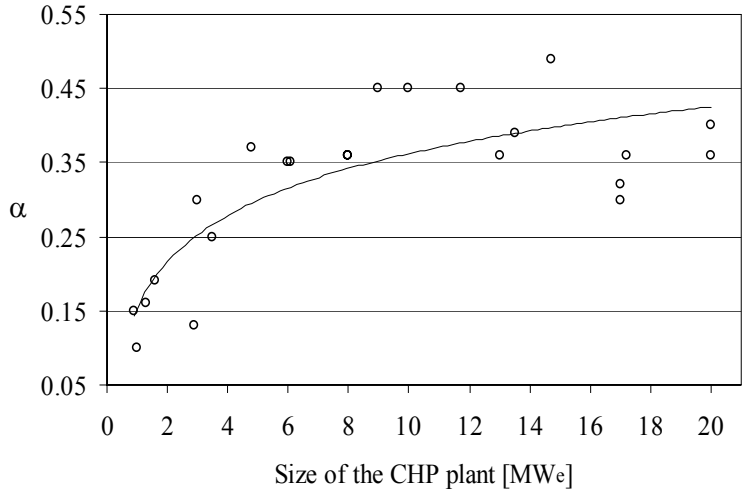

Figure 1. Power-to-heat ratios (α) versus the plant size of some Finnish and Swedish biomass-fuelled CHP plants producing 1–20 MW_e (Wahlund et al., 2000; Salomón et al., 2002; Kirjavainen et al., 2004).

In Finland there is potential to increase the CHP production especially in smaller heating plants corresponding to the power production of 1–20 MW_e. These plants are usually using biomass fuels. However, in the plants of this size range the ratio between produced power and produced heat is often lower than in larger plants. Furthermore, the power-to-heat ratios tend to decrease as the CHP plants get smaller as presented in Figure 1.

The decision to invest in a new CHP plant or to extend the current CHP production requires a corresponding heat demand. Therefore, to maximise the profit from the plant the power production of the plant should be as high as possible. To increase the economic feasibility of the small-scale CHP plant investments more electricity should be extracted from the process per produced heat unit. In addition to the higher electricity production, the increased power-to-heat ratio could also reduce the fuel consumption and the CO_2 production per produced energy unit.

The factors that are limiting the power-to-heat ratios in the small-scale CHP plants are mostly material properties and economical issues. For example, the superheated steam temperature in the process is limited mostly by the materials used in the superheaters and in the steam turbine, whereas many other process features that are commonly used in larger plants are considered to be too expensive for smaller size ranges. Thus, the trade-offs between costs, the complexity of the process, and the increased power production are important factors when defining the most profitable process for a CHP plant investment. Currently, the small-scale CHP processes are kept as simple as possible in new plant investments in order to maintain the economic feasibility of the plants. However, to improve the economic feasibility of the plant investments it would be important to know the CHP plant sizes, in which the different process changes increasing the power-to-heat ratio could become profitable.

2. State of the art for technologies

2.1 Small-scale CHP plants using biomass

2.1.1 Combined heat and power (CHP) processes based on a steam Rankine cycle

The biomass-fuelled CHP plants producing less than 20 MW_e are usually based on a Rankine cycle with steam superheating. The steam after the boiler is superheated at the constant pressure to a higher temperature than the saturation point. A flowsheet example of this process is presented in Figure 2. If the process is producing only power with a condensing steam turbine, the heat exchanger after the steam turbine uses cooling water to condensate the steam into water. The steam expansion in the steam turbine is limited by the moisture content of the steam after the turbine. The maximum value for moisture is around 12%. The cooling water temperature after the heat exchanger is 20–30 ^{o}C, so the heat transferred to the cooling water in condensation usually cannot be utilised because of the low temperatures. If the process is used also for heat production, e.g. in a district heating (DH) network, the forward temperature of the heated water has to be higher, at least 85–110 ^{o}C depending on the outdoor temperature. This defines the temperature and the corresponding pressure of the steam after the turbine. Thus the process is often called back-pressure process. The higher temperature and pressure after the back-pressure turbine reduces the power production as can be seen from Figures 3 and 4, where the temperature vs. entropy (T,s) -diagrams and the enthalpy vs. entropy (h,s) -diagrams of the condensing and back-pressure processes are compared. In the Figures 2–4 the letter A refers to the superheated steam, B is the steam after the back-pressure turbine, C is the steam after the condensing steam turbine, D is the water after the condenser in the condensing process and E in the back-pressure process, F is the feed water at the saturation temperature, and G is the saturated steam after the evaporator. In D and E two points are marked as also the pressure increase in the pump is taken into account. B’ and C’ are the corresponding isentropic steam values after the turbine.

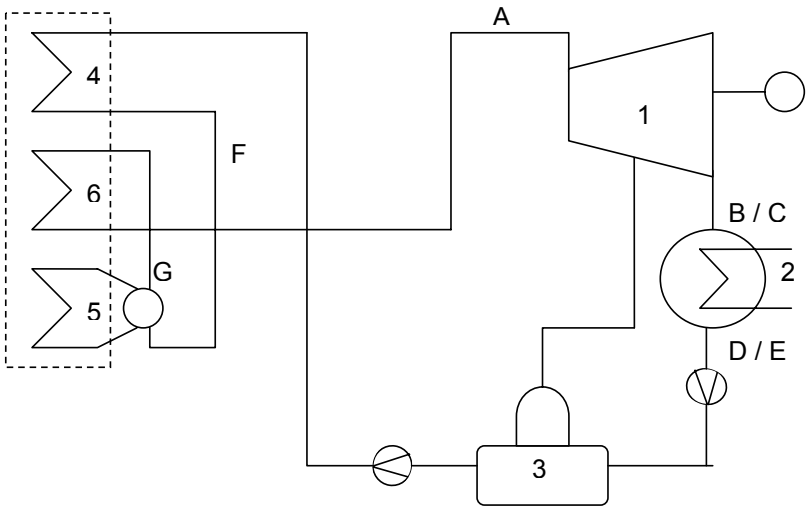

Figure 2. Simple power plant based on a steam Rankine cycle with steam superheating. 1 = Turbine, 2 = Condenser / DH exchanger, 3 = Feed water tank, 4 = Economiser, 5 = Evaporator, 6 = Superheater.

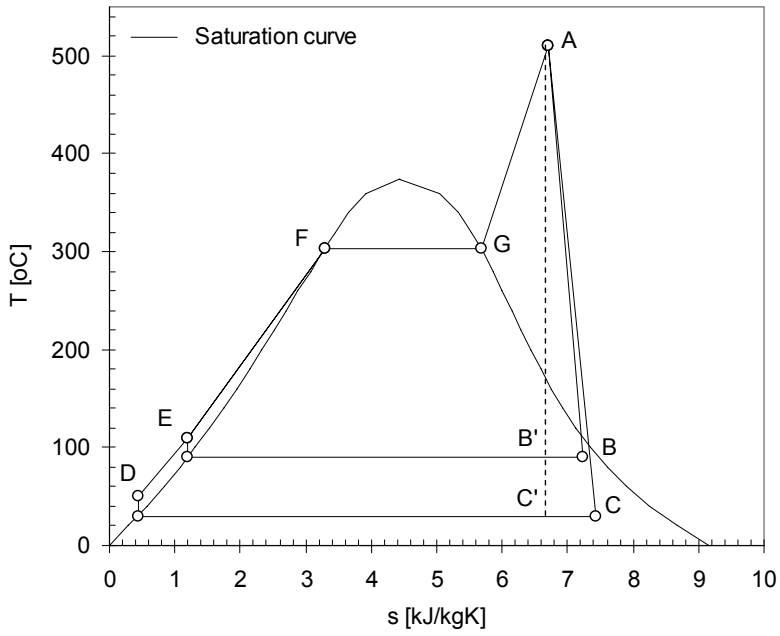

Figure 3. T,s -diagram comparison of a steam Rankine processes with steam superheating for a condensing power plant (ACDFG) and for a back-pressure CHP plant (ABEFG).

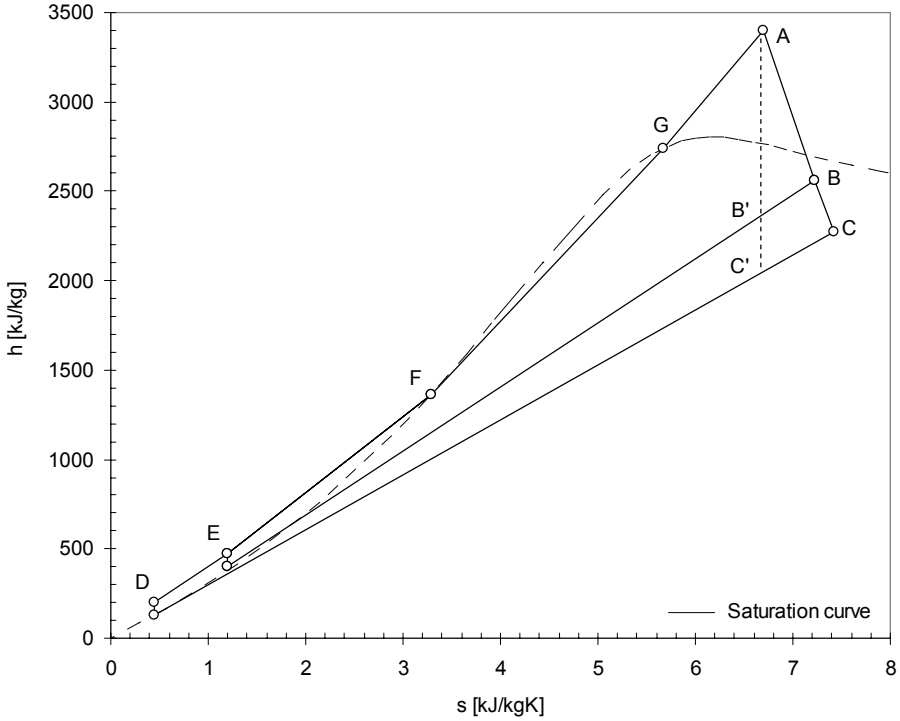

Figure 4. h,s -diagram comparison of a steam Rankine processes with steam superheating for a condensing power plant (ACDFG) and for a back-pressure CHP plant (ABEFG).

Reduction in mechanical work from a steam turbine, when producing both district heat and power, equals the difference between AB and AC. When also the turbine losses, η_{loss}, and the generator efficiency, η_{gen}, are taken into account, the difference presented in Eq. (1) gives an estimation of the difference in the electricity production, ΔP_{gen}, between the condensing and the back-pressure processes:

$$\Delta P_{gen} = AB \cdot \eta_{loss} \cdot \eta_{gen} - AC \cdot \eta_{loss} \cdot \eta_{gen} \quad (1).$$

The electrical efficiency, η_e, of a power plant process can be defined

$$\eta_e = \frac{P_{net}}{Q_{fuel}} \quad (2)$$

where P_{net} is the net power production of the plant and Q_{fuel} is the fuel input energy to the plant. The total efficiency, η_{tot}, of the back-pressure process producing power and district heat can be defined as

$$\eta_{tot} = \frac{P_{net} + Q_{dh}}{Q_{fuel}} \quad (3)$$

where Q_{dh} is the district heat produced in the plant. For a condensing power plant the Q_{dh} = 0. Though Eq. (3) is used widely it is not completely logical in the energy technology point of view, as it considers the electricity and heat to be equally valuable products. In reality electricity is a more valuable product as it can be transformed to any other energy form, whereas the Carnot efficiency restricts the transformation of heat.

Although η_{tot} is higher in CHP plants than in condensing plants, η_e remains lower in CHP plants than in condensing plants because of the smaller power production as shown in Figures 3 and 4. For the 1–20 MW_e biomass-fuelled CHP plants η_e varies from 17% to 29% depending on the plant size (Wahlund et al., 2000; Salomón et al., 2002; Kirjavainen et al., 2004), while it can be around 45% for a condensing power plant. With the heat production η_{tot} is in the CHP plants over 90% (LHV).

The CHP plants are characterized by a parameter indicating the produced power versus the produced heat called the power-to-heat ratio, α:

$$\alpha = \frac{P_{net}}{Q_{dh}} \tag{4}.$$

α corresponds to the ratio

$$\alpha = \frac{AB \cdot \eta_{loss} \cdot \eta_{gen} - P_{process}}{BE} \tag{5}$$

where AB and BE refer to the Figures 3 and 4 and $P_{process}$ corresponds to the power used in the CHP plant, e.g. in pumps and blowers. η_{loss}, η_{gen} and $P_{process}$ have usually only a small effect on AB, so a rough estimate, corresponding the upper bound of α, can be calculated with a ratio between AB and BE.

For an economical operation of the CHP plant a high α is preferred. The district heating CHP plants are usually operated according to the heat demand in the network, so a plant with a high α produces more electricity to the grid with the same heat demand than a plant with a low α. A special problem in the small-scale biomass-fuelled CHP plants is that α has remained fairly low compared to the larger plants. Currently, α is between 0.10 and 0.30 in the 1–5 MW_e CHP plants and between 0.35 and 0.45 in the 5–20 MW_e CHP plants (Wahlund et al., 2000; Salomón et al., 2002; Kirjavainen et al., 2004). In larger back-pressure CHP plants producing district heat the ratio α is usually 0.45, but with other competing CHP processes α can be much higher. In gas turbine processes with a simple recovery cycle α can be 0.55, in a gas turbine process with combined steam cycle 0.95, and in an internal combustion engine process with heat recovery 0.75 (Orispää, 2000). Improvement of α would increase the power production and could improve the economic feasibility of the new small-scale CHP plant investments.

2.1.2 Organic Rankine Cycle CHP plant

Abbreviation ORC comes from the words Organic Rankine Cycle. It is a Rankine process, where instead of the water some organic compound is used as a flowing media (toluene, isobutene, isopentane or silicon fluids).

Heat of evaporation for organic fluid is less than that of the water. That is why an organic process boiler with one pressure level can reach better efficiency than a water boiler with two pressure levels. The organic media will evaporate with lower heat amount than the water and ORC process can utilise lower temperature cells than the water evaporating process. The evaporating process of ORC and water process is illustrated in Figure 5.

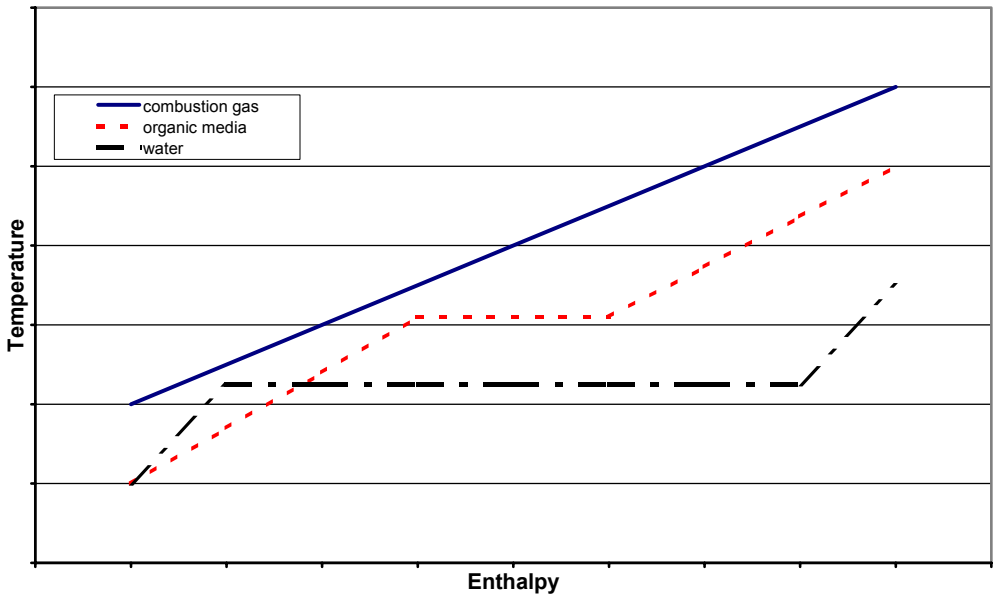

Figure 5. Steaming process of the water and ORC-media.

Enthalpy drop is lower for the organic media than for water and a small one step turbine for ORC media has better efficiency than a steam turbine. Organic media is superheated all the time through the turbine and droplets do not exist as in a steam process. This makes possible a good efficiency also in part loads.

ORC process with high speed technique has a rotation speed 20 000–30 000 rpm. A reduction switch is not used and super frequency current is produced that is why the generator is connected to the network with a frequency converter. An organic liquid feed pump is connected directly to the axis of the turbogenerator. For preventing cavitation a prefeeding pump is used. A principle scheme of super speed ORC-plant is presented in Figure 6. As circulating media is used toluene, isobutene and isopentane. High speed ORC plant is until now built only for research and demonstration use.

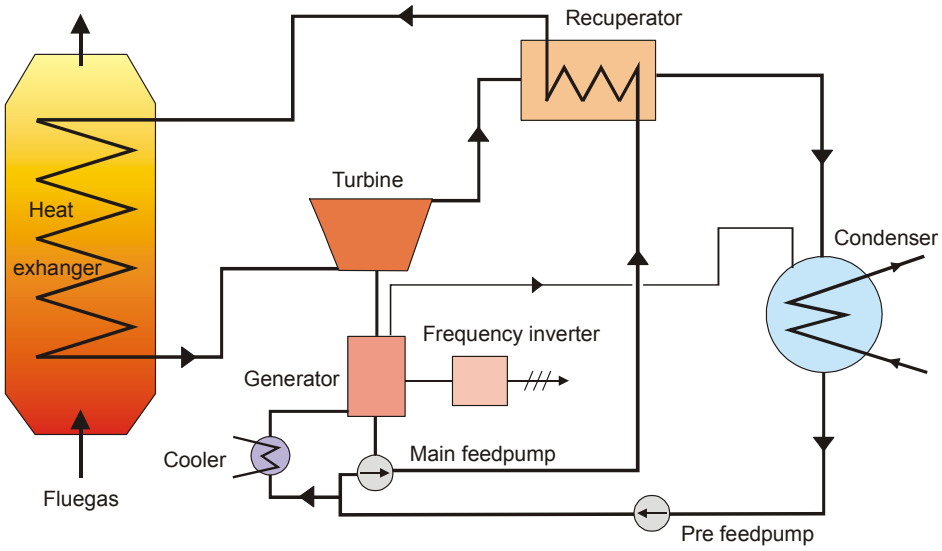

Figure 6. Super speed ORC- plant (Alakangas & Flyktman, 2001).

Low speed ORC process is built in electric output of 400–1100 kW and electricity to heat ratio of 0.18–0.22. The ORC-concept has two circuits, one for thermal oil and another for organic fluid. Heat from burning biomass or other fuel will be transferred through oil circle in temperature 250–300 °C to heat exchanger steaming and super heating the organic silicon fluid. The super heated organic steam is led through the turbine into the condenser, which can also be a district heat exchanger. The condensed ORC-liquid will be pumped through the regenerator to the evaporator in 12 bar pressure. The low speed ORC plant in Admont is present as an example in chapter 5.2.

The most used circulating media is methylenebentzen called Toluene, which is easily flammable, evaporative liquid. The boiling point is 111 °C, melting point –95 °C, density 0.867 kg/m^3, steam pressure 3.73 kPa (25 °C) and flashing point 4 °C. Toluene is classified detrimental to health.

The other media is thermal silicon oil. They have typical evaporating point of 280 °C, when steam pressure is 2.1 kPa, density 696 kg/m^3 and thermal capacity 2.83 kJ/kg K. Silicon oil is not dangerous to surrounding, not toxic and does not destroy the ozon zone. It is however easily flammable, so the pipeline system must be carefully sealed.

2.2 Small-scale biomass CHP potential in Finland

2.2.1 CHP potential including all fuels

CHP (Combined Heat and Power production) has long traditions in Finland. First CHP plants were built in 1960s and big coal and peat fired CHP plants were built in 1970s. Building of CHP plants was based on large enough district heating activities in towns, where CHP plants are located.

In 2000 there were 48 places in Finland, which have CHP production connected to DH-network. The total capacity was 4128 MW electricity and 5671 MW heat. Helsinki has the biggest CHP capacity 1017 MW in electricity and 1300 MW in heat. CHP plants produce about 76% of Finnish district heating energy.

CHP extra potential in Finland has been evaluated to be 941 MW of electricity and 1670 MW of heat with 6000 hours annual peak load time based on district heat energy consumption in 2000. The CHP potential is evaluated to be 3685 MW electricity and 5020 MW heat with 2000 hours annual peak load time. The total amount of possible CHP units is 194 divided in seven categories. The distribution of CHP units is shown in Figure 7 categorised by the unit size.

In evaluating the CHP potential CHP plants have to be able to drive 6 000 h/a or 2 000 h/a based on heat load in existing Finnish DH-systems in 2000. The same principle is used in those places, where CHP production already exists. The potential of the heat capacity is evaluated based on the rest of heat load after CHP production already existing. The share of existing CHP production can not be more than 80% of total annual heat demand.

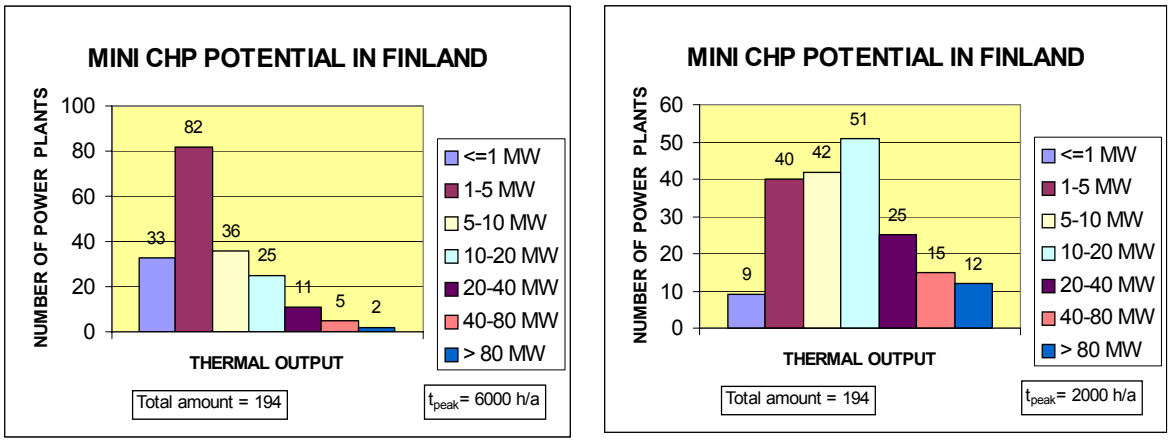

Figure 7. Number of the extra potential CHP plants in Finland.

The potential electricity capacity of CHP is calculated based on the power to heat ratio (black line) shown in Figure 8. Maximum and minimum of the power to heat ratio are shown also based on today's technology. Potential capacity of CHP plants is shown in Figure 9 divided in seven categories.

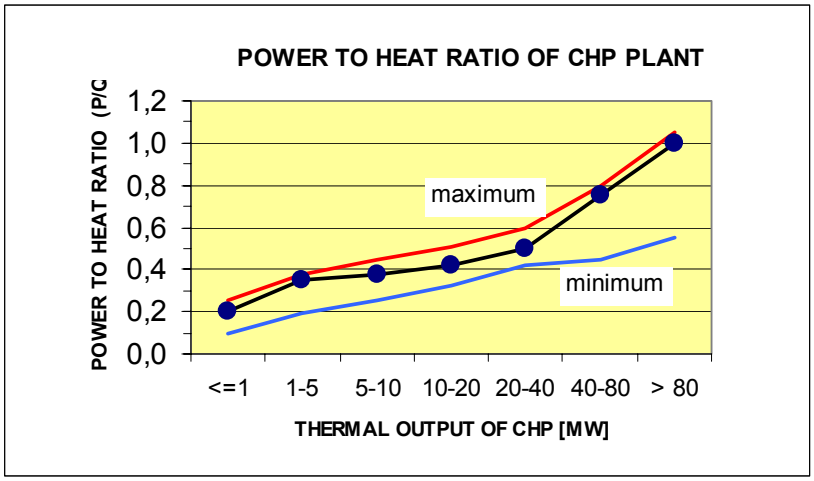

Figure 8. Power to heat ratio of CHP plant as a function of heat capacity.

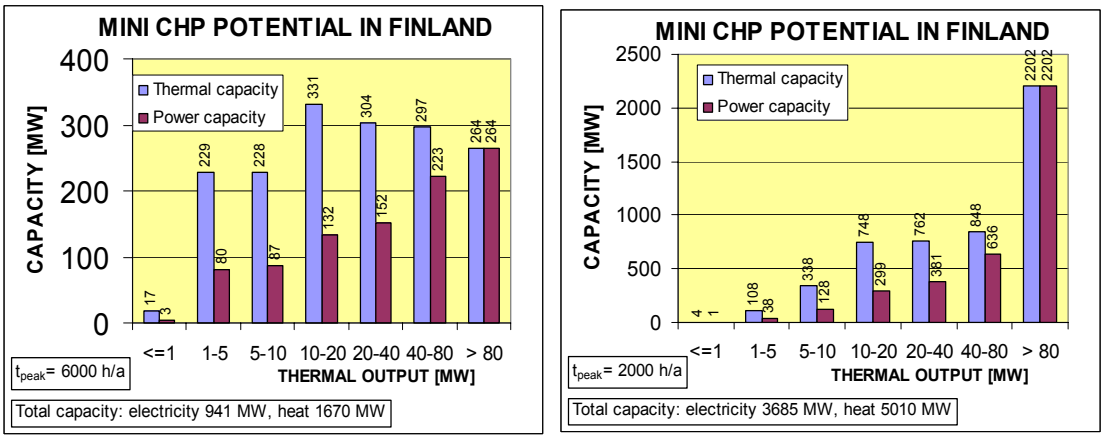

a) b)

Figure 9. CHP potential categorised in thermal output of the plants.

2.2.2 CHP potential including bio fuels, peat and natural gas

CHP potential has been evaluated to be 611 MW of electricity and 1044 MW of heat with 6000 hours of annual peak load time based on district heat energy consumption produced on bio fuel, peat and natural gas in 2000. The CHP potential is evaluated to be 3685 MW electricity and 5010 MW heat with 2000 hours of annual peak load time. The total amount of possible CHP units is 116. If the peat fuel is not included, the amount of CHP plants is 85 and total heat capacity is 481 MW_e/822 MW_{th}. The distribution of the number of CHP units is shown in Figure 10 categorised by the unit size. The fuels are presented in Table 1.

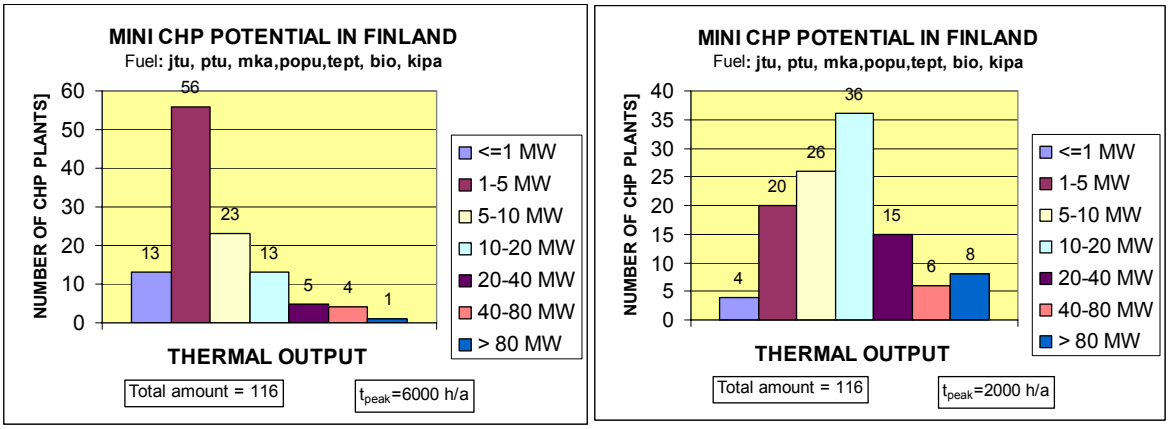

a) b)

Figure 10. Number of the potential CHP plants using bio fuels, peat or natural gas in Finland.

We see that 91% of potential CHP plants exist in category less than 20 MW of thermal effect, if 6 000 h/a of peak load demand is required. The range 1–5 MW covers the most part of the CHP amount having proportion of 48%. Correspondingly the proportion in the thermal size of 20 MW or less is 74%, if 2 000 h/a peak load time is demanded including biggest proportion of 31% in the category of 10–20 MW.

Table 1. Acronyms for fuels.

Fuels	
jtu	milled peat
ptu	sod peat
mka	natural gas
popu	forest fuel
tept	industrial wood waste
pjät	wood industrial liquid waste
bio	biogas
kipa	renewable fuel

The potential capacity of CHP is calculated based on the power to heat ratio shown in Figure 8. Potential capacity of CHP plant is shown in Figure 11 divided in seven categories. CHP plants need gas or gasified fuels to increase the power to heat ratio in category more than 40 MW.

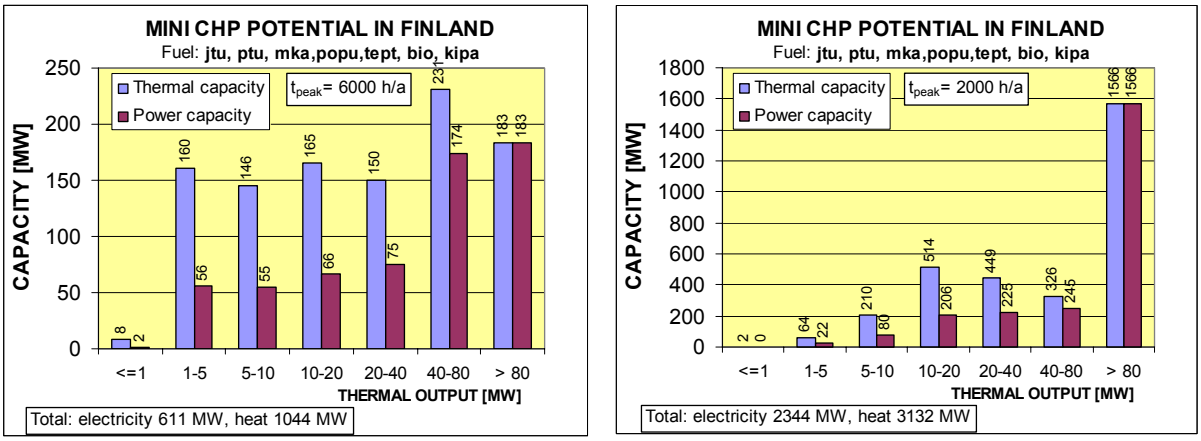

a) b)

Figure 11. CHP potential categorised in thermal output of the CHP plants, if bio fuels, peat or natural gas is used.

2.2.3 CHP potential including only biofuels

CHP potential has been evaluated to be 80 MW of electricity and 214 MW of heat with 6000 hours of annual peak load time based on district heat energy consumption produced on bio fuel in 2000. The CHP potential is evaluated to be 293 MW electricity and 641 MW heat with 2000 hours of annual peak load time. The total amount of possible CHP units is 51. The distribution of CHP units is shown in Figure 12 categorised by the unit size.

We see that 90% of potential CHP plants belong to the category less than 10 MW of thermal effect, if 6000 h/a of peak load demand is required. The range 1–5 MW covers the most part of the CHP amount having proportion of 53%. Correspondingly the proportion in the thermal size of 20 MW or less is 82%, if 2000 h/a peak load time is demanded including biggest proportion of 31% in the category of 10–20 MW.

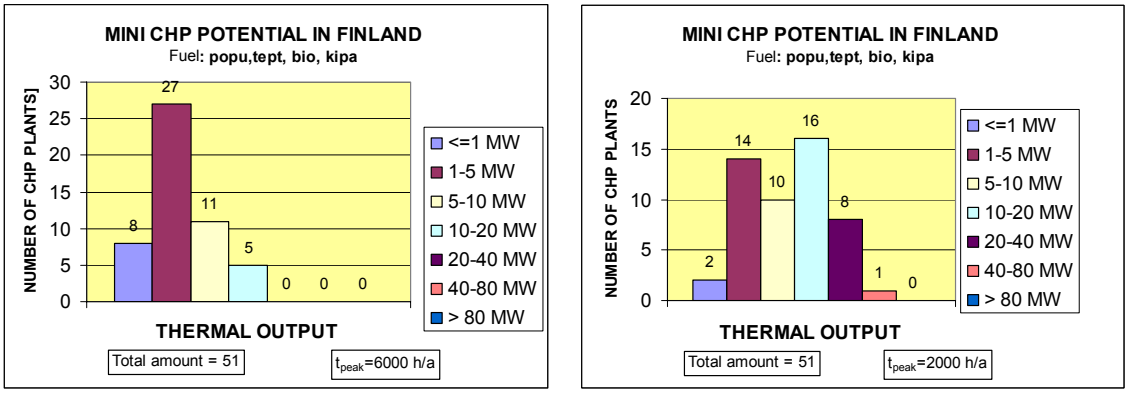

a) b)

Figure 12. Number of the potential CHP plants using bio fuels in Finland.

The potential capacity of CHP is calculated based on the power to heat ratio shown in Figure 8. The potential capacity of CHP plants is shown in Figure 13 divided in seven categories.

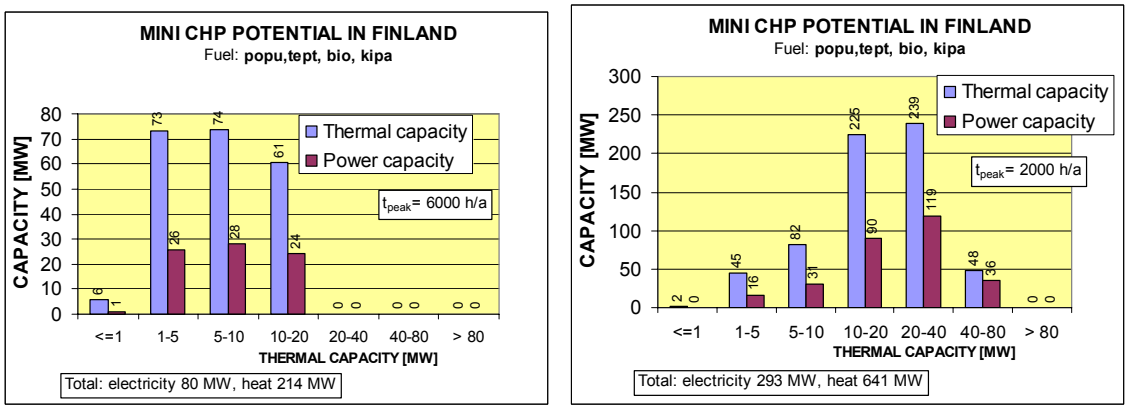

a) b)

Figure 13. CHP potential categorised in thermal output of the CHP plants, if biofuel are used.

The potential capacity of biofuel CHP is located on the map of Finland in Figures 14 and 15. The total demand of fuel is about 2 TWh, when peak load time is 6 000 or 2 000 hours a year. Difference of the estimated fuel production and existing demand in 2010 before those extra CHP installations has been evaluated also in Figure 14 (the column on the right side). The four columns from the left side are number of new CHP plants, heat production, electricity production and annual fuel demand of the CHP plants. As we can see in figure there are four main areas, where biofuel installations are possible:

1. South Savo, Finnish Karelia North and Kainuu: 10 possible CHP plants with fuel demand of 304 GWh a year when the estimated fuel production will be 38.1 TWh in 2010. Main part of the fuel will be forest fuels.

2. Lapland and Middle Ostrobothnia: 5 possible CHP plants with fuel demand of 163 GWh a year when the estimated fuel production will be 57.8 TWh in 2010. Main part of the fuel will be peat.

3. South coast and Häme-Uusimaa: 8 possible CHP plants with fuel demand of 454 GWh a year when the estimated fuel production will be 1.8 TWh in 2010. Main part of the fuel will be renewables.

4. Ahvenanmaa: 1 possible CHP plant with fuel demand of 300 GWh a year when the estimated fuel production will be 0.5 TWh in 2010. Main part of the fuel will be renewable.

It would be possible to build 24 small-scale CHP plants with total capacity of 136 MW_e/306 MW_{th} and annual fuel demand of 1.22 TWh. If district heat energy market will increase 2% a year in those four areas, the market potential after 10 years will be about 22% higher than in 2000.

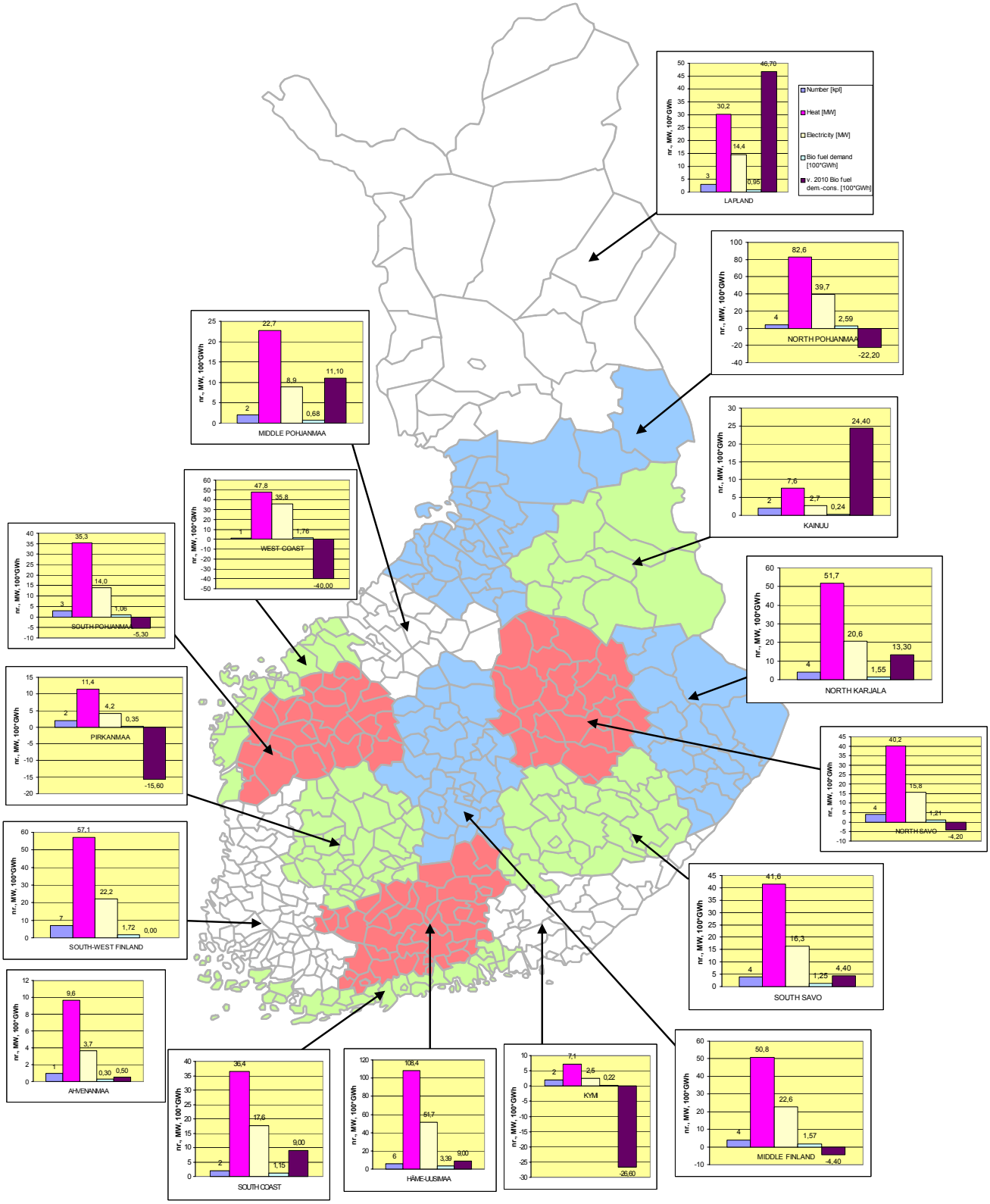

Figure 14. Areal potential of bio-CHP production and biofuel resources in Finland.

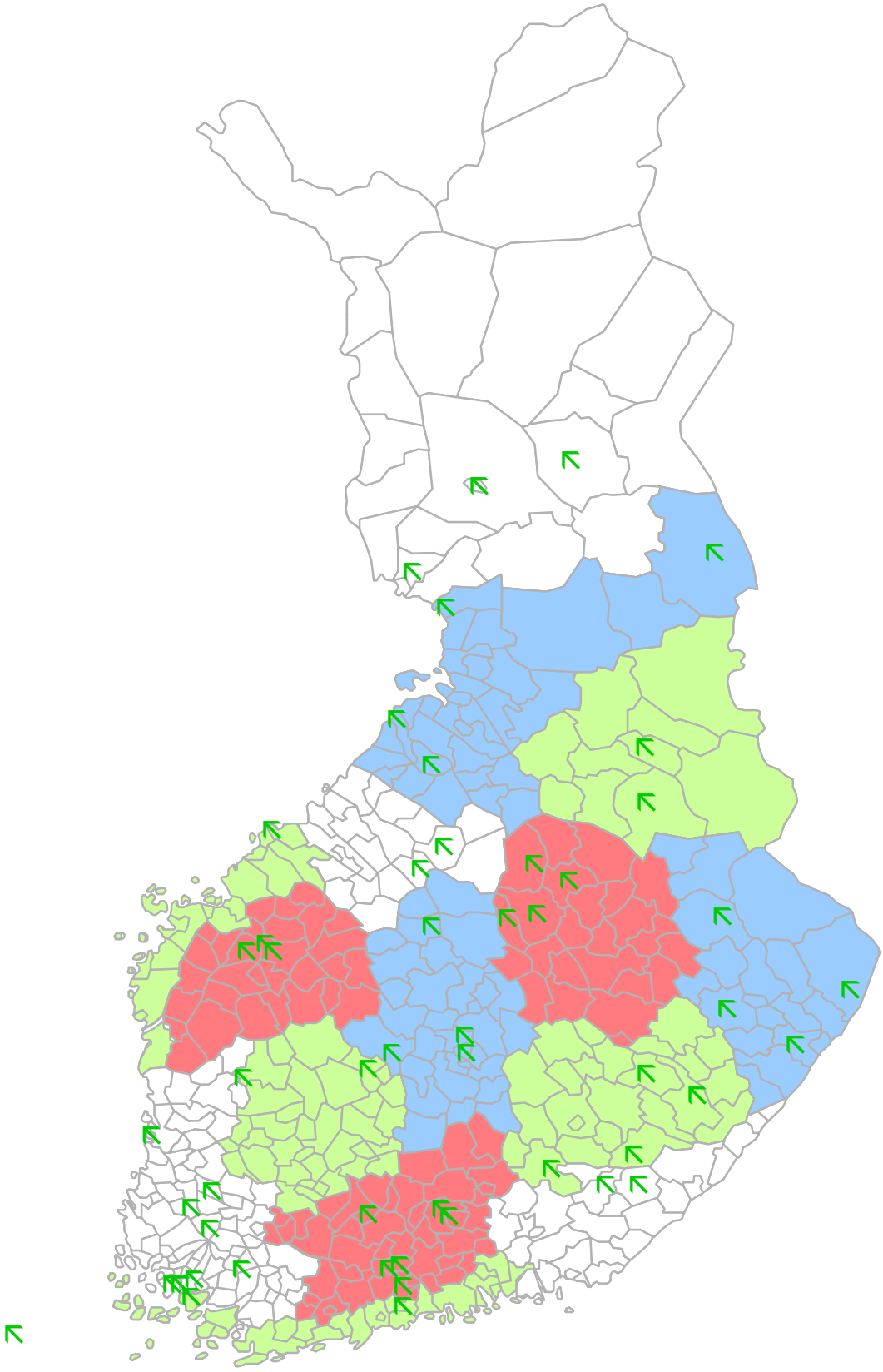

Figure 15. 51 Small-scale biofuel CHP located on the map of Finland.

2.2.4 CHP potential if oil is replaced by biofuel

CHP potential has been evaluated to be 501 MW of electricity and 776 MW of heat based on district heat energy consumption, if production by oil fuel and coal fired heat only boilers could be replaced by biofuels in 2000. Criteria for evaluation are the same as mentioned earlier in this chapter. The total amount of possible CHP units is 61. The distribution of potential CHP plants is shown in Figure 16 in seven categories. The capacity of CHP plants is shown in Figure 17. The power to heat -ratio is shown in Figure 8.

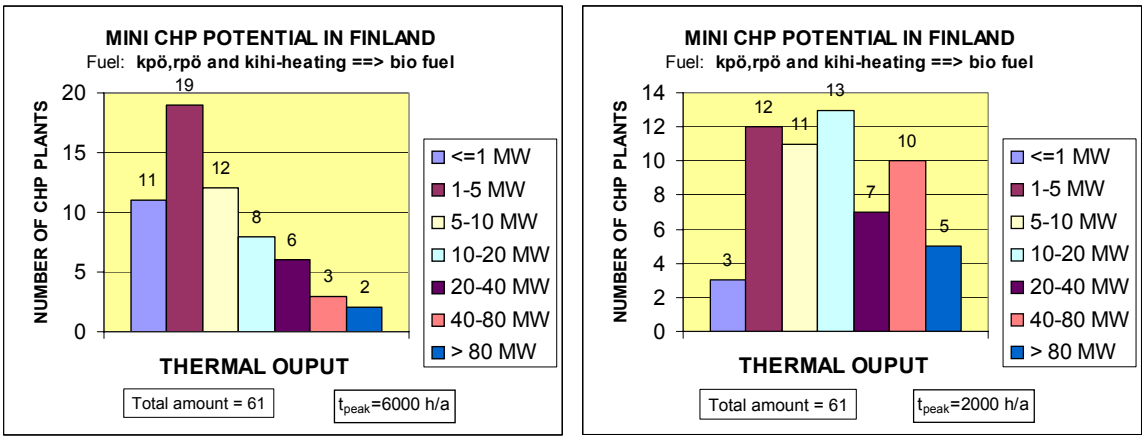

a) b)

Figure 16. Number of the potential CHP plants; if production by oil fuel and coal fuel in coal fired heat only boilers could be replaced by biofuel.

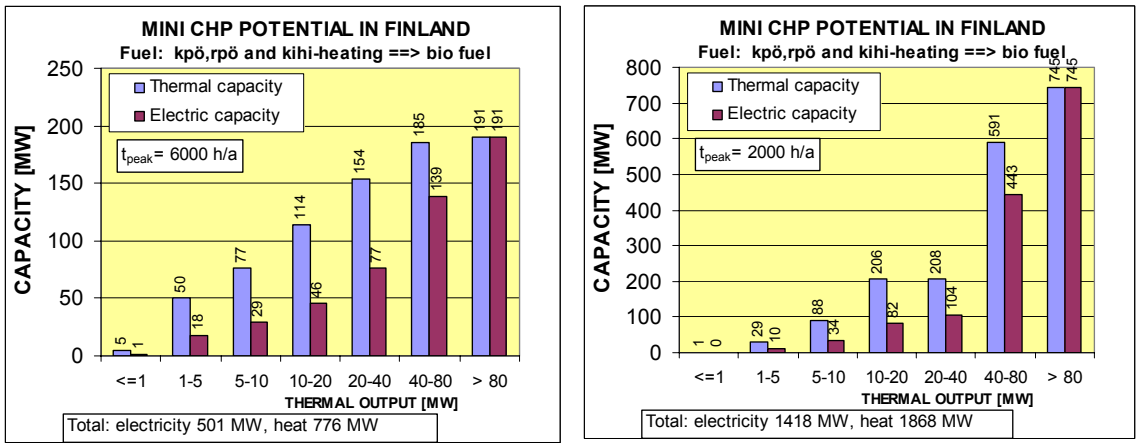

a) b)

Figure 17. CHP potential categorised in thermal output of the plants, if production by oil fuel and coal fuel in coal fired heat only boilers could be replaced by biofuel.

2.3 Review of 1–20 MW_e biomass-fuelled CHP plants in Finland and Sweden

In the year 2003 about 76% of the district heating and 38% (27.2 TWh_e) of the electricity in Finland was produced with CHP plants. The CHP was produced with natural gas (37%), coal (27%) and domestic fuels including peat, wood, and biogas (28%) (Finergy, 2002). Although there is a high share of CHP plants in Finland and many large-scale power plants have been converted to CHP plants, there are still possibilities to increase the amount of CHP by converting regional small-scale district heating plants to combined power and heat production (Kirjavainen et al., 2004). The potential to increase the CHP production in Finland has been estimated to be around 5.5–7.5 TWh_e per year (Kirjavainen et al., 2004). In Sweden only 10% of the district heat (STEM, 2001) and 6% (8.7 TWh_e) of the electricity (STEM, 2004) is produced in CHP processes. The main reason for these low shares is the abundance of affordable electricity from hydro and nuclear power plants. The future potential for CHP in Sweden is estimated to be 10–20 TWh_e per year. From this around 20% could be small-scale CHP plants (Ambiente Italia srl et al., 2001).

Summaries of the biomass-fuelled CHP plants producing less than 20 MW_e and built during the last fifteen years in Finland and Sweden are presented in Tables 2 and 3. Most of the plants producing 3–20 MW_e are based on a steam Rankine cycle with steam superheating as described in Section 2.1.1. The furnaces used in the processes are circulating fluidised beds (CFB), bubbling fluidised beds (BFB), and grate furnaces. In the under 1 MW_e size range, there have been two technologies used in new CHP plants. At Tervola, the CHP plant produces 0.47 MW_e with a new process, where the fuel is gasified with a combined counter and parallel flow gasifier. The dirtier product gas from the counter flow process is burned with a separate gas boiler, and the cleaner product gas from the forward flow process is cleaned and burned in a gas engine. In Kiuruvesi, Karstula, and Tranås the grate technology designed for biomass firing is used together with a steam engine. In addition to these technologies, an integrated gasification combined cycle process has been demonstrated in Värnamo with a 5.5 MW_e CHP plant. The plant was based on a pressurised biomass gasifier and on combustion of the cleaned gasification gas in a gas turbine. The flue gases of the gas turbine were utilised in a heat recovery boiler, which produced steam for a steam turbine. However, the plant is currently out of operation.

Table 2. Biomass-fuelled CHP plants producing 1–20 MW_e constructed in Finland between 1990 and 2004 (Kirjavainen et al., 2004).

Power plant	Power MW_e	Heat MW	Fuel MW	η_e %	η_{tot} %	α	Steam values bar/°C/kgs^{-1}	Fuel	Technology	Start up
Tervola	0.47	1.13	2.0	24	82	0.42	-/-/-	wood	gasification and gas engine	2002
Kiuruvesi	0.9	6	8.1	11	85	0.15	25/350/2.8	bark, sawdust, wood chips	grate and steam engine	1999
Karstula	1	10	12.9	8	85	0.10	24/350/	bark, sawdust	grate and steam engine	2000
Renko	1.3	8	10.9	12	85	0.16		wood	grate	2004
Vilppula	2.9	22.5	29.9	10	85	0.13	50/450/	bark	grate	2004
Kuhmo	4.8	12.9	20.1	24	88	0.37	81/490/	wood residues	CFB	1992
Kuusamo	6.1	17.6	27.6	22	86	0.35	61/510/8	peat, wood chips, sawdust	BFB	1993
Kankaanpää	6	17	26.0	23	89	0.35	60/510/7.9	peat, wood	BFB	1992
Lieksa	8	22	33.9	24	89	0.36	61/510/8	peat, wood	BFB	1994
Ristiina[1]	10	64[1]	86.0	12	86	0.16		wood	BFB	2002
Iisalmi	14.7	30	48.0	31	93	0.49	93/515/17.5	peat, wood, REF	BFB	2002
Kotka	17	56	81.1	21	90	0.30	62/480/21	bark, wood, peat	BFB	2003
Savonlinna	17	53	81.0	21	86	0.32	92/523/28	bark, wood, peat	BFB	2003
Forssa	17.2	48	71.7	24	91	0.36	62/510/22.8	wood, REF	BFB	1996
Kokkola	20	50	78.7	25	89	0.40	80/482/27	peat, wood	BFB	2002

[1]Main product of the plant is process heat.

Many CHP plants in Sweden have also flue gas condensing which increases the heat production. The humidity of the flue gases is condensed and the heat is transferred to the returning district heating water. This process increases the η_{tot} of the plant often by 10–30%. This can result in total efficiencies over 100%, as the lower heating value of the fuel is used in the calculations. In Tables 2 and 3 α has been calculated without the heat from flue gas condensation, to make a comparison of the CHP plants possible. The flue gas condensing requires that there are profitable possibilities to utilise the additional heat from the condenser. This has made the flue gas condensing unattractive for the CHP plants in the Finnish markets for the last ten years.

Table 3. Biomass-fuelled CHP plants producing 1–20 MW_e constructed in Sweden between 1990 and 2002 (Wahlund et al., 2000; Salomón et al., 2002; Kirjavainen et al., 2004).

Power plant	Power MW_e	Heat MW	Fuel MW	η_e %	η_{tot} %	α	Steam values bar/°C/kgs^{-1}	Fuel	Tech-nology	Start up
Tranås	1.6	8.3+2.7[2]	11.5	14.5	104	0.19	16/345/3.4	sawdust, bark	grate,steam engine	2002
Malå	3	10	16.3	18	85	0.30	41/480/4.4	wood	BFB	1991
Lomma	3.5	14	18.3	19	93	0.25	60/510/5.7	wood, paper	FB	1995
Värnamo[1]	5.5	9	18.5	30	76	0.67	40/455/-	wood	IGCC	1994
Falun	8	22+8[2]	35	23	109	0.36	63/490/10.2	bark, wood	BFB	1993
Nässjö	9	20+6[2]	36	25	100	0.45	85/490/12	wood	CFB	1990
Sala	10	22	36	28	89	0.45	80/480/12.6	wood	BFB	2000
Härnösand	11.7	26+7[2]	42	28	106	0.45-0.49	92/510/14	wood, bark, peat	BFB	2002
Hudiksvall	13	36	60	22	82	0.36	67/475/18	wood, peat	grate	1992
Kristianstad	13.5	35	55.5	24	87	0.39	65/510/17.5	wood	CFB	1994
Lycksele	14	28	50	32	84	0.51	88/520/17.5	wood	CFB	2001
Karlstad	20	55+20[2]	88	20	108	0.36	66.7/500/29	wood	CFB	1992

[1] Currently out of operation.

[2] Some heat is produced with flue gas condensing, and is considered when calculating η_{tot} but not when calculating α.

3. Optimisation of the CHP and district heating system[1]

3.1 Description of the system

The goal of this part of the project is to find out the optimal parameters for a small-scale CHP-system and estimate, what would be the feasible combinations of electricity prices and investment costs.

The evaluation is done using non-linear mathematical programming. Relations affecting the transport, production and consumption of energy are used in the model as equality or inequality constraints. The object function to be optimised consists of the investment costs (the electricity price is predetermined), electricity price (investment costs are given) or production costs (only the production parameters act as variables). Based on these, a model of a district heating system is created and optimised and the required range of electricity prices and investment costs are obtained as results. The district heating parameters are variables, so the optimisation will also provide values to the parameters, that give the economic optimum.

Production parameters are optimised separately for each outside temperature. The temperature drop and the required mass flow at a substation are evaluated with the help of a Visual Basic -macro. The network used in the study is a small, separate network located in western Finland.

3.2 The optimisation model

A district heating system can be considered to consist of three separate systems and the links between these systems; heat production and the heat transfer to the district heating water, transfer of the district heating water from the plant to the customer and heat transfer from the district heating water to the water circulating in the building. The system inside the building could be considered the fourth, but in this study we stop at the distrcit heating substation, where the energy is transfered to be then delivered further by the customer himself.

In this section we present the composition of the model as well as the structure of each of the components included in the model.

---

[1] This chapter is based on the paper (Keppo & Savola, 2005) submitted to Energy Conversion and Management.

3.2.1 The general structure of the model

The operational optimisation of the model is based on dividing the year into 10 different bins, denoted with a subscript *i*, based on the outside temperature. Division by outside temperatures allows one to take into account the effects this temperature has on the operation of a district heating substation, where the temperature of the water in the radiator circuit depends on the outside temperature. A division based on seasons, times of the day and days of the week, which is done in (Henning, 1997; Sundberg, 2000, 2002; Rolfsman, 2004), would not allow these temperatures to be taken into account. The design level of the optimisation takes the results from these bins into account and decides the dimensioning of the plants based on investment costs and the operating costs which are weighted according to the probabilities of the bins.

The model is built as a nonlinear model, without integer variables. The general form for a problem like this is:

$$\min f(x)$$

$$\text{s.t.} \quad \begin{aligned} h(x) &= 0 \\ g(x) &\le 0 \\ x &\in X \subseteq \Re^n \end{aligned}$$

Here x is a vector of continuous variables. If any of the functions is nonlinear, the problem also becomes a nonlinear programming problem.

3.2.2 The production facilities

Three actual small-scale biomass CHP plants are chosen to represent the current situation. These three plants are mostly used as examples of current CHP *technology* and therefore their sizes and investment costs are varied considerably during this study. These particular plants are chosen based on (Kirjavainen et al., 2004) and they all started their operation in 2002. Two of these plants are located in Sweden and one in Finland. The plants are simulated using software called PROSIM and the mathematical representation of the production is formulated from these results. More about the simulations and the mathematical model can be found in Savola and Keppo, 2005. Some basic data for the original plants is presented in Table 4.

Table 4. Summary of the plants studied (Savola & Keppo, 2005).

Power Plant	Plant A	Plant B	Plant C
Power output, MW	1.6	11.7	14.7
Heat output, MW	8.3 + 2.7[a]	26 + 7[a]	30
Fuel input, MW	11.5	42	48
Electrical efficiency	0.145	0.28	0.31
Total efficiency	1.04	1.06	0.93
Fuel	sawdust, bark	wood, peat	wood chips, sawdust, bark, peat, REF
Technology	Biograte + steam engine	BFB	BFB
Power-to-heat ratio	0.19	0.45-0.49	0.49
Approximate investment cost, €/kW, el	3888[b]	1496	1429

a Produced with flue gas condensing. Not taken into account in simulations, but included in the efficiencies.

b Approximated from several sources describing similar projects of the manufacturer.

The fuel consumption for a CHP plant is described as (Savola & Keppo, 2005):

$$Q_{f,i} = a_f \cdot Q_{CHP,i} + D \cdot b_f \cdot T_{h,i} + D \cdot c_f \cdot T_{c,i} + D \cdot d_f \quad (6).$$

The power production follows from Eqs. (2–6):

$$P_i = a_p \cdot Q_{CHP,i} + D \cdot b_p \cdot T_{h,i} + D \cdot c_p \cdot T_{c,i} + D \cdot d_p - w_{1.i} - w_{2,i} \quad (7)$$

$$w_{1,i} \geq \left(L_1 \cdot Q_{inv} - Q_i\right) \cdot r_1 \quad (8)$$

$$w_{2,i} \geq \left(L_2 \cdot Q_{inv} - Q_i\right) \cdot r_2 \quad (9)$$

$$w_{n,i} \geq 0 \quad (10)$$

$$D = \frac{Q_{CHP,inv}}{Q_{CHP,inv0}} \quad (11).$$

This formulation is used to describe the reduction in power production during part-load operation. Since fuel consumption only depends on the heat load, *w* gets values of zero as long as the electricity price is positive or the load is above the limit *L*. Below limit *L* power production is reduced according to Eq. (8) and (9) making the power production a piecewise linear function.

Table 5. Coefficients for fuel consumption and power production.

	Plant A	Plant B	Plant C
a_f	0.265285	0.501837	0.579103
b_f	-0.013420	-0.049631	-0.047802
c_f	0	0	-0.012534
d_f	0.770670	2.810384	2.449670
a_p	0.170036	0.407082	0.480720
b_p	-0.013255	-0.049126	-0.047368
c_p	0	0	-0.012324
d_p	1.493472	4.938716	4.868050
r_1	0.073020	0.070207	0.079772
r_2	0.057123	0.087737	0.095694
L_1	0.9	0.85	0.8
L_2	0.7	0.6	0.6

Coefficients needed for Eqs. (6–9) are shown in Table 5. These are calculated from the simulation results and they therefore refer to the original plants. Variable *D* is used to scale the coefficients so that they can be used for plants of variable scales. $Q_{CHP,inv}$ refers to the maximum heat production of the plant we are studying while $Q_{CHP,inv0}$ refers to the maximum heat production of the original plant. $Q_{CHP,inv}$ is defined as:

$$Q_{CHP,inv} \geq Q_{CHP,i} \quad (12).$$

For more information about the simulations and estimation of the coefficients, see Savola and Keppo, 2005. Note that the temperature of the cold district heating water was also changed for this study. The coefficient of determination is over 0.995 for all descriptions of power production and fuel consumption.

The investment cost depends on the maximum nominal power production and this is calculated from Eq. (7) by replacing the variables followingly: $Q = Q_{CHP,inv}$, $T_h = 115$ ºC and $T_c = 50$ ºC. The temperatures are chosen because they represent typical design temperatures in Finland.

It is also required, that the power production is always non-negative. This means, that the plant must always be used once an investment is made. However, the price difference between the fuel and electricity prices used is large enough to make sure this restriction does not affect the optimal production strategy. But this restriction can have an effect on the dimensioning of the plant; a plant can not be dimensioned such, that its minimum load would be above the minimum demand.

In addition to the CHP plant, it is assumed, that there is an old oil boiler available. We also study cases, where an investment is required for the boiler. These plants are described simply as boilers transforming the fuel energy into heat with the efficiency of 0.9. When investment is needed, Eq. (12) is used also for the heat-only boilers.

The energy balance for bin *i* is

$$Q_{CHP,i} + P_{pump,i} + Q_{boiler,i} = c_p \cdot \dot{m}_i \cdot \left[T_{h,i} - T_{c,i}\right] + Q_{loss,i} \qquad (13).$$

The power needed for pumping is assumed to turn into heat (Benonysson et al., 1995; Zhao et al., 1998). The heat loss, $Q_{loss,i}$, and the pumping energy are defined in the next section. In the case of several heat-only boilers, another $Q_{boiler,i}$ is added on the left side of Eq. (13).

3.2.3 District heating network

In this study it is assumed that there is already an existing network and therefore no investment is needed. The network used, is located in South-Western Finland. The maximum heat load of all the customers is about 4.5 MW. The system is currently operated with oil fired boilers. The information available for the network contains the lenghts of the pipelines, the locations of customers and pipes and the maximum heat load of each substation. An approximation is made for the dimensions of the pipes by making sure, that the pressure loss in design conditions is no more than 1 bar/km. The total length of this tree-shaped network is somewhat over two kilometers.

The critical customer is the one, to whom the pressure loss is the biggest. The route from the production plant to that particular customer is the critical route. The pressure loss for a pipe is according to Darcy-Weisbach equation

$$\Delta p = \xi \cdot \frac{8 \cdot l}{\pi^2 \cdot \rho \cdot d_{inner}^5} \cdot \dot{m}^2 \qquad (14)$$

where ξ is the friction factor, l the length of the pipe, ρ the density of the water, d_{inner} the inner diameter of the pipe and $\dot{m}$ the mass flow of the district heating water.

The friction factor can be estimated from Swamee- Jain equation, which is

$$\xi = 0.25 \cdot \left[\lg\left(\frac{5.74}{\mathrm{Re}^{0.9}} + \frac{\varepsilon}{3.71} \right) \right]^{-2} \quad (15).$$

Re refers to the Reynolds number

$$\mathrm{Re} = \frac{4 \cdot \dot{m}}{\pi \cdot \mu \cdot d_{inner}} \quad (16)$$

and ε to relative roughness (pipe roughness, k, divided by the inner diameter). μ is the dynamic viscosity.

Using these functions the critical route is defined. It is verified with a simulation software Heat Nexus^{Tm}, that the critical customer remains the same during all relevant operating conditions.

Since the costs connected to the network are usually not vital (Zhao et al., 1998) and the small size of the network used here makes its operation even less important economically, following simplifications are made:

- The efficiency of the pump is considered to be always 1.
- The density and dynamic viscosity of the water are assumed to be constants.

In addition to these, the friction factor is estimated for typical flow conditions on the critical route and used then as a constant. Doing this, we get from Eq. (14) for the critical route:

$$\sum_{cr} \xi_c \cdot \frac{8 \cdot l_{cr}}{\pi^2 \cdot \rho \cdot d_{inner,cr}} \cdot \dot{m}_{cr}^2 = 16.807 \cdot \dot{m}_{total}^2 \frac{1}{kg \cdot m} \quad (17).$$

The subscript *cr* refers to a pipe along the critical route. The mass flow on the right side of Eq. (17) refers to the total mass flow and the relation between that and the mass flow along the critical route is defined from the corresponding heat loads.

The required power for pumping can now be calculated from

$$P_{pump,i} = \dot{m}_i \cdot \left(\frac{2 \cdot 16.807 \cdot \dot{m}_i^2 + \Delta p_{\min}}{\rho} \right) \quad (18).$$

Δp_{min} is the pressure loss for a substation and it is assumed to be 60 kPa. The unit for minimum pressure difference in the equation is pascal and the power is given in watts.

Since the network is very small, the temperature drop of the district heating water from the plant to the substation is not calculated and the heat loss for a pipe is determined for steady-state conditions:

$$\frac{Q_{loss,i}}{l} = G \cdot \left(\frac{T_{h,i} + T_{c,i}}{2} - T_{ref} \right) \quad (19).$$

T_{ref} is the reference temperature of the soil, taken to be +5 ºC through the year, and G is the total heat transfer coefficient for two buried pipes. Since G only depends on the dimensions and characteristics of the pipe, soil and insulation, it is constant for pipes of similar dimensioning. For the calculation of G, see e.g. Energy-Economic Society, 1989. The heat losses are calculated from Eq. (20), where the sum includes all the pipes in the network. For this particular network, the sum is 934.4298 W/K.

$$Q_{loss,i} = \left(\frac{T_{h,i} + T_{c,i}}{2} - T_{ref} \right) \cdot \sum_{pipe} G_{pipe} \cdot L_{pipe} \quad (20)$$

3.2.4 District heating substations

The district heating substations are modelled to find out how the temperature of the district heating water changes while going through the heat exchangers at the substation during different outside temperatures. Two-stage coupling is used for the substations in this study.

The outside temperature range for the modelling is from –30 to +19 ºC. The temperature of the hot district heating water can vary from 115 ºC to 60 ºC. The design conditions are based on outside temperature of –30 ºC and district heating water temperature of 115 ºC.

The cold domestic water temperature is 10 ºC, hot domestic water 55 ºC and the circulating water coming back to the heat exchanger 50 ºC. The consumption of the hot domestic water flow is assumed to be constant and the flow is calculated in such a way, that the energy needed to heat that flow is 30% of the energy needed for space heating during the year. In reality the consumption has a lot of variation, but to take this into account, an operational study with very small time steps would be required.

The heat load for space heating is linear and equals zero when the outside temperature reaches +20 °C. The temperatures of the water in the radiator circuit depend on the outside temperature as follows:

$$T_{r,hot} = 40 - T_{outside} \quad (21)$$

$$T_{r,cold} = 28 - \frac{2}{5} \cdot T_{outside} \quad (22).$$

$T_{r,hot}$ refers to the temperature the water has when it is leaving the heat exchanger and going to the radiators. $T_{r,cold}$ is the temperature of the same water when it is returning to the heat exchanger.

The heat transferred in a heat exchanger is calculated from Eq. (23):

$$Q = A \cdot U \cdot \Delta T_{lm} \tag{23}.$$

A is the heat exchange area, U the overall heat transfer coefficient and ΔT_{lm} is the log-mean temperature difference for a counterflow heat exchanger.

The overall heat transfer coefficient for a heat exchanger is calculated from Eq. (24):

$$\frac{1}{U} = \frac{1}{\alpha_{dh}} + \frac{1}{\alpha_s} \tag{24}.$$

α_{dh} is the convection heat transfer coefficient for circuit with district heating water and α_s is the same coefficient for the secondary circuits, the radiator and the hot domestic water circuits. The equation is a simplification, since the conduction term has been left out as insignificant. In the following calculations it is assumed to be constant and similar on both sides of the heat exchanger. The flow is also assumed to be turbulent.

Convection heat transfer coefficient can be calculated from Eqs. (25–27):

$$\alpha = \frac{Nu \cdot \lambda}{d_{hyd}} \tag{25}$$

$$Nu = C \cdot \mathrm{Re}^n \cdot \mathrm{Pr}^m \tag{26}$$

$$\mathrm{Pr} = \frac{c_p \cdot \mu}{\lambda} \tag{27}.$$

Following substitutions are used:

$$\frac{\dot{m}_{dh,design}}{\dot{m}_s} = S_{design} \tag{28}$$

$$\frac{\dot{m}_{dh}}{\dot{m}_{dh,design}} = S \tag{29}.$$

The index *design* refers to design conditions. d_{hyd} is the hydraulic diameter of the heat exchanger. The consumption of the hot domestic water is assumed to be constant. The heat capacity and dynamic viscosity are also assumed to remain constant. These assumptions reduce the accuracy, but the model should still be accurate enough for the purposes it is created for.

Taking into consideration the simplifications, Prandtl's number is a constant and same for both sides of the heat exchanger. Reynold's number is a function of the mass flow. Thus we get from Eqs. (25–28):

$$\frac{\alpha_{dh,design}}{\alpha_s} = S_{design}^n \tag{30}.$$

Combining Eq. (24) and Eq. (30) leads to:

$$\frac{1}{U_{design}} = \frac{1}{\alpha_{dh,design}} + \frac{S_{design}^n}{\alpha_{dh,design}} = \left(1 + S_{design}^n\right) \cdot \alpha_{dh,design}^{-1} \tag{31}.$$

Using Eq. (29) in a similar way we get:

$$\frac{\alpha_{dh}}{\alpha_{dh,design}} = S^n \tag{32}$$

$$\frac{1}{U} = \frac{1}{\alpha_{dh,design} \cdot S^n} + \frac{S_{design}^n}{\alpha_{dh,design}} = \left(S^{-n} + S_{design}^n\right) \cdot \alpha_{dh,design}^{-1} \tag{33}.$$

Combining Eq. (31) and Eq. (33):

$$\frac{U}{U_{design}} = \frac{1 + S_{design}^n}{S^{-n} + S_{design}^n} \tag{34}.$$

The product of the heat exchanger area, A, and the total heat transfer coefficent, U_{design}, is calculated from the design conditions, since the design temperatures and the heat load are known. The product of A and U is then calculated for other operating conditions from Eq. (34). Eq. (23) defines the heat transferred.

The required mass flow and the resulting temperature of the cold district heating water are calculated for all outside temperatures using different temperatures of the hot district heating water. For the calculations a small program is created with Visual Basic. The program iterates all heat exchangers taking into account how they are connected to each

other. If Eq. (23) is not fulfilled, mass flow is increased. A temperature difference of 5 ºC is required in the inlet and outlet of a heat exchanger. Therefore there are some restrictions on the hot water temperatures that can be used for the colder outside temperatures. The resulting temperatures for cold district heating water as a function of hot district heating water and outside temperature are shown in Figure 18.

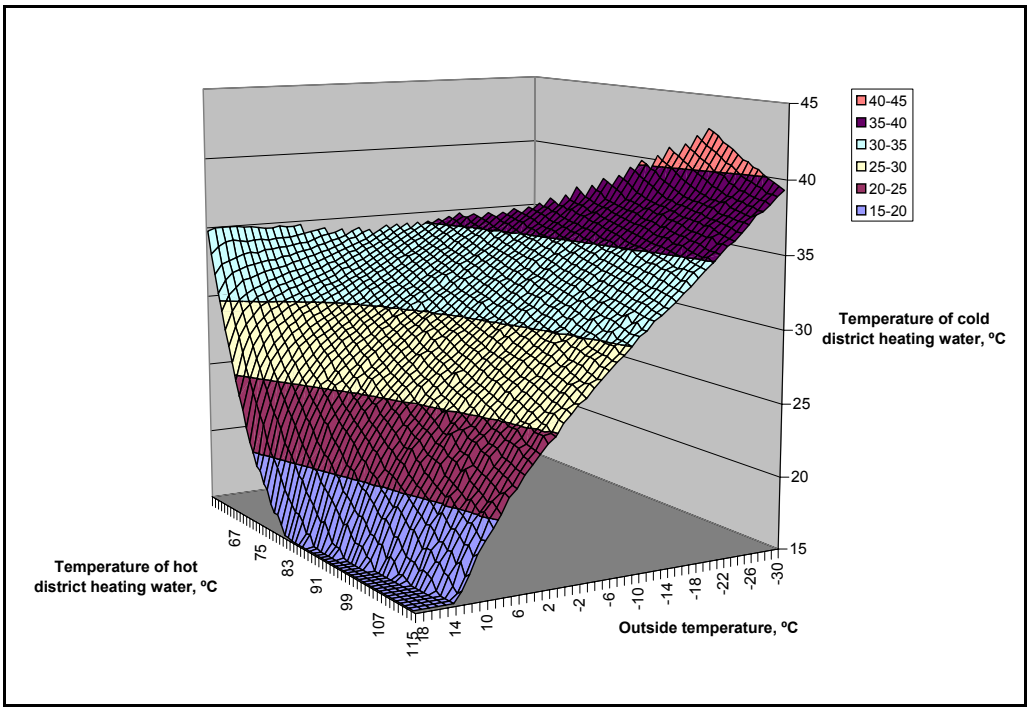

Figure 18. The temperatures of the cold district heating water.

The temperature of the cold water is taken as linearly dependent of the temperature of the hot district heating water for each temperature bin i:

$$T_{c,i} \geq a_i \cdot T_{h,i} + b_i \tag{35}$$

$$T_{c,i} \geq 15^{\circ} C \tag{36}.$$

The coefficients for Eq. (35) are different for each bin i and they are determined using least square estimations. Constraint (36) is added, since the relationship between $T_{c,i}$ and $T_{h,i}$ can not be described with a single line with high outside temperatures. This is also the reason for not using an equality constraint. The inequality constraint does not affect the result, since using a certain hot water temperature, it is always beneficial to have as low cold water temperature as possible. The higher the cold water temperature, the higher is the required mass flow and thus pumping costs (Eq. (18)), the higher are the heat losses (Eq. (20)) and the lower is the power production (Eq. (7)). R^2 for the regression estimates is over 0.93 for all bins.

The temperature of the hot district heating water is restricted in three ways: 1) it must always be at least 70 ºC, but no more than 115 ºC, 2) it must be at least 5 ºC above the highest temperature in the secondary circuit at the substations and 3) the mass flow can not be more than approximately 15% above the original design flow. The required mass flow follows from the energy balance:

$$\dot{m}_i = \frac{Q_{i,demand}}{c_p \cdot (T_{h,i} - T_{c,i})} \quad (37).$$

3.2.5 The weather data, the price of electricity and the objective function

The outside temperatures are organised in 10 bins and the frequency of these bins is used to weight the costs associated with a particular bin in the objective function. The temperature distribution is calculated based on (Soini, 1982). The temperature measurements in (Soini, 1982) were done four times a day for four years and the total number of observations is 5844.

The outside temperatures are divided into bins as is shown in Table 6.

Table 6. The weather data.

Bin number, *i*	Upper limit for bin	Lower limit for bin	Temperature used	Frequency for bin
1	-26	n.a.	-28	0.003080
2	-21	-25	-23	0.010951
3	-16	-20	-18	0.030972
4	-11	-15	-13	0.049110
5	-6	-10	-8	0.095311
6	-1	-5	-3	0.130903
7	4	0	2	0.190794
8	9	5	7	0.139117
9	14	10	12	0.167180
10	n.a.	15	18	0.182580

The column ”Temperature used” refers to the outside temperature according to which the heat loads and temperatures are calculated for the substations. Since the hot domestic water consumption is assumed to be constant, the heat loads and their duration can be estimated on the basis of the outside temperatures alone. Figure 19 shows the heat load duration curve for the system in question. It also has a curve describing the heat loads before they are assigned to the bins.

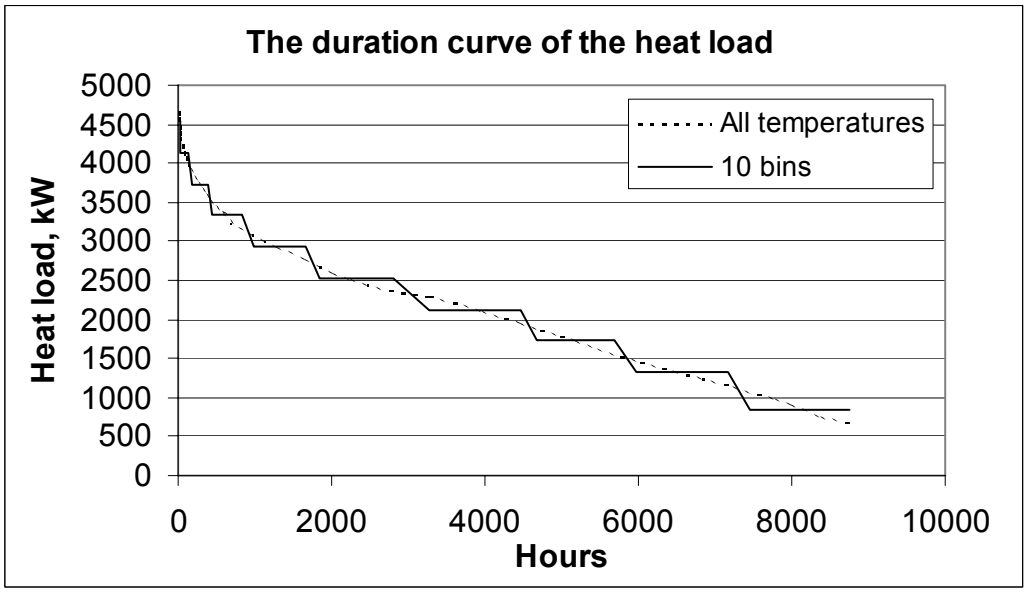

Figure 19. The duration curve for the heat load.

This estimation seems to correspond reasonably well to results derived from actual measurements (Gustafsson, 1998; Harvey et al., 2000). However, some of the peaks are naturally lost when dealing with average values.

The price of electricity has a lot of seasonal and yearly variation. Because of its large share, the status of the hydro power is the most important element in determining the price of electricity in the Nordic electricity market area. The level of the reservoirs, the expected rainfall and the production structure of the market area largely define, what price the hydro power producer requires for the electricity produced. The outside temperature has an effect on the demand and therefore on the price, but it is not the most important factor in determining the price. For our study, the use of averages should give a relatively good approximation.

Seasonal averages are calculated based on the data from the Nordpool from the beginning of 1996 to the beginning of April in 2003. Each season consists of three months, winter starting with December. The average prices for these seasons are 27.18 €/MWh during winter, 19.21 €/MWh during spring, 16.92 €/MWh during summer and 21.67 €/MWh during autumn.

The weather data from (Gustafsson, 1998) is used to connect an electricity price to an outside temperature. If $C_{Tout,el}$ is the electricity price for outside temperature T_{out}, C_{season} the average price of electricity for a particular season and $p_{Tout,season}$ is the share of observations of this temperature in a season, the electricity price for outside temperature T_{out} is

$$C_{Tout,el} = \sum_{season} p_{Tout,season} \cdot C_{season} \quad (38).$$

The electricity prices for the bins are calculated according to Eq. (39), which takes also into account the different probabilities of different outside temperatures within the bin *i*:

$$C_{el,i} = \frac{\sum_{Tout} p_{Tout} \cdot C_{Tout,el}}{\sum_{Tout} p_{Tout}} \quad (39).$$

In Eq. (39) T_{out} includes the outside temperatures of bin *i*. The limits for bins are shown in Table 6. Figure 20 shows the dependance between the outside temperature and the calculated electricity prices.

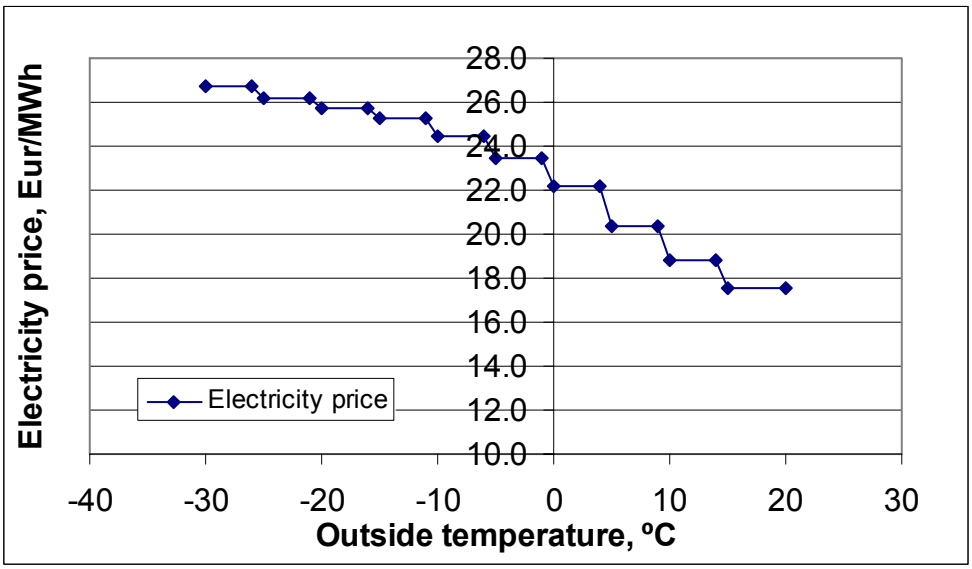

Figure 20. The relation between outside temperature and the price of electricity.

The income or costs from the emerging emissions trading are not included in the model. The reason for this is, that many of the small district heating networks are too small to have quotas and plant specific restrictions for their production facilities. The price of oil does include tax, which is partly based on CO_2 emissions. The emission trading is also likely to increase the price of electricity. Due to the uncertainities connected to the future market price of electricity, a sensitivity analysis is carried out.

The objective function being minimised, is

$$C_{tot} = \frac{C_{inv} + \sum_i f_i \cdot C_{o,i}}{\sum_i f_i \cdot Q_{i,demand}} \quad (40).$$

C_{tot} is the total cost in €/MWh, f_i is the frequency (see Table 6) and $Q_{i,demand}$ the heat demand for bin i. C_{inv} is the investment cost and $C_{o,i}$ the operational cost, both in €/h. Investment costs and operational costs are determined according to Eqs. (41, 42):

$$C_{inv} = \frac{Ann \cdot \sum_{plant} Q_{plant,inv} \cdot c_{plant,inv}}{8760} \tag{41}.$$

Ann is the annuity factor, calculated for discount rate 5% and operation time of 20 years. $c_{plant,inv}$ is the specific investment cost in €/kW. For a CHP plant, $Q_{plant,inv}$ refers to the maximum electricity output and the original values for $c_{plant,inv}$ are taken from Table 1. The specific investment cost is 133 €/kW_{heat} for an oil boiler and 200 €/kW_{heat} for a biofuel boiler (Helynen et al., 2002; Elomatic Oy, 2002).

$$C_{o,i} = \frac{C_{oil} \cdot Q_{oil,i}}{\eta_{oil}} + C_{bio} \cdot \left(\frac{Q_{bio,i}}{\eta_{bio}} + Q_{f,i} \right) - C_{el,i} \cdot \left(P_i - P_{pump,i} \right) \tag{42}$$

The first term refers to the production of the oil fired boiler. The efficiencies of both heat-only boilers are 0.9 and they are considered not to be affected by changes in load or other parameters. The second term refers to production, where biofuel is used, either in a heat-only boiler or in a CHP plant. The fuel consumption of the CHP plant is presented in Eq. (6). Last term concerns the production, consumption and sale of electricity. Electricity price is predetermined according to Eq. (39), power production follows from Eq. (7) and pumping power from Eq. (18). The prices for fuels are 10 €/MWh for biofuel and 20 €/MWh for oil. (Turunen, 2003.)

3.3 The result of the optimisation

In the first case studied, an old oil boiler is assumed to be still available. Biofuel-fired boiler is not among the options. Therefore the options are either to produce heat using the old oil boiler or to invest in a CHP plant. The second case assumes that no old plant is available. In this case it is also possible to invest in a biofuel-fired boiler. GAMS/conopt is used to formulate and solve the problem.

In both cases the investment costs are varied to give an idea on how the situation would change, if investment costs were higher. This would be the case, if the plants studied were built as smaller versions of the actual plants. A sensitivity analysis is done for the electricity prices. All three plants are studied separately.

3.3.1 Results for the case with an old oil-fired boiler available

The results of the optimisation of the first case are presented in Table 7. Original investment costs and electricity prices were used. Different starting levels were tried for the variables to make it more likely, that the global optimum is found instead of a local one.

Table 7. Results for the case with an old boiler and a CHP-plant.

Plant	A	B	C
Total production costs, €/MWh	17.358	14.348	14.400
Total fixed costs, €/MWh	6.644	6.921	6.778
Total variable costs, €/MWh	10.714	7.427	7.622
Invested heat production for CHP, kW	2169	2570	2277
Invested power output, kW	361	977	1002
Plant peak production time	6958	6297	6757
Share of energy produced	89.3%	95.8%	91.0%
Share of peak load	47.8%	56.7%	50.2%

An investment is made with all three plants. The oil-fired boiler has a variable cost of 22 €/MWh, but it still covers almost 50% of the peak load with all three plants. Plant B is able to produce the heat with the lowest average cost. Plant B suffers from the high specific investment cost and has therefore circa 20% higher average production costs than the other two plants. It has to be taken into account, that the size of the original plants has an impact on their investment costs and some performance related characteristics (e.g. power to heat ratio).

As with earlier studies (Zhao et al., 1998), also here it turns out, that the costs from heat losses and pumping are low compared to the costs resulting from energy production and the investment. Since the specific investment cost (€/kW_{el}) for a plant is not taken as size-dependent and the original specific investment costs are used, the result for plant A can not be directly compared to the results for plant B and C. Size-dependent investment costs are not used, because there is too little data on small biofuel-fired CHP plants to form a description for specific investment costs, that would not only take the

size of the plant as such into account, but would also consider the combined effect of power to heat ratios and size. Figure 21 shows the optimal temperature levels of the district heating water as a function of the outside temperature.

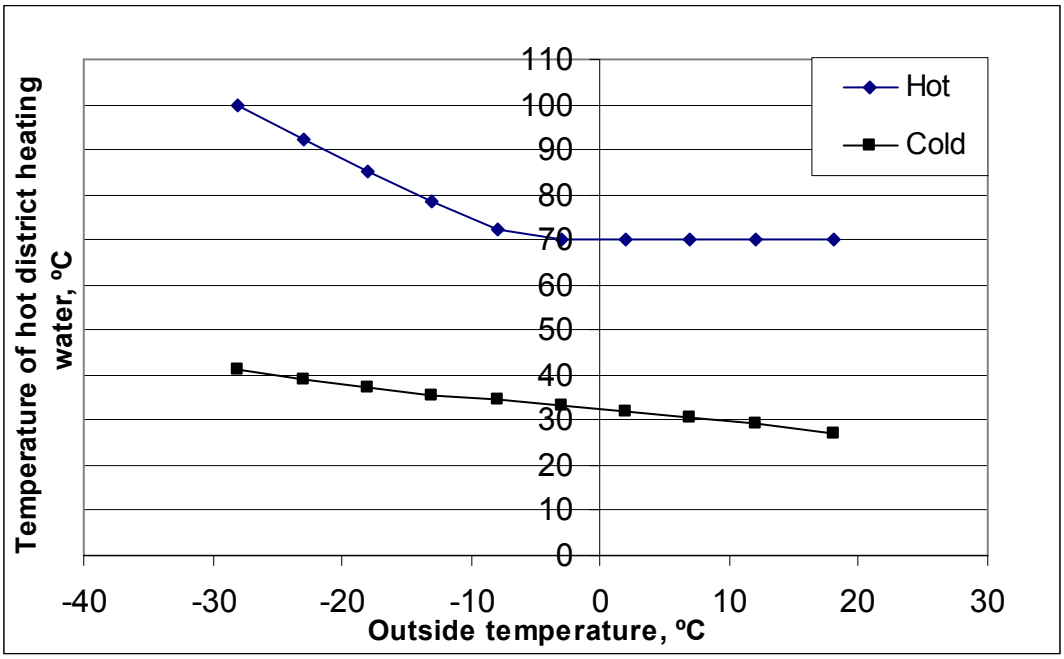

Figure 21. The optimal temperature levels of the district heating water.

The temperatures shown in Figure 21 correspond to the lowest temperatures allowed. It turns out, that the same result is achieved with all further cases. This result is somewhat expected and similar results have been reported before (Zhao et al., 1998).

To compare the technical characteristics of the three plants, these plants should have approximately similar specific investment costs. This is not the case for plant A, because it is clearly smaller than the other two plants. To compare the performance of these three plants, same specific investment cost is used for all three plants. A raised specific investment cost for plants B and C also describes a situation, where these plants are built as smaller versions of what the original plants were.

When similar specific investment cost is used for all plants, plant A benefits and is clearly the cheapest option. This is not suprising, since the specific investment cost is attached to the maximum electricity output and since plant A has a low power to heat ratio, it can produce an equal amount of electricity and much more heat with the same investment cost. If the specific investment cost is lowered to 3000 €/kW_{el}, plant A is affected by the minimum load restriction and the fact that it can not be shut down. If the specific investment cost is 4000 €/kW_{el} or more, no investment is made on plant C. The same applies to plant B, when the specific investment cost reaches 4500 €/kW_e. Plant A

would be built, even if the specific investment cost was as high as 5000 €/kW_{el}. Figure 22 shows how the average production costs of plants B and C change, when the specific investment cost is varied. The original specific investment cost is used as the reference value. Plant A is not included, since its original specific investment cost already reflects its small size.

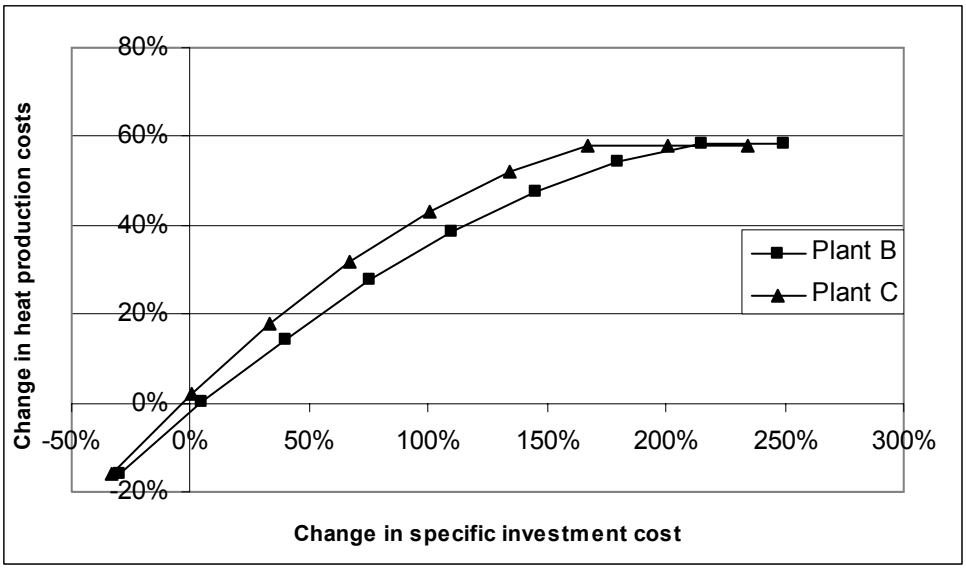

Figure 22. The relation between specific investment cost and average heat production cost.

The price of electricity is important for the viability of the CHP plants. The prices used here are derived from the data of the past few years. However, this does not tell us, whether these prices describe the future as well. Therefore, a sensitivity analysis should be performed.

If the original investment costs are used, but the price of electricity is changed, plant A remains the most expensive option. However, plant C is able to produce electricity slightly more than plant B and therefore a uniform price increase of 2 €/MWh_{el} is enough to make it the best option. If the same average price increase is distributed differently and instead of a uniform absolute price increase, a uniform relative increase is used, all plants perform better. This is because in absolute numbers the increases are higher during winter, when the heat demand, and therefore the load of the plant, are also the highest. The plants with a high power to heat ratio benefit the most. Figure 23 shows the relation between changes in average electricity price and average heat production costs. A uniform price increase is used and the original weighted average price of electricity is 20.95 €/MWh_{el}. No price reductions were considered, since in the long run such changes can not be considered very likely. This is especially true, when the effects of the pending emissions trading are considered.

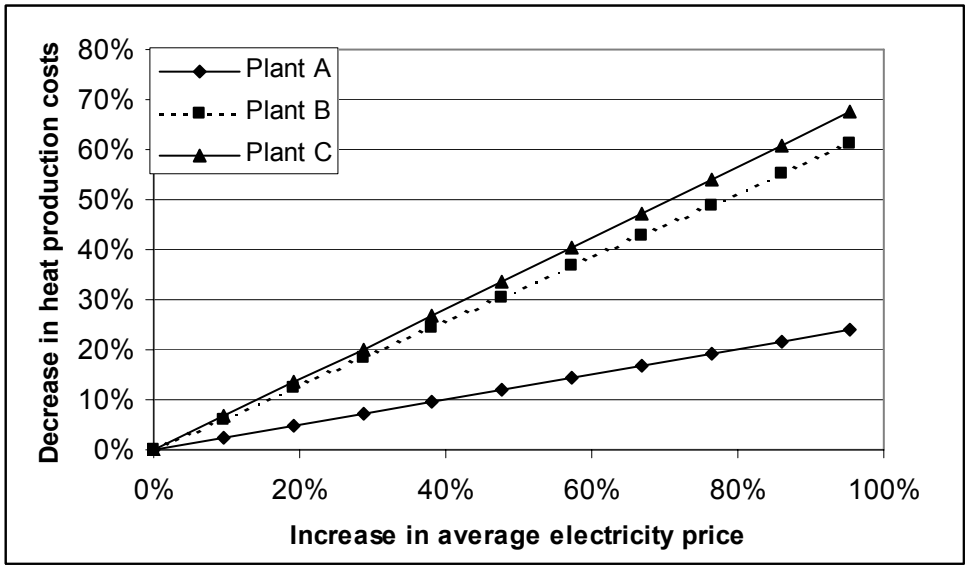

Figure 23. Relation between changes in average electricity price and average heat production costs.

If an equal specific investment cost is used, plant A is again the cheapest option. However, the larger the increase in electricity price, the narrower the gap between the production costs of the plants.

3.3.2 Results for the case with an investment in boilers required

The results for the first case do not yet tell, how much of the benefit of not relying only on the oil-fired burner can be attributed to the cheaper fuel and how much to the possibility to produce electricity. This is studied next by introducing the option to invest in a biofuel-fired heat boiler. In addition to this, it is also assumed, that the old oil-fired boiler has to be removed. A new oil-fired boiler is among the investment options. The investment costs for the boilers are 133 €/kW_{heat} for the oil-fired boiler and 200 €/kW_{heat} for the boiler using biofuel. Table 8 has the results for a case, where original investment costs and electricity prices are used.

Table 8. Results for the case where investments in boilers are required.

Plant	Plant A	Plant B	Plant C
Total costs of heat production, €/MWh	15.425	14.911	14.840
Total fixed costs of heat production, €/MWh	3.963	6.770	6.952
Total variable costs of heat production, €/MWh	11.462	8.141	7.888
Heat production capacity of the CHP-plant, kW	0	1607	1472
Heat production capacity of the oil-fired boiler, kW	1217	1217	1217
Heat production capacity of the boiler using biofuel, kW	3377	1770	1905
Invested power output, kW	0	611	648
CHP-plants peak production time, h	0	7734	7929
Share of heat produced with the CHP plant	0%	73.6%	69.1%
CHP-plants share of the peak load	0%	35.5%	32.5%

The results in Table 8 differ from those in Table 7 significantly. The CHP plants cover less of the peak load with plants B and C and no investment is made in plant A. Plant C is now the most economic option instead of plant B. The biofuel-fired boiler is the largest unit no matter which CHP plant is considered. Oil-fired boiler is used to cover the demand during peak load hours.

A sensitivity analysis is performed for the price of electricity. Figure 24 shows the share of the peak load delivered by the CHP plant, when the electricity price is varied. The dimensioning of the oil-fired boiler remains unchanged (about 27% of the peak load) and the remaining share is delivered by the biofuel-fired boiler.

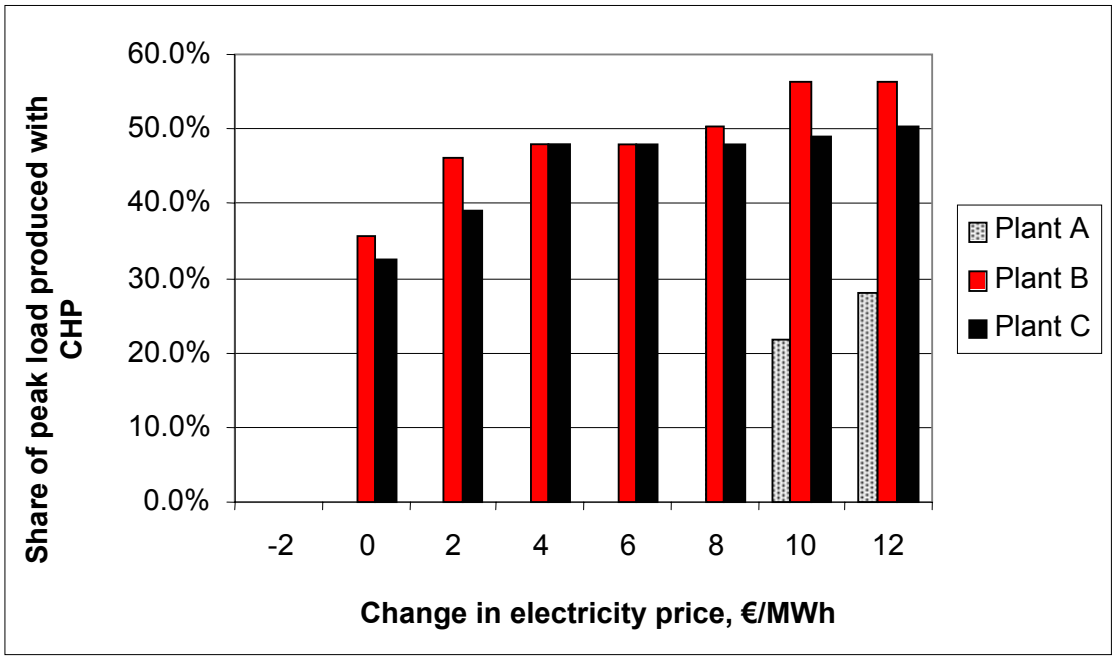

Figure 24. The effect of electricity price on dimensioning of the plants.

According to Figure 24, it seems that plant A would require a uniform electricity price increase of 10 €/MWh, before it would be part of the optimal solution. Plants B and C do get built with the original electricity prices, but a reduction of 2 €/MWh in electricity price is enough to remove them from the optimal solution. Table 9 shows the limits for investment costs and electricity prices after which the plants are not built.

Table 9. Requirements for the electricity prices or investment costs to make an investment viable.

Plant	Plant A	Plant B	Plant C
Maximum specific investment cost, €/kW$_e$	2517	1725	1664
Allowed/required change in electricity price, €/MWh	9.16	-1.75	-1.85
Allowed/required change in electricity price. Percentage change.	43.6%	-7.5%	-7.2%

”Percentage change” refers to a case, where all the prices for the bins are raised with an equal percentage instead of an equal absolute amount. As can be seen from Table 9, significant changes are needed to make plant A profitable. The specific investment costs could increase slightly for plants B and C, before no investment is made in them. It is, however, quite likely that this cost would go up more than what Table 9 allows, if these plants were to be scaled down. The investment cost might very well rise as high as with plant A, since plants B and C have more complicated technology. It should also be mentioned, that a low interest rate was used in the calculations. If the interest rate was raised to 8%, the result with each of three CHP plants would include only the two heat-only boilers.

The results here indicate, that much higher electricity prices or lower investment costs would be needed to make plants in the size range of plant A economical. Plants B and C are originally much bigger and have much lower specific investment costs. However, as Table 9 indicates, there is little room for changes in the undesirable direction and the specific investment cost would move to this direction, if these plants were to be dimensioned considerably smaller. The small margin connected to the fact, that the cashflows from the sale of electricity include a high level of uncertainity, make the situation look grimmer for these plants, too.

4. Increasing the power production of small-scale CHP steam Rankine cycle processes

4.1 Objective and focus of the work

As described in Section 2.3 there are several new biomass-fuelled CHP plants producing less than 20 MW_e in Finland and Sweden. Many of these biomass plants can be considered to represent the best current technology of small-scale CHP processes. Plants producing over 3 MW_e are based on a steam Rankine cycle with steam superheating and include a bubbling or a circulating fluidised bed boiler and a steam turbine. Grate boilers designed for biomass firing and steam engines have been used in smaller plants. Although the recently built biomass-fired CHP plants are of a high standard, there still exists a significant difference in the efficiencies of the small-scale and the large-scale CHP plants.

The objective of this sub-task is to find profitable process designs that could raise the efficiencies of the small-scale CHP plants closer to the efficiencies of the large-scale ones. Prior to constructing the optimisation model some profitable process changes that could raise the efficiencies of the small-scale CHP plants closer to the the large-scale ones needed to be selected. The process designs should be based on the current biomass-fired CHP processes.

The biomass-fired CHP plants producing less than 20 MW_e are of interest because they are often the most economical alternatives to utilise biofuels near the fuel source. Furthermore, in Finland, with a high share of CHP production, the potential to increase cogeneration is in transforming the small heating plants to CHP production. In Sweden, where there is large nuclear and hydro power production, the potential for new CHP production is in the regions with increasing district heat demand and in the regions that are planning for new district heating networks. CHP plants are often used in the industry. The industrial CHP plants are usually providing primarily steam with constant pressure to the process and generating power as a secondary product. The industrial CHP plants are heavily dependent on the steam properties needed by the industrial process. Therefore, this work concentrates mainly on the small-scale CHP plants connected to district heating networks.

The heat demands in the smaller district heating networks are often limited, so the possibilities to improve the efficiencies of the small-scale CHP plants in an economical way is either to increase their power generation, or to convert heating plants to CHP production. Currently, the power-to-heat ratio in the CHP plants producing less than 3 MW_e is 0.10–0.19. In the 3 MW_e processes the power-to-heat ratio is 0.25–0.30, and in

the CHP plants producing 5–20 MW_e it increases gradually from 0.35 to 0.45 (Wahlund et al., 2000; Salomón et al., 2002; Kirjavainen et al., 2004). In larger back-pressure CHP plants the power-to-heat ratio is 0.45 or over. In competing CHP processes, like in a gas turbine with a recovery boiler, in an internal combustion engine process with heat recovery, or in a gas turbine process with combined steam cycle the power-to-heat ratios can be 0.55, 0.75, and 0.95, respectively (Orispää, 2000). These processes use natural gas as fuel. However, in the more remote areas natural gas might not be available. The biomass is preferred also, because it is a CO_2 neutral fuel and does not increase fossil CO_2 emissions.

The first part of the research problem of this sub-task was to find process changes that could increase the power production and power-to-heat ratio of biomass-fuelled small-scale CHP plants. Second part of the reasearch problem was to construct a mixed integer nonlinear programming (MINLP) model that would be able to optimise the most profitable process change combinations for the CHP plants. The optimisation model should take into account the trade-offs between the increased power production, the investment costs, and the additional fuel costs. Also, the changes in the fossil CO_2 emissions should be calculated.

The work was carried out by selecting four CHP plants of different sizes, from Finland and Sweden to represent the best current CHP processes between 1–20 MW_e, and by implementing the possible process changes to case plants with simulation and optimisation tools. Simulation gave the possibility to define more extensive process data of the case plants on the basis of the received process values. In addition, the part load behaviour of the CHP process could be simulated. When modifying the processes with the possible changes, the simulations gave the possible process parameters and their acceptable region in the modifications. Optimisation could be used to include the trade-offs between the additional power production, the investment costs, and the additional fuel costs resulting from the changes. It was also possible to study the effect of the price of electricity on the selected process changes with optimisation. Furthermore, changing from case to case was more flexible in an optimisation model than in simulations.

The research tasks of this work were

(i) mapping and collecting data of the existing small-scale CHP plants in Finland and Sweden

(ii) selecting good CHP case plants representing different sizes between 1 and 20 MW_e

(iii) constructing simulation models of the case plants and analysing the sensitivities of the models

(iv) simulating the power production of the case plants in part load (off-design) operation

(v) mapping the possible process changes that could increase the power production and the power-to-heat ratio in small-scale CHP plants

(vi) simulating the changes by applying them to the case plant models

(vii) analysing the effects of the process changes on production, costs, and fossil CO_2 emissions of the case plants

(viii) using optimisation tools to show the trade-offs between the increased power production and the costs due to the process changes, and to calculate the most profitable changes; in addition, evaluating the saved fossil CO_2 emissions

(ix) constructing a generalised optimisation model suitable for the process design optimisation of 1–20 MW_e CHP plants based on steam Rankine cycle with steam superheating. The sizes of the CHP plants are not limited by the formulation of the model but by the selected process changes, most of which often already exist in larger CHP plants.

The work done in this sub-task is presented more detailed in Savola and Keppo (2005) and in Savola and Fogelholm (2005a and 2005b). As a part of this work a mixed integer nonlinear programming (MINLP) model for the process change optimisation in small-scale CHP plants was constructed. The formulation of the mathematical model was partly based on the rigorous MINLP model for optimal synthesis and operation of the utility plants presented by Bruno et al. (1999). Special for the model developed in the current work is that its superstructure is based on a typical process design used in 1–20 MW_e biomass-fuelled CHP plants, and that it includes alternatives for process design changes relevant to these plants. Examples of the alternatives not used in previous models are the selection of a single- or two-stage district heat exchanger and the integration of the exhaust gas from a gas engine or a gas turbine as combustion air in the biomass boiler. Furthermore, the cost functions and cost coefficients have been modified to correspond to the situation in these smaller plants. For example, the cost functions of gas engines and gas turbines are here specifically developed for small sizes. Therefore, unlike the other corresponding models, this model includes the designs and regression coefficients specifically suitable for small-scale CHP plants.

4.2 Possibilities to improve the power production in small-scale CHP plants

4.2.1 Temperature and pressure of superheated steam

Important factors defining the power generation in Rankine cycles with steam superheating are the temperature and pressure of the superheated steam. Their current levels are mostly defined by the material limitations of the turbine. For example, the

maximum temperature in high and medium pressure stages of the turbine is 600 °C if high alloy steels are used and 550 °C if low allow steels are used. In low pressure parts of the turbine the non-alloy steels with maximum temperatures of 350 °C are often used. A review by Fridh (2001) on the admission temperatures and pressures of 600 steam turbines producing from 1 to 25 MW_e noted that the admission temperatures to small-scale steam turbines are generally below 520–540 °C, which is 40–60 °C lower than the usual temperatures in large-scale plants. The economical feasibility of small-scale plants with higher steam temperatures depends on the possibilities to reduce the use of the more expensive materials in high temperature applications and on the successful scaling of these results from large-scale plants to smaller sizes.

T,s -diagrams of the temperature increase at constant pressure and of the simultaneous temperature and pressure increases are presented in Figure 25. The different points marked in the figure are discussed in Section 2.1.1. If only the temperature of the superheated steam is increased, the steam moisture content after the turbine decreases and the steam after the turbine may become even slightly superheated. If both the pressure and the temperature of the superheated steam are increased, the steam moisture content after the turbine increases. In back-pressure CHP processes, where the forward temperature of the DH water defines the pressure after the turbine, there may be potential for the steam moisture content to increase before the limitations of the turbine materials are met.

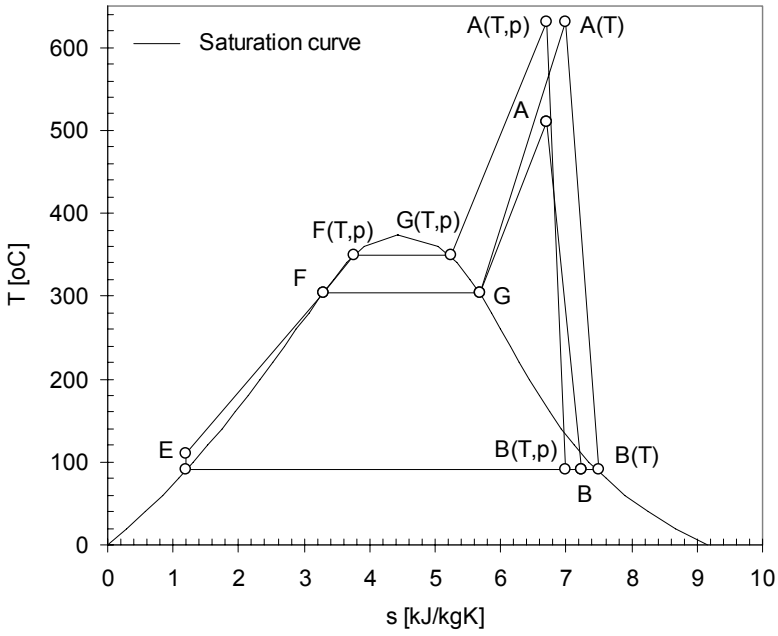

Figure 25. T,s -diagram comparison of the superheated steam temperature increase in constant pressure (A(T)) and of the simultaneous temperature and pressure increase (A(T,p), F(T,p), G(T,p)).

4.2.2 Steam reheating

Another possibility to increase the power production is to extract the superheated steam from the steam turbine and to reheat it with flue gases to a higher temperature. In the case of a condensing plant, turbine materials limit the steam moisture content and thus the steam exit pressure from the turbine. Reheating makes it possible to have a lower exit pressure than without reheating. In CHP plants with back-pressure turbines the steam exit pressure from the turbine is defined by the forward temperature of the DH water. In the back-pressure turbine processes reheating improves power production, if the extraction pressure of the reheated steam is selected so that the reheating increases the average temperature of the incoming heat to the process. All the heat that is transferred to the process in reheating (A2–A1 in Figure 26) can be used for power generation in a steam turbine. Usually the extraction pressure of the reheated steam is selected so that the steam can be reheated to the same temperature it had before entering the turbine. This makes it possible to use the same material both in a superheater and in a reheater. Reheating is common in larger power plants but in smaller plants it has not been used as its economical feasibility has been considered to be low.

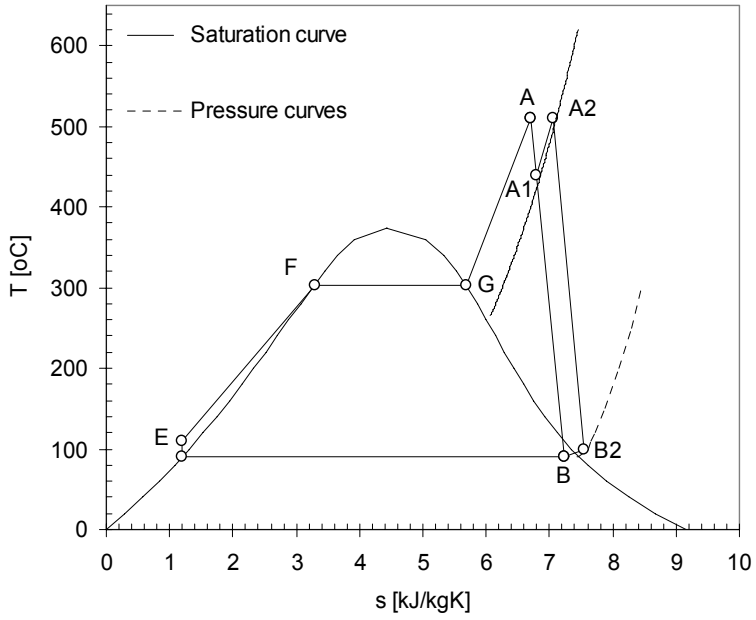

Figure 26. T,s -diagram of the steam reheater (A2) addition.

4.2.3 Feed water preheater

The efficiency of a power plant can be improved also by increasing the temperature of the feed water before the economiser. The temperature can be increased by extracting steam from the turbine before and after the feed water tank extraction and using this steam to preheat the feed water. A T,s -diagram of the feed water preheating is presented in Figure 27.

4.2.4 Two-stage DH exchanger

One possibility to increase the power generation of a back-pressure steam turbine is to reduce the steam exit pressure by dividing the DH exchanger into two or more stages, and by extracting the steam from the turbine to DH exchangers in several phases. The exit pressure of the saturated steam from the turbine is then defined by the DH water temperature after the additional stage of the DH exchanger, which may be significantly lower than the forward temperature as shown in Figure 28. The increase of power generation resulting from the two-stage DH exchanger compared to a single-stage corresponds to the difference between T_b and T_a. The two-stage DH exchangers have already been used in the CHP plants producing from 15 to 20 MW_e, but their economical feasibility in smaller plant sizes has not yet been demonstrated.

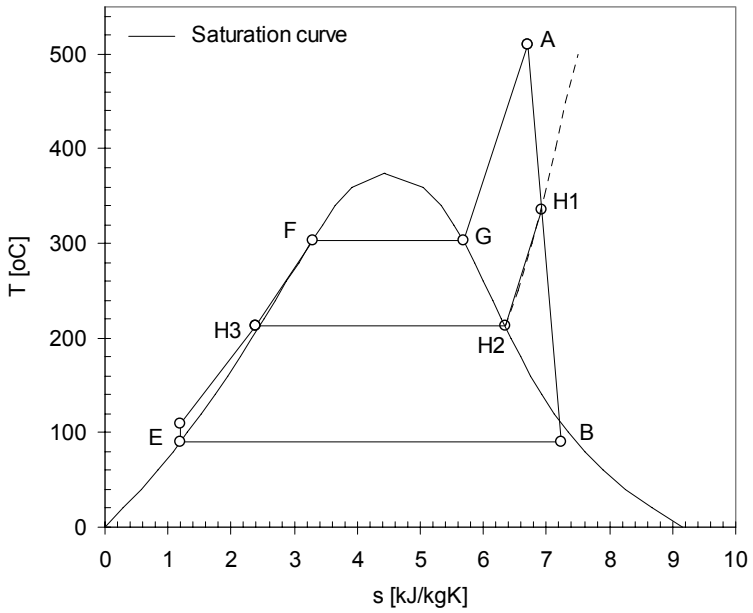

Figure 27. T,s -diagram of a feed water preheater (H1–3) addition.

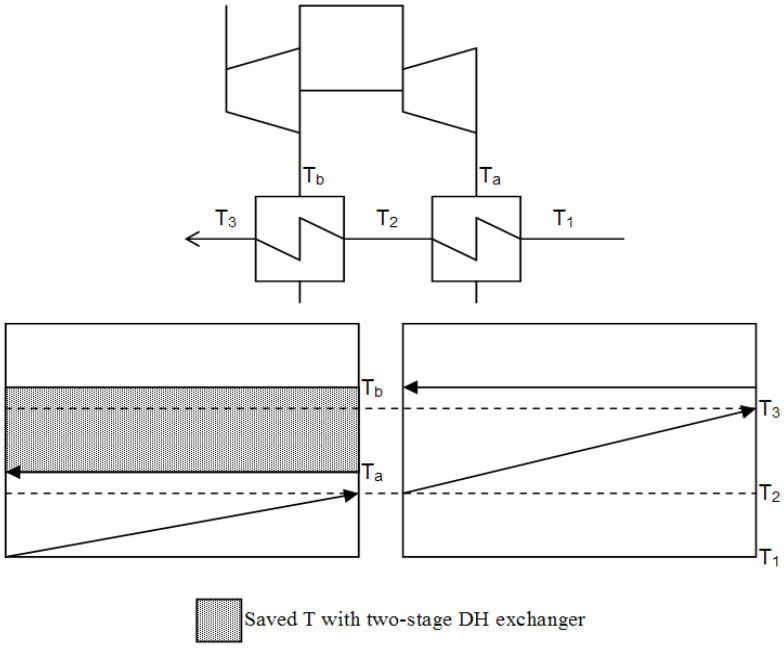

Figure 28. Saved temperature T_b–T_a in two-stage DH exchanger.

4.2.5 Fuel drying

The moisture content of the biofuels can be up to 55 weight-%, so fuel drying with flue gases or steam has a good potential to increase the power production of a biomass-fired CHP plant. An overview of the current fuel drying technologies is presented by Wimmerstedt (1999) and Brammer et al. (1999). In the case of a power plant situated near large biofuel resources it may be also profitable to dry the fuel for transportation to the more remote plants. Wahlund et al. (2002) describe a system configuration for a CHP plant, where a fuel dryer producing wood pellets is utilising steam during the low heat demand and thus increasing the annual power production of the plant.

4.2.6 Gas turbine or gas engine

A gas turbine and a gas engine integration to the CHP plant is an efficient way to increase the electricity generation and the power-to-heat ratio of the plant. In larger CHP plants, a gas turbine is often connected directly to a heat recovery boiler, but the turbine can also be integrated to a solid fuel fired boiler by using the exhaust gas from the gas turbine in a feed water preheater, or using the gas turbine exhaust gas as combustion air in the boiler. Manninen and Zhu (1999) have presented a method for finding the optimal integration of a gas turbine to the utility. Harvey et al. (2000) have studied gas turbine CHP plant performance including part loads and its effects on district heating costs and CO_2 emissions. Carcassi and Colitto Cormacchione (2001)

presented a comparison of the gas turbine part load performances in the heat recovery boiler CHP application. In smaller plants especially the investment costs of a gas turbine or a gas engine integration may become critical, as the investment per generated power increases when the size of the turbine of engine decreases.

4.3 Simulation of the small-scale CHP process improvements

4.3.1 Simulation method

A steady state simulation program Prosim produced by Endat Oy was used as a simulation tool in this work. A steady state simulation program was sufficient for this study because although the CHP processes needed to be simulated also in part loads, no detailed time dependent behaviour of the process was required. Some backgroud information on simulation methods and their implementation to CHP plants is summarised in Savola (2005). The simulations are described more detailed in Savola and Keppo (2005).

The process flowsheets in the used simulation program are constructed from modules and streams. The modules can be chosen from a module library, which contains most of the typical power plant equipment (e.g. burners, boilers, turbines, and heat exchangers). Stream analyses (e.g. fuel analysis) are available from an analysis library. After the process model is constructed and the relevant parameters for the modelling case are inserted, the design simulation of the process model can be run. In a design simulation the energy and mass balances of the process modules are calculated. In addition, the physical properties of the plant equipment modules are calculated according to the given data. For each module the program uses an iterative Newton-Raphson method for the balance calculations, which are performed in the order of the user defined numbering of the modules. After the design model of the process has been created the properties of the modules can be fixed for off-design calculations. In off-design mode the properties of the process modules are defined according to the calculated design case and only the stream values (e.g. fuel input) in the process can be changed.

4.3.2 Design and off-design simulation models of the case plants

Four existing CHP plants producing 1.8 MW, 6 MW, 11 MW, and 14.7 MW electricity were selected to present the state-of-the-art steam Rankine processes with steam superheating in the CHP production from biomass. Some basic data of these processes at full load design conditions is presented in Table 10. All of the selected plants were quite new and three of them had started their operation in the year 2002, when also the process data of these CHP plants was collected.

The simulation models were constructed following the basic properties of the simulation program described in Section 4.3.1. The fuel used in the processes was wood, the lower heating value of which was 6.24 MJ/kg. The excess combustion air factor, λ, was 1.1 and the temperature of the combustion air after the air preheater was adjusted in design case to be between 200 °C and 300 °C. In the processes with bubbling fluidized bed the evaporator and the superheater were considered to be placed parallel to each other in the fluidised bed. This means that the bed temperature (850–870 °C) indicated the flue gas exit temperature from both the evaporator and the superheater. Therefore the bed temperature defined the steam mass flow in the fluidised bed design cases, if the fuel input and thus the flue gas flow remained constant. In the grate boiler case a radiant furnace model with an evaporator was used and the flue gas exit temperature from the radiant furnace defined the steam flow in design case with the constant fuel flow.

The operation of a CHP plant depends usually on the district or process heat demand. The minimum load of a general biofuelled steam turbine CHP system is in previous studies mentioned to be 30% of the full load (Marbe et al., 2004). The part load operation of the modelled CHP plants was here simulated by changing the fuel mass flow into the fluidised bed or grate boiler in the off-design mode. The minimum heat load used in off-design simulations depended on the plant size and was 35% for the larger 11 MW_e and 14.7 MW_e plants and 45% for the smaller 1.8 MW_e and 6 MW_e plants.

Table 10. Basic data of the modelled CHP processes at full load conditions.

Process	MW_e	1.8	6	11	14.7
Boiler type		grate	BFB	BFB	BFB
Wood fuel input	MW	11.5	26	42	48
Temperature after boiler / in bed	°C	650	850	870	850
Steam values	°C/bar kg/s	355/16.5 3.8	510/60 7.9	510/92 13.8	515/93 16.1
Condenser pressure	bar	0.68	0.68	0.68	0.68 /0.37
District heat in/out temperature	°C	55/85	55/85	55/85	55/70/85
Feed water tank temperature	°C	105	120	160	158
Flue gas exit temperature	°C	174	176	172	174
Net electricity production	MW_e	1.8	6.2	11	13.6
District heat production	MW	8.3	16.5	25.8	28.4
Electrical efficiency (η_e)		0.16	0.24	0.26	0.28
Power-to-heat ratio (α)		0.22	0.38	0.43	0.48
Total efficiency (η_{tot})		0.88	0.87	0.88	0.88

A steam turbine was modelled as several turbine modules each corresponding to a group of one to five turbine stages (i.e. the expansion between two steam extractions). A similar decomposition principle of steam turbines for modelling purposes has been presented by Chou and Shih (1987). The forward temperature of the DH water defines the back-pressures in the steam turbine both at full and at part loads. The pressures of the other turbine stages are defined by the turbine constant, which can be derived from the cone rule presented e.g. in Traupel (2001), and is calculated from the data given in the design point. To keep the pressure of the superheated steam constant also at the partial steam loads, the first turbine stage is a regulating stage, which adjusts the steam flow so that the required constant pressure in the boiler is obtained. The friction losses in blading and the relative efficiency changes of the regulation valves adjusting the steam flow decrease the efficiency of the regulation stage at part loads. The efficiency of the regulation stage is typically designed to be at its maximum at partial steam load (90% load).

Here the part load performance of the regulation stage is defined in the turbine module as user defined second order polynomial functions, which are calculated for each CHP plant case separately. The functions are based on the estimation that the maximum efficiency of the regulation stage, 0.80, is gained at around 90% steam load. At full steam load the efficiency is 0.75 and as the steam load decreases towards 10% the efficiency goes to zero. This estimation, where the maximum efficiency of the regulation stage is gained at part load, corresponds to the usual conditions in a CHP plant. With these estimations the efficiency of the regulation stage starts to decrease rapidly, when the steam load is less than 80–70%.

The efficiencies, η_{ts}, of the working turbine stages are calculated by Prosim using Eq. (43), which is based on the turbine design specifications from the late 1990's:

$$\eta_{ts} = 0.023521 \cdot \ln(\upsilon) + 0.749538 \tag{43}.$$

The average volume flow, υ, is calculated as

$$\upsilon = \frac{m \cdot \Delta h_s}{p_{in} - p_{out}} \tag{44}$$

where m is the mass flow of the steam, Δh_s is the isentropic enthalpy change and p is the pressure.

When the mass flow of steam decreases during the part load operation, the inlet pressure of the turbine stage decreases accordingly. Thus the average volume flow and therefore the isentropic efficiency of the turbine stage are not affected by the load changes. Overall, the part load operation affects the efficiency of the whole turbine system by changing the efficiency of the regulation stage and the exhaust losses at the turbine exit.

The exhaust losses of the last turbine stage were calculated according to the reference data of exhaust loss versus relative volumetric flow. A detailed description of the models, their sensitivity analysis, and the off-design simulations of the CHP plant models are presented in Savola and Keppo (2005).

4.3.3 Process improvement simulations of the case plants

The simulation models of the base case CHP plants were modified according to the selected process changes. The process changes were divided to those using only biomass fuels and to those including the gas turbine or gas engine and requiring the use of natural gas as additional fuel. The process improvement simulations are described more detailed in Savola and Fogelholm (2005a).

4.3.3.1 Process changes using the biomass fuels

The process changes of the CHP plants considered here were higher superheated steam temperature and pressure before the turbine (the current maximum of 540 ^{o}C / 92 bar and a long-term goal of 600 ^{o}C / 170 bars), steam reheating and feed water preheating, and the division of the DH exchanger into two stages. For the smallest plant, producing 1.8 MW_e no simulations of superheated steam temperature and pressure increase were conducted as they would have required substantial changes to the process.

The power and heat productions of the process were simulated using the same wood fuel input flow as in the models without the changes. The part load behaviour of the changed processes was simulated by varying the fuel flow in the off-design models from 100% to 45% in 1.8 MW_e and 6 MW_e processes and from 100% to 35% in 11 MW_e and 14.7 MW_e processes.

The off-design simulation results for the base cases and the process changes without natural gas usage in different CHP plant cases are presented in Figures 29–32. Also the power-to-heat ratio, α, and the electrical efficiency, η_e, for the changes at full load are presented in the figures. For the 1.8 MW_e process the power production increase after the addition of a reheater and a two-stage DH exchanger were close to each other. For the 6 MW_e and 11 MW_e plants the superheated steam temperature and pressure increase to 600 ^{o}C and 170 bars offered the highest power production. For the 14.7 MW_e process, in which the base case already included the two-stage DH exchanger, the highest power production was gained with a steam reheater and a feed water preheater.

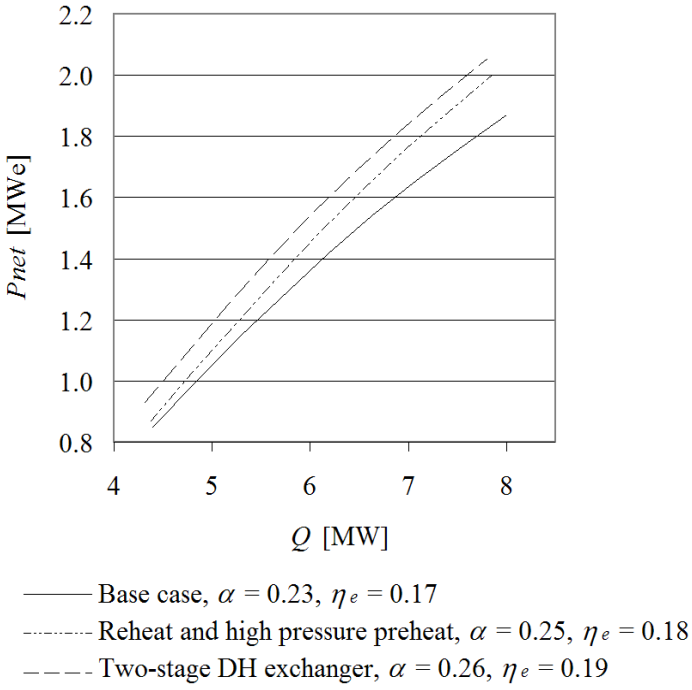

Figure 29. The power and heat production of the 1.8 MW_e case with selected changes.

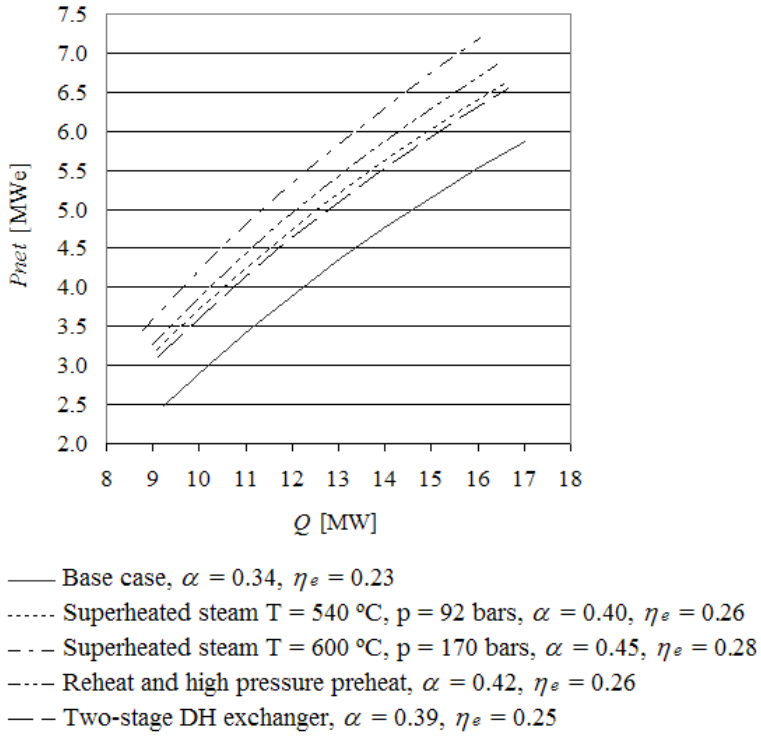

Figure 30. The power and heat production of the 6 MW_e case with selected changes.

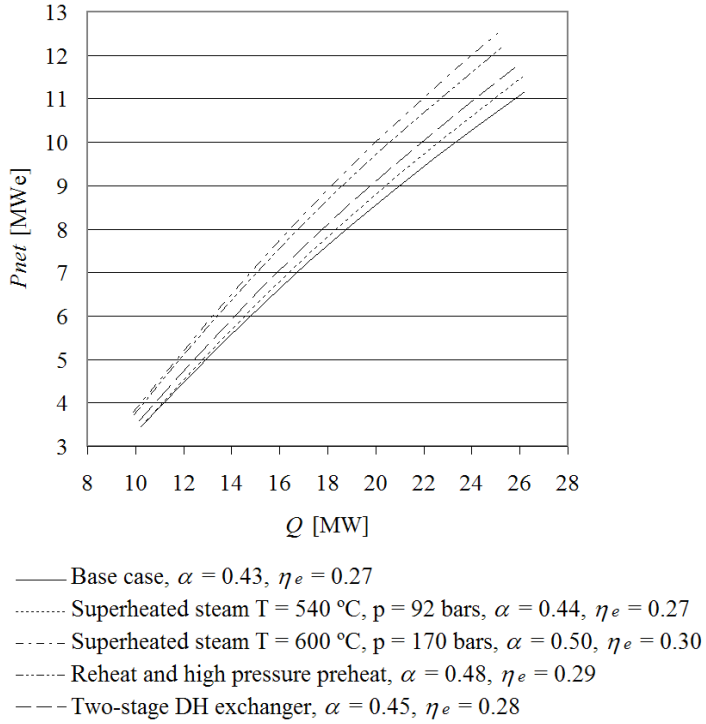

Figure 31. The power and heat production of the 11 MW_e CHP plant with selected changes.

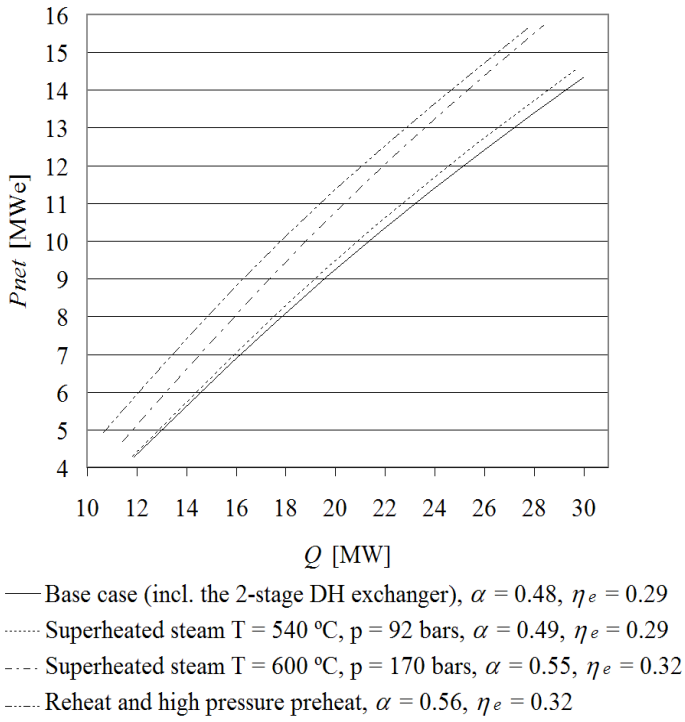

Figure 32. The power and heat production of the 14.7 MW_e CHP plant with selected changes.

4.3.3.2 Process changes using biomass fuels and natural gas

The use of natural gas to increase the power-to-heat ratio was considered by integrating a gas turbine and a gas engine to the case plants. The concept for the gas turbine or engine integration was to use the flue gas flow from the turbine or engine, containing about 15% and 12.5% oxygen, respectively, as combustion air in the biomass boiler. Furthermore, some additional combustion air was injected into the boiler to cover the total oxygen need. However, the effect of the flue gas flow increase on the size of the furnace or the fluidised bed was unknown. The gas turbine and engine sizes used in the simulations were selected so that they corresponded to 10, 25, and 50% of the power production of the base case plants. The excess heat in the flue gases of the biomass boiler after the gas turbine or engine integration was utilised in a steam reheater, in a feed water preheater, and in a fuel dryer.

In the processes, using both natural gas and biomass fuel, the input of both fuels was reduced at the same rate during the off-design simulation. Usually, the gas turbines or engines integrated into the CHP plants are operated at full load until the outdoor temperature has reached a certain limiting value, while the CHP boiler load is reduced according to the heat demand. When the limiting outdoor temperature is reached, the load in the gas turbine is reduced until the gas turbine load is at the minimum level of 50–30% (Harvey et al., 2000; Carcasci et al., 2001). The result is an increased α at part loads. In this study the goal was to simulate the design of a process that produces electricity with biomass and avoids fossil CO_2 emissions. Thus the gas turbines and engines were operated in a same way as the boiler at part loads during the lower heat demand. This means that throughout the part load operation the loads of the gas turbine or the engine and the boiler were reduced at the same rate. If the optimal operation of the CHP process would have been the goal of the optimisation, it would have been done differently.

An example case of the off-design simulation results of the addition of gas turbines and gas engines to the 6 MW_e CHP processes is presented in Figure 33. The gas turbine and engine additions to the other case plants gave similar results. In the 1.8 MW_e process the α increased up to 0.35 and the η_e up to 0.22 with gas turbine or engine integration. The ratio between biomass and natural gas ratio was 5.1 in gas engine integration and 3.4 in gas turbine integration. For the 11 MW_e process the integration of gas turbine and engine increased the α and η_e up to 0.65 and 0.33, respectively. In this case the ratio between biomass and natural gas ratio was 3.2 in gas engine integration and 2.4 in gas turbine integration. For the 14.7 MW_e process the α increased up to 0.63 and the η_e up to 0.32, with the biomass to natural gas ratio of 3.0 for gas engine and 1.9 for gas turbine integration.

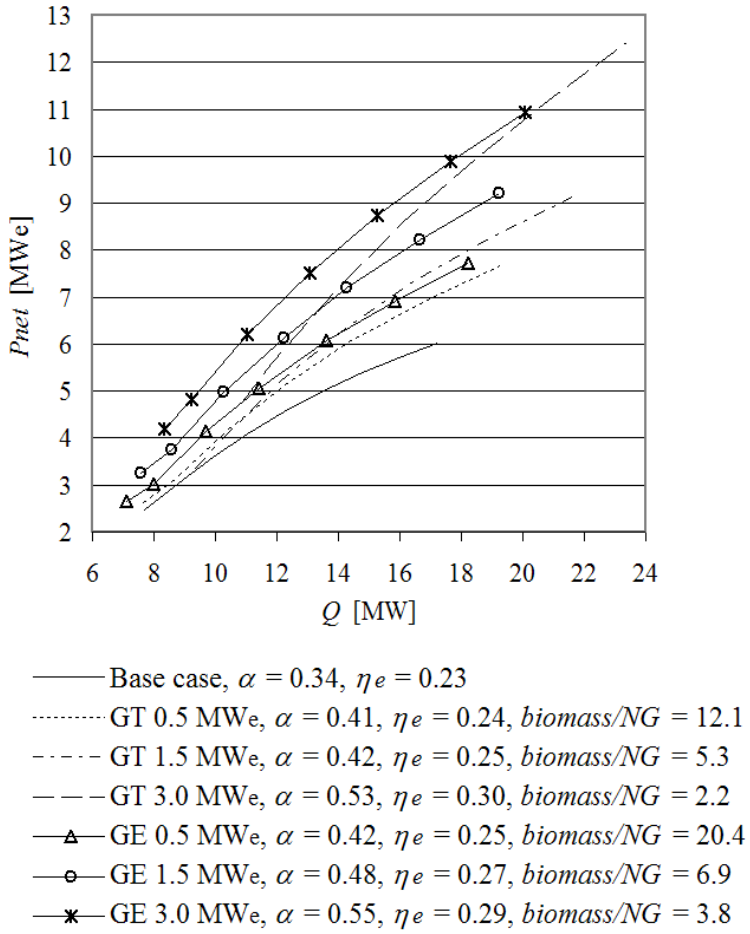

Figure 33. The power and heat production, the efficiencies, and the biomass to natural gas ratio of the 6 MW_e CHP plant with differently sized gas turbines (GT) and gas engines (GE).

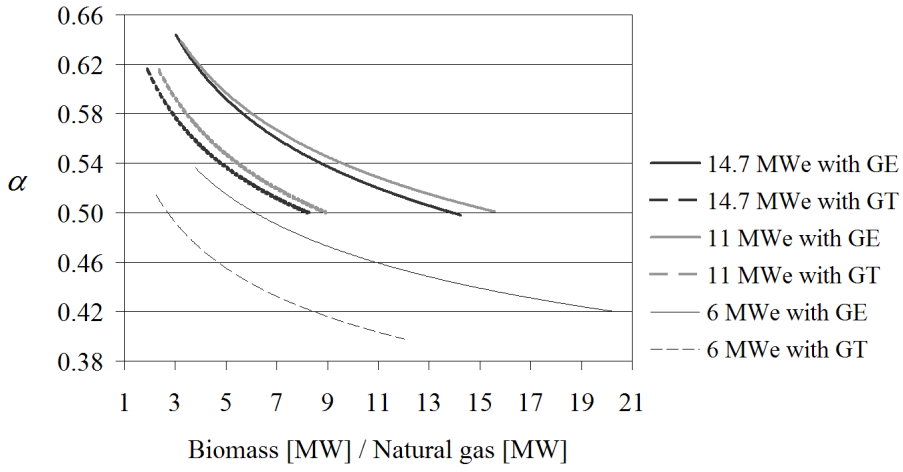

Figure 34. Effect of the biomass and natural gas ratio on the α of the CHP processes with gas engine (GE) and gas turbine (GT) integration.

At full load the α of the CHP processes with gas engines were slightly higher than in the processes with gas turbines but the η_e of the gas engine and turbine processes were almost the same. The increase in the α and in the η_e given by the integration of a gas turbine or engine depended on the size of the plant and of the gas turbine or engine selected. The α that can be gained with gas turbine or engine integration in the 6 MW_e, 11 MW_e, and 14.7 MW_e cases are presented as functions of natural gas usage in the processes in Figure 14. The lower the biomass to natural gas ratio is, the larger the integrated gas turbine or engine. The larger the gas engine or turbine integrated into the process, the more it increases the α and η_e of the whole CHP process. The curves in Figure 34 thus indicate the size of the gas turbine or engine that has to be selected for integration in order to gain a certain level of α in the process.

4.3.4 Production, cost, and CO_2 analysis

The economic feasibility of the simulated changes in the differently sized CHP processes was evaluated by analysing the improvements in the power and heat production, the income and the investment costs of the process changes, and the CO_2 emissions after the changes. The investment cost analysis was based on the best available data of the power plant equipment prices, so the analysis presents the level of the economic feasibility of the process change rather than the exact amount of the profit gained. Summaries of the profitable changes for each case process and the increases in the efficiencies are presented in Table 11. The detailed calculation principles of the investment costs and profits as well as a more extensive presentation of the results can be found in Savola and Fogelholm (2005a).

The profit in Table 11 refers to the additional profit gained with the changes compared to the base case process. So the profit is calculated by subtracting the investment costs of the changes and the cost of the natural gas, if used in the process, from the additional power production resulting from the changes. The costs of the biomass fuel can be excluded from the analysis, as the amount of biomass fuel in the processes remains the same regardless of the process changes. The changes in the income from the DH production were not included in the cost analysis. The district heat was here considered to be a less profitable product than electricity, so changing from heat production to power production was considered to be always beneficial in these cases. The electricity price used in the analysis was 30 €/MWh and the natural gas price 15 €/MWh. The interest rate used when calculating the annuity was 5% and the lifetime of the plant 15 years.

A second estimate of the profit, including the saved CO_2 emissions due to the changes, was also calculated. The CO_2 emissions were included in the analysis by calculating how much fossil CO_2 can be saved in comparison with the situation where the

additional electricity production resulting from the process changes were to be produced in a coal-fired condensing power plant with 45% electrical efficiency. In the cases where the process changes include the addition of the natural gas to the process, the fossil CO_2 emissions resulting from the use of natural gas are subtracted from the CO_2 benefits of the changes. The price used for a ton of CO_2 was 8 €.

Table 11. Profitable process changes according to the simulations.

Process change	Profit (with CO_2) [k€/a]	CO_2 saved [t/a]	Efficiencies		
			α	η_e	η_{tot}
1.8 MW_e					
Base case	0	0	0.23	0.17	0.90
Two-stage DH exchanger	19.7 (23.8)	520	0.26	0.19	0.90
Reheat and high pressure preheat	7.7 (9.6)	235	0.25	0.18	0.90
6 MW_e					
Base case	0	0	0.34	0.23	0.90
Two-stage DH exchanger	33.2 (40.2)	876	0.39	0.25	0.89
Reheat and high pressure preheat	73.7 (88.6)	1 864	0.42	0.26	0.90
GE 0.5 MW_e, reheat, preheat and fuel dryer	98.0 (137.0)	4 873	0.41	0.24	0.84
GE 1.5 MW_e reheat, preheat and fuel dryer	79.7 (140.0)	7 538	0.42	0.25	0.84
GE 3.0 MW_e reheat, preheat and fuel dryer	44.2 (129.2)	10 623	0.53	0.30	0.83
11 MW_e					
Base case	0	0	0.43	0.27	0.89
Two-stage DH exchanger	70.2 (84.5)	1 793	0.45	0.28	0.90
Reheat and high pressure preheat	134.5 (161.7)	3 394	0.48	0.29	0.90
GE 1.1 MW_e, reheat, preheat and fuel dryer	126.5 (186.7)	7 524	0.50	0.27	0.79
GE 2.75 MW_e, reheat, preheat and fuel dryer	96.0 (188.1)	11 517	0.57	0.29	0.80
GE 5.5 MW_e, reheat, preheat and fuel dryer	32.4 (174.7)	17 781	0.65	0.32	0.81
14.7 MW_e					
Base case	0	0	0.48	0.29	0.90
Reheat and high pressure preheat	201.8 (243.5)	5 210	0.56	0.32	0.88
GT 1.4 MWe, reheat, preheat and fuel dryer	270.7 (362.4)	11 582	0.50	0.28	0.83
GE 3.5 MWe reheat, preheat and fuel dryer	9.3 (97.6)	11 036	0.56	0.30	0.82

The investment costs of the increased temperature and pressure of the superheated steam depend on the used heat exchanger and turbine materials and are difficult to estimate. Therefore the profits from the higher superheated steam temperatures and pressures could not be estimated reliably enough to include them to the analysis.

Overall, it seems that both adding a reheater and a feed water preheater and adding a two-stage DH exchanger, can be profitable ways to increase the power production and the power-to-heat ratio in the 1–20 MW_e CHP plants. Additionally, the increase in the superheated steam temperature and pressure provides substantial income in all cases but the investment costs are unknown. The feasibility of the addition of a gas engine improves as the CHP plant size increases from 1.8 MW_e to 11 MW_e. For the 14.7 MWe plant the addition of a gas engine is not as feasible as in other cases, as this plant has already a high power-to-heat ratio at the base case, because of the two-stage DH exchanger. In these 1–20 MW_e CHP plants, and with the selected electricity and natural gas prices, the addition of a gas turbine seems to be economically feasible only for the largest 14.7 MW_e case. The factors that strongly affect the profitability of the addition of a gas turbine and engine are the price of the turbine or the engine, the price of the electricity, and, especially, the price of natural gas.

4.3.5 Further analysis based on calculations

The simulation results show that the addition of a steam reheater and a feed water preheater and the addition of a two-stage DH exchanger are economically feasible alternatives for all CHP plants between 1–20 MW_e. The increase of the superheated steam temperature and pressure to the high values of 600˚C and 170 bars offered, in most cases, the best opportunity to increase the power-to-heat ratio. However, it was not possible to evaluate the investment costs and thus the economic feasibility of this change. The addition of a steam reheater provided high power production but the mere addition of a two-stage DH exchanger also increased power production significantly in comparison to the base cases.

The integration of an engine to the CHP process offered profitable solutions in the 6 MW_e and 11 MW_e plants and also in the 14.7 MW_e plant if the CO_2 savings were included in the analysis. However, increases in the power-to-heat ratio and the economic feasibility are heavily dependent on the size of the integrated gas engine.

The simulations and cost analysis show that there is potential to increase the power-to-heat ratio and electrical efficiency of small-scale biomass CHP plants in an economically feasible way. However, simulation study of all the interesting process change combinations for finding the most profitable one would be very work

consuming. The optimisation tools could be used to include the trade-offs between the power production increase and the investment costs in the selection of the process changes and their combinations. Although simulation is a good tool for the preliminary studies of the process change possibilities, optimisation makes it easier to find the optimal combinations of the possible process changes and to include the economic considerations to the selection of the best process changes. The simulations showed that the changes selected for a CHP process should be chosen according to the plant size and the plant properties, which affect strongly the overall investments, profits, and CO_2 savings.

4.4 Optimisation model for increased power production in smal-scale CHP plants

4.4.1 Optimisation method

The mixed integer nonlinear programming (MINLP) method was used for finding the best process changes for the CHP processes. Integer programming was needed to have a possibility to include and exclude modules to the process. Nonlinear optimisation was required, e.g., in order to formulate the energy balances without fixing both the temperatures and pressures in the model. There were also nonconvexities in the model, which made finding the global optimum challenging with the available solvers.

The MINLP problem was solved using the General Algebraic Modeling System (GAMS) by GAMS Development Corporation and the Standard Branch and Bound (SBB) solver by ARKI Consulting & Development A/S. The NLP solver used in the SBB was CONOPT3. The SBB solver is especially suitable for problems with complex nonlinearities but fairly small combinatorial problem. In this case there were only 13 binary variables connected to the combinatorial possibilities, but the nonlinear functions in the model presented some complexities and are fairly nonconvex. Although the SBB was able to solve the problem, the global optimalities of the solutions could not be guaranteed and the solutions were sensitive to the selected starting points. The methods of process synthesis optimisation and their implementation to the CHP plant design and operation analysis are summarised in Savola (2005).

The mathematical formulation of the optimisation model is presented in Appendix A. The optimisation model and results are originally described in Savola and Fogelholm (2005b).

4.4.2 Problem statement for the optimisation model

The objective of the optimisation was to increase the power production of the small-scale biomass-fuelled CHP plant by changing the process design of the plant and to maximise the additional profit from these changes. The superstructure for the optimisation problem is presented in Figure 35. The MINLP model should find the process change combination that increases the power production of a selected CHP plant and results in the highest possible profit with the selected prices of the electricity and natural gas. The biomass fuel input to the model is fixed but it is possible to dry the biomass fuel in a fuel dryer utilising the excess heat of the flue gases. Three different gas turbines and gas engines can be integrated to the CHP process using the oxygen content of their exhaust gases, 15% and 12.5%, respectively, as combustion air in the biomass boiler. Additional combustion air can be preheated and injected to the boiler. The steam turbine construction is divided into separate stages in the superstructure as suggested by Chou and Shih (1987). Four different steam turbine configurations can be selected for the process: the base case steam turbine, a steam turbine with a steam reheater, a steam turbine with a feed water preheater, and a steam turbine with both a steam reheater and a feed water preheater. The DH exchanger used in the process can be either a single-stage or a two-stage heat exchanger.

The DH production in the CHP plant can be slightly lower after the process changes than in the base case but the total efficiency of the plant should remain close to 0.90. Primarily the process changes should increase the power-to-heat ratios and electrical efficiencies without degrading the heat production.

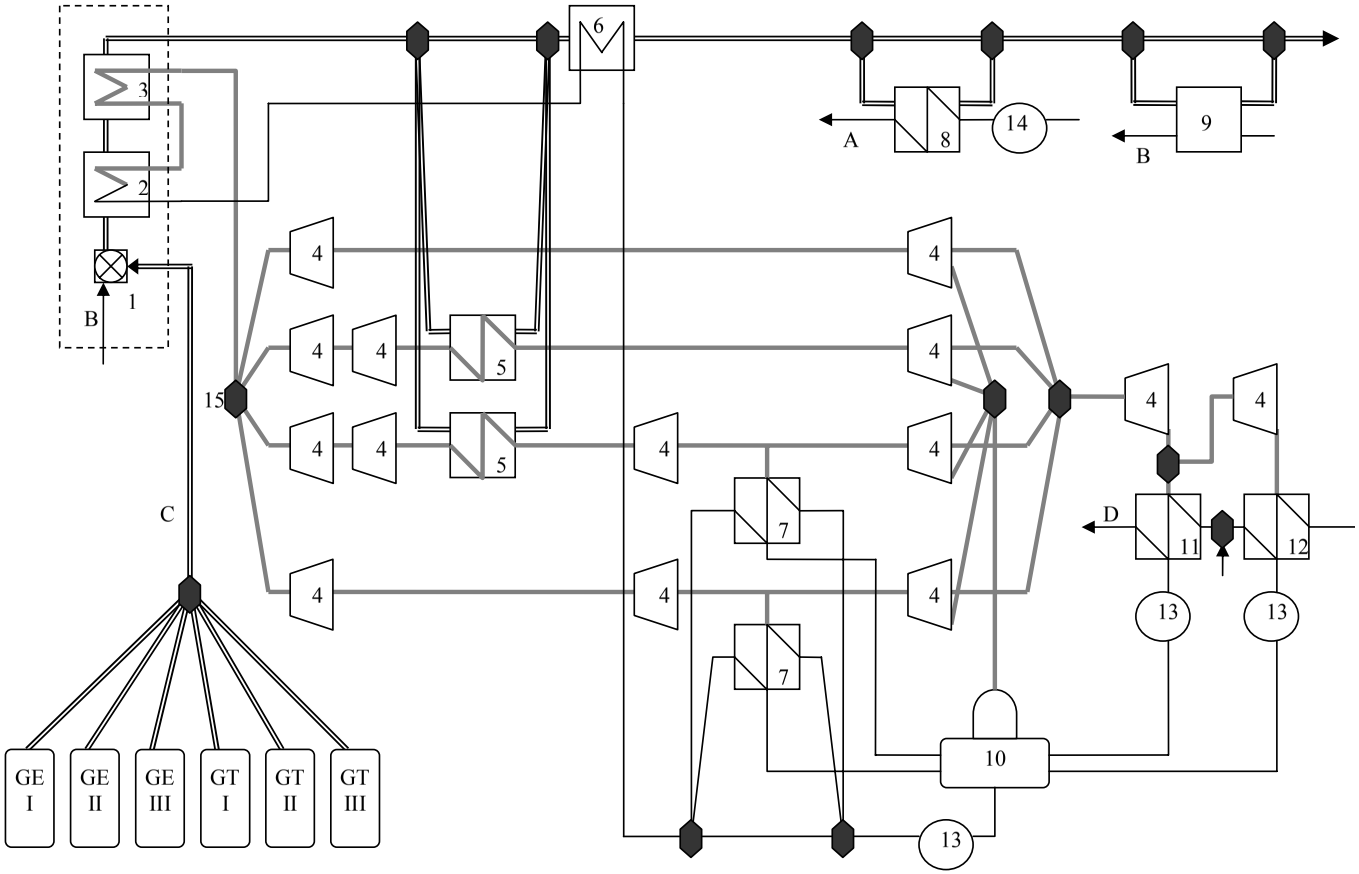

Figure 35. The superstructure of the optimisation problem. 1. Burner, 2. Evaporator, 3. Superheater, 4. Turbine stage, 5. Reheater, 6. Economiser, 7. Feed water preheater, 8. Air preheater, 9. Fuel dryer, 10. Feed water tank, 11. DH exchanger, 12. 2nd stage of DH exchanger, 13. Pump, 14. Blower, 15. Selection node, GE I-III: Gas engine alternatives, GT I-III: Gas turbine alternatives, A=Air, B=Fuel, C=Exhaust gas, D=DH water.

4.4.3 Results from the case plant optimisations

The MINLP model was used to optimise the configuration of four existing CHP plants producing 1.8 MW_e, 6 MW_e, 11 MW_e, and 14.7 MW_e. The goal for the optimisations was to increase the power-to-heat ratios and the electrical efficiencies of the processes in the most profitable way.

The size of the CHP plant was defined in the optimisation model by giving the biomass input flow to the boiler and the maximum temperature of the superheated steam. In addition, the net power production of the base case process was given, so that the changes in the process can be compared to that. It was also possible to change the sizes of the integrated gas turbines and engines by defining their natural gas and air input flow, exhaust gas temperature, and the electrical efficiency. Some general parameters used in the model and the case related parameters that were needed for the models are summarised in Savola and Fogelholm (2005b).

The electricity price used in the optimisation was varied between 20 €/MWh and 50 €/MWh and the natural gas price used was 17 €/MWh. The interest rate used when calculating the annual income and costs was 5% and the lifetime of the investments 15 years. The annual income from the process changes included the additional production of electricity. The cost of natural gas was subtracted from this income, if gas was used as an additional fuel in the process. Similarly to the simulations, the changes in the income from the district heat production were not included in the cost optimisation because changing from heat production to power production was considered to be always beneficial in these cases.

In these cases the CHP plants were modelled only at the design load. A heat load duration curve was adopted from Harvey et al. (2000) and scaled for different cases so that at the full load the CHP plant would produce 65% of the annual peak load of the DH network and so that about 80% of the annual energy generation of the network was produced with the CHP plant.

The results of the optimisation cases are presented in Figure 36, where the additional profit gained with the process changes is presented as a function of the electricity price to natural gas price ratio. When calculating the ratio, the natural gas price was held constant (17 €/MWh) and the electricity price was varied. The saved CO_2 emissions and efficiencies of these profitable process changes are summarised in Table 12.

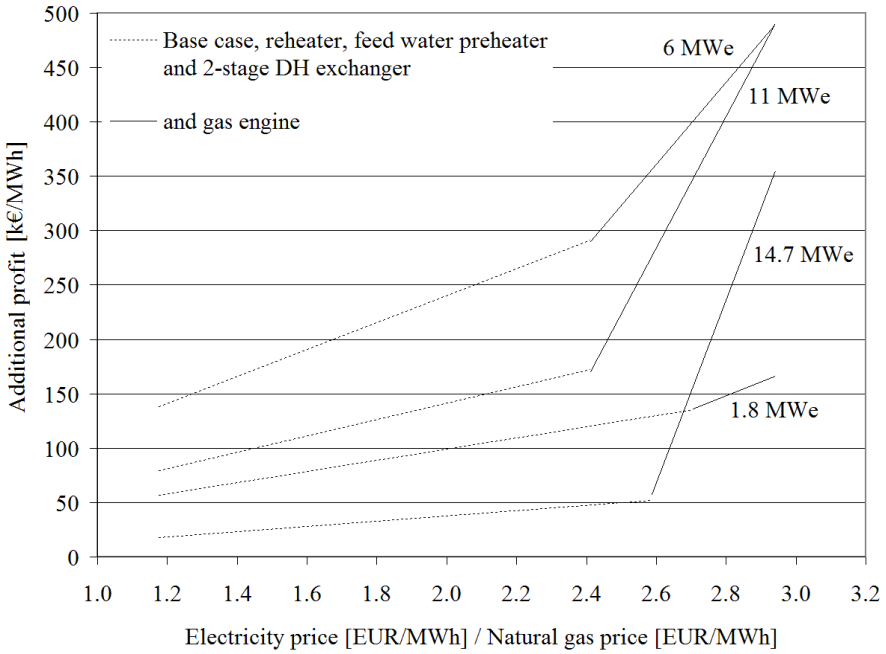

Figure 36. Results of the optimal process changes for the 1.8 MW_e, 6 MW_e, 11 MW_e, and 14.7 MW_e plants. A fuel dryer was added in the 6 MW_e case at the electricity price to natural gas price ratios 1.2–2.8 and in the 11 MW_e case at ratios 2.4–2.8.

For the 1.8 MW_e CHP process the addition of a feed water preheater, a steam reheater, and a two-stage DH exchanger gave some additional profit when the price of the electricity varied from 20 €/MWh to 45 €/MWh. When the price of the electricity was higher than 45 €/MWh, the addition of a gas engine became profitable. In this smallest CHP plant case the fuel dryer was not included to the process with a gas engine.

For the 6 MW_e CHP process the addition of a steam reheater, a feed water preheater, a two-stage DH exchanger, and a fuel dryer was profitable between the electricity prices of 20 €/MWh and 42 €/MWh. When the price of the electricity increased from 42 €/MWh, it became profitable to add a gas engine to the process.

Similarly to the 6 MW_e process, the breaking point for the process changes for the 11 MW_e CHP process was the electricity price of 42 €/MWh. Below that price the profitable change was to add a feed water preheater, a steam reheater, and a two-stage DH exchanger to the process. Above this price the addition of a gas engine and a fuel dryer was the profitable process change.

Table 12. The saved CO_2 emissions and the efficiencies of the most profitable process changes in the optimisation.

Process change	CO_2 saved	Efficiencies		
	[t/a]	α	η_e	η_{tot}
1.8 MW_e				
Base case	0	0.23	0.17	0.90
Feed water preheater, reheater, and 2-stage DH exchanger…	2237	0.45	0.28	0.90
… and gas engine	5087	0.59	0.31	0.85
6 MW_e				
Base case	0	0.34	0.23	0.90
Feed water preheater, reheater, 2-stage DH exchanger, and fuel dryer…	5381	0.49	0.29	0.90
… and gas engine	16 252	0.66	0.35	0.87
11 MW_e				
Base case	0	0.41	0.27	0.94
Feed water preheater, reheater, and 2-stage DH exchanger…	3269	0.47	0.29	0.90
… and gas engine and fuel dryer	24 958	0.66	0.35	0.87
14.7 MW_e				
Base case (with feed water preheater and 2-stage DH exchanger)	0	0.50	0.30	0.90
Reheater…	1079	0.50	0.30	0.90
…and gas engine	34 943	0.78	0.36	0.81

In the 14.7 MW_e case there were a two-stage DH exchanger and a feed water preheater already at the base case plant. Therefore, the efficiency increase and the additional profits from the process changes that were calculated in comparison with the base case results remained lower than in other cases. For the electricity prices between 20 €/MWh and 44 €/MWh the addition of a steam reheater was slightly profitable. No fuel dryer was added to the process in this case with a steam reheater. When the price of the electricity increased, the addition of a gas engine became profitable. The integration of a gas turbine was not profitable to any of the case plants with the used natural gas price and the electricity price range. The ratio of the electricity price and the natural gas price should have been much higher, at least 3.5–4.0, before the gas turbine integration would have became profitable.

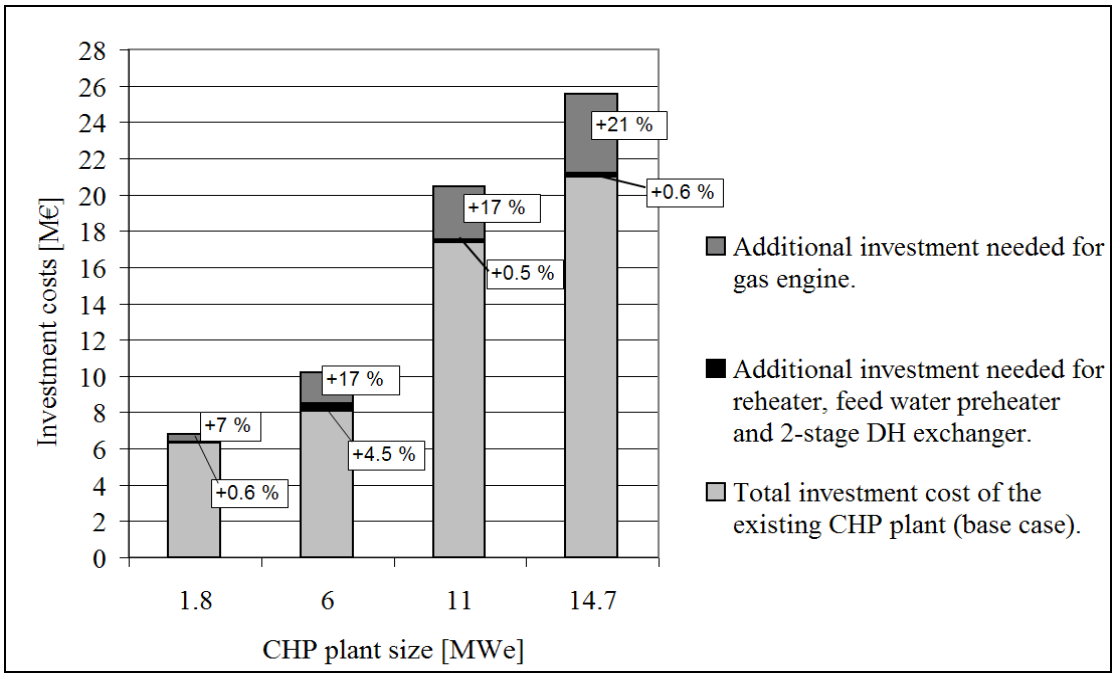

Figure 37. Effects of the process changes on the total investment costs of the 1.8 MW_e, 6 MW_e, 11 MW_e, and 14.7 MW_e plants. In the 6 MW_e case also a fuel dryer was added with a reheater, a feed water preheater, and a 2-stage DH exchanger. In the 11 MW_e case a fuel dryer was added with a gas engine.

The effects of the process changes on the total investment costs of the case plants are presented in Figure 37. According to the optimisation results some improvement in the power production and efficiencies can be gained with fairly low investment costs. The addition of a feed water preheater, a two-stage DH exchanger, and a steam reheater increased the CHP investment costs only by 0.5–0.7%. In the 6 MW_e case also a fuel dryer was added with the reheater, the feed water preheater, and the two-stage DH exchanger. This increased the investment costs by 4.5%. However, the investment costs of a two-stage DH exchanger did not include the costs of an additional extraction in a steam turbine, which increases the total investment costs of a two-stage DH exchanger. The integration of a gas engine increased the investment costs by about one fifth except in the smallest CHP process where the increase was below 10%. Because injecting the exhaust gases from a gas engine or a gas turbine to a biomass boiler is a novel technology, there are still many uncertainties in the investment cost evaluation. Changes may be required, e.g., to the boiler structure that increase the costs of this change. Overall, it may be concluded that the addition of a two-stage DH exchanger, a feed water preheater, a steam reheater, and a fuel dryer provide good solutions for a moderate increase in the power-to-heat ratio and the electrical efficiency of a small-scale CHP plant. Higher improvements may be gained with the integration of a gas engine, but more work should be done to find detailed process modification needs and cost estimates for this new process.

4.4.4 Further analysis of the results

The results of the MINLP model show that with this model profitable solutions for increasing the electrical efficiency and the power-to-heat ratio in the case plants can be found with optimisation tools. The electrical efficiency increased up to 0.28–0.30 and the power-to-heat ratio up to 0.45–0.50, depending on the CHP plant size, with additions of a two-stage DH exchanger, a feed water preheater, and a steam reheater. A gas engine and a fuel dryer integration increased the electrical efficiency further to 0.31–0.36 and the power-to-heat ratio to 0.59–0.78. The effect of a two-stage DH exchanger, a feed water preheater, a steam reheater, and a fuel dryer addition on the CHP plant investment costs was small, but the integration of a gas engine increased the investment costs in most cases by one fifth.

The MINLP model that was applied to the existing CHP plants showed its capability to handle the trade-offs between efficiency and costs, when different process alternatives were compared and when profitable process changes for current process designs were searched for. In the future work the model could be improved by removing some non-convexities from the mathematical formulation. This could make it possible to find better local optimums with different initial starting points and to reach the global optimum with the used initial starting points. With the improved model it could be easier to include more accurate, and also more complex, nonlinear enthalpy and entropy functions with free pressures to the model. This would enable the pressure optimisation of the process changes, e.g., in the steam turbine extractions for the steam reheat and the feed water preheat. Furthermore, the multiperiod properties of the CHP operation in a DH network could be included in the improved model. Overall, the MINLP model gives good solutions already at its current state and provides a good basis for the future modelling of the CHP plants and their integration to the DH network.

4.5 Conclusions from the results

In this work possibilities to increase the power production and the power-to-heat ratio of 1–20 MW_e CHP plants using biomass fuels were studied with simulation and optimisation tools. Especially, a MINLP optimisation model was constructed to find the most profitable process changes increasing the CHP plant efficiencies. The basis for the simulations and optimisations was the data collected from Finnish and Swedish small-scale CHP plants between 2002 and 2004. The process changes that were selected to be evaluated for the power production increase were

(i) high temperature and pressure of superheated steam (only in simulations, no cost analysis)

(ii) steam reheater

(iii) high pressure feed water preheater

(iv) two-stage district heat exchanger

(v) fuel dryer

(vi) gas engine or gas turbine integration.

In this case a novel concept for the addition of a gas engine and a gas turbine to the small-scale CHP plant was suggested, in which the exhaust gases, with 12.5% and 15% oxygen content, from a gas engine or a turbine were used as combustion air in a fluidised bed or grate furnace firing biomass.

In order to test the considered changes four existing CHP plants from Finland and Sweden were selected to represent the different size CHP processes. Simulation models of these case plants were constructed, and the process changes were added to these models. The simulation results and the cost analysis showed that there were possibilities to increase the power production of the CHP plants with the selected process changes. With the current electricity price of 30 €/MWh, the addition of a two-stage district heat exchanger, the steam reheater and a feed water preheater had potential to be profitable changes for all the case plants. Furthermore, the integration of a gas engine gave profit in some cases, but the costs of a gas engine and a gas turbine integration were quite uncertain. The addition of a fuel dryer was connected to the integration of a gas engine and a gas turbine, as this provided extra heat to the flue gases that could be used for fuel drying.

Testing all the possible profitable combinations with the simulation models would have been a very time consuming task. To include the simultaneous trade-off between power production, increased efficiencies, and the resulting costs in the evaluation of the process changes an optimisation model for the improvement of a CHP process was developed. The mixed integer nonlinear (MINLP) model included all the considered process changes and their cost effects. In most cases only the costs of the equipment were included in the investment functions, as the installation etc. costs were very uncertain.

The profitable process changes of the case processes with the current electricity price (30 €/MWh) according to the optimisation model were:

(i) 1.8 MW_e case: Addition of a feed water preheater, a steam reheater, and a two-stage district heat exchanger. This increased the investment costs of the total plant by 0.6%, the electrical efficiency to 0.28, and the power-to-heat ratio to 0.45, while the total efficiency remained at 0.90. A saving of 2237 t/a in fossil CO_2 emissions was estimated compared to the case where the additional power was to be produced with coal-fired condensing plant.

(ii) 6 MW_e case: Addition of a feed water preheater, a steam reheater, a two-stage district heat exchanger, and a fuel dryer. This increased the investment costs of the total plant by 4.5%, the electrical efficiency to 0.29, and the power-to-heat ratio to 0.49, while the total efficiency remained at 0.90. The savings of fossil CO_2 emissions were estimated to be 5381 t/a.

(iii) 11 MW_e case: Addition of a feed water preheater, a steam reheater, and a two-stage district heat exchanger. This increased the investment costs of the total plant by 0.5%, the electrical efficiency to 0.29, and the power-to-heat ratio to 0.47, while the total efficiency remained at 0.90. The savings of fossil CO_2 emissions were estimated to be 3269 t/a.

(iv) 14.7 MW_e case: Addition of steam reheater (while the base case already included a feed water preheater and a two-stage district heat exchanger). This increased the investment costs of the total plant by 0.6%, but the electrical efficiency, the power-to-heat ratio, and the total efficiency remained at 0.30, 0.50, and 0.90, respectively. The savings of fossil CO_2 emissions were estimated to be 1079 t/a.

For all cases the electricity prices over 42–45 €/MWh, with the natural gas price of 17 €/MWh, were needed before the addition of a gas engine became profitable. The addition of a gas engine had potential to increase the electrical efficiency to 0.31–0.36 and the power-to-heat ratio to 0.56–0.78 depending on the plant size. The integration of a gas turbine to the case plants was not profitable in the analysed electricity price range. The ratio of electricity price to natural gas price should have been at least 3.5–4.0 before the gas turbine integration to these cases would have become profitable.

Overall, the addition of a feed water preheater, a steam reheater, and a two-stage district heat exchanger seemed to be the most promising alternatives for increasing the power production in all the case plant sizes between 1–20 MW_e. When the simulation results and the optimisation results were compared, higher profits were gained with the process change combinations suggested by the optimisation model than with the separate process changes evaluated one-by-one with the simulation models. Thus, when applied to the existing CHP plants, the constructed MINLP model showed its capability to handle the trade-offs between power production, efficiency, costs, and the complexity of the process.

4.5.1 Significance of the results

Prior to this work the possibilities to improve the power production by modifying the currently used process design of 1–20 MW_e biomass-fuelled CHP plants were not studied systematically nor reported publicly. In the industry there was knowledge of the

currently used best practices but the potentials of the process changes in increasing the power-to-heat ratios and power production in the plants were not accurately known. However, this knowledge is vitally important in the future development of the CHP production especially in Finland, where the potential for increasing the CHP production is in the conversion of small heating plants into combined heat and power production. If the economical feasibility of these CHP investments could be improved by using process designs with higher power production capabilities and higher power-to-heat ratios, the new CHP investments could become more lucrative and the biomass fuels used in the heating plants could be utilised more efficiently. Furthermore, the fossil CO_2 emissions could be decreased, if the power produced in the CHP plants could replace coal-fired condensing power.

In this work process data of the state-of-the-art biomass-fuelled 1–20 MW_e CHP plants was summarised and some possible process changes that could improve the power production of the small-scale CHP plants were selected. The simulation and optimisation models constructed in this work provided knowledge on the efficiencies, profitability, and CO_2 emission savings of the different changes. The results were based on four existing small-scale CHP case plants from Finland and Sweden. The results from these cases give good basis for the future case-by-case considerations of the process designs of the biomass-fuelled CHP plants.

For the case-by-case evaluations of the process changes a MINLP optimisation model including the most promising process change possibilities was developed. The model is based on a well established mathematical formulation presented e.g. by Bruno et al. (1999) but the regression models and constraints describing the process changes and their cost functions are specially developed for the small-scale plants. The optimisation model gives possibilities to simultaneously combine different process changes to the CHP case plants and to evaluate their profitability. The case related parameters including the cost coefficients can be changed in the model according to the selected case. Unlike the other corresponding models, the model includes the design configurations and regression coefficients specifically suitable for small-scale CHP plants. For example, the selection of a single- or two-stage district heat exchanger and the integration of the exhaust gas from a gas engine or a gas turbine as combustion air in the biomass boiler have not been included in the previous optimisation models. In addition, the cost functions of gas engines and gas turbines used here are specifically developed for small sizes. Thus the model can be used as a tool in the future decision making when the process design changes of the small CHP plants are considered. With the developed optimisation model it is possible to evaluate the trade-offs between the investments and the profits gained from the increased power production, and also to evaluate the saved fossil CO_2 emissions.

4.5.2 Recommendations for future work

Currently, the developed optimisation model requires that the pressures in the modelled CHP process are fixed. This is undesirable when the process changes are optimised as the selected pressure may have significant effect on the profitability of the changes. Especially, for the profitability of a steam reheater and a feed water preheater the pressure in which the steam is extracted from the steam turbine may be very important. In order to model the pressures as free variables, the more complex enthalpy and entropy functions, depending on both temperature and pressure, should be added to the model. However, as the model is already in its current formulation nonlinear and fairly nonconvex, the addition of the more detailed enthalpy and entropy functions would make the solving of the model more difficult with commercial solvers. Thus the formulation of the model should be more convex and robust before making it more complex. There are many convexifying techniques suggested for the nonconvex functions of the optimisation models (e.g. Floudas, 1999; Pörn, 2000) and some of these transformations will be applied to the current model in the future. The formulation of the model into a more convex one would make the optimisation less sensitive to the starting points and would help the solvers to find the global optimum of the problem instead of the local ones.

The current model considers the design of the CHP process only at its design load. The annual operation is evaluated by calculating how long the plant should be operated annually at design load to correspond to the annual heat demand. However, the small-scale CHP plants are usually operated long time periods at part loads. Therefore, the changes in the efficiency of the CHP process during the part load operation have a major impact on the profitability of the total investments. In the future work the model will be transformed into a multiperiod one, where each period would correspond to the process conditions at a certain partial heat load and where the annual duration of the specific loads would be taken into account. After the addition of the multiperiods to the CHP plant optimisation model, the model could be combined with a district heating network model. Thus, also the effects of the process changes and the increased power production on the operation of the district heating network and on the other CHP plants in the network could be evaluated.

5. Possibilities to make more effective small-scale organic Rankine cycle (ORC) process concept

5.1 Property functions of the organic working medium

In an ORC (Organic Rankine Cycle) process an organic substance is used as working medium instead of water. By using the SOLVO software developed by Fortum, it is possible to simulate the cycle process of an ORC plant but, obviously, the software does not contain properties of every possible organic substance in the form of functions used in simulation.

Therefore, these property functions for any organic substances must be evaluated separately and attached to the SOLVO software in order to enable simulation. The examined working medium being chosen, it takes several working phases to include this organic substance to SOLVO: calculation of the substance properties with given initial parameters, forming property functions from the calculation points by using a curve-fitting software, programming the functions with Fortran language and compiling the Fortran functions and attaching them to the SOLVO software. VTT Processes is responsible for the entire work excluding the compiling and the attachment of the functions, which are performed by Fortum.

5.1.1 Calculation of the substance properties

In order to calculate the substance properties, ASPENPLUS software was used. This software evaluates by using given parameters, quantities of chemical thermodynamics for the chosen substance. Before the calculation by ASPEN, the grid of initial parameters must be formed. ASPEN calculates several thermodynamical quantities but merely pressure, temperature or the steam quality can be used as parameters.

Forming the grid is not quite straightforward since there are three different ”areas” in which the thermodynamical dependencies of the parameter quantities (pressure, temperature and steam quality) differ. There are three thermodynamical areas: liquid, moist steam and dry steam.

Naturally, the steam quality alters only in the moist steam area, and in liquid area the steam quality has a value 0 and in dry steam area a value 1. In the moist steam area temperature is dependent fully on pressure and, therefore, the thermodynamical quantities must be calculated in this area as functions of pressure and steam quality.

Obviously, in the liquid and dry steam areas steam quality is irrelevant and thermodynamical quantities are calculated as functions of pressure and temperature.

The first organic substance to be evaluated is Diphenyl-DiphenylEther which is a mixture of two substances. The grid was formed initially as follows: Pressure has values between 2 bar and 40 bar with 2 bar steps; temperature between 20 ^{o}C and 600 ^{o}C with 10 ^{o}C steps; steam quality has steps of 0.1 between 0 and 1. From the first calculations it was observed that in a pressure over 36 bar some evaluated quantities were erroneus, hence the pressure was limited to 36 bar. In addition, due to the condensing water required in the cycle process pressure must be as low as 0.01 bar. Therefore, the grid was extented to 0.01 bar by using logarithmically decreasing steps. The grid being sufficient, the required thermodynamical quantities were calculated with ASPEN.

In order to form property functions used in SOLVO, several thermodynamical quantities are required. These quantities with symbols and units are represented in the following:

P: pressure (bar)

T: temperature (^{o}C)

X: steam quality

H: specific enthalpy (kJ/kg)

S: entropy (kJ/kg K)

C: specific heat capacity (kJ/kg K)

M: dynamic viscosity (kg/m s)

K: thermal conductivity (W/m K)

V: specific volume (m^3/kg).

Enthalpy and entropy differ from the other quantities above, since their absolute values are irrrelevant. In thermodynamics only the differentials of enthalpy or entropy are calculated. For example, the entropy values given by ASPEN are based on the standard formation entropy values of chemical thermodynamics, and in the case of the substance examined here the entropy values are negative. On the other hand, negative entropy values cannot be used in SOLVO. Since only the differentials are important, these negative values can be scaled by adding a constant in order to obtain positive entropy values. In this case of calculation an addition of 5 kJ/kg K is sufficient.

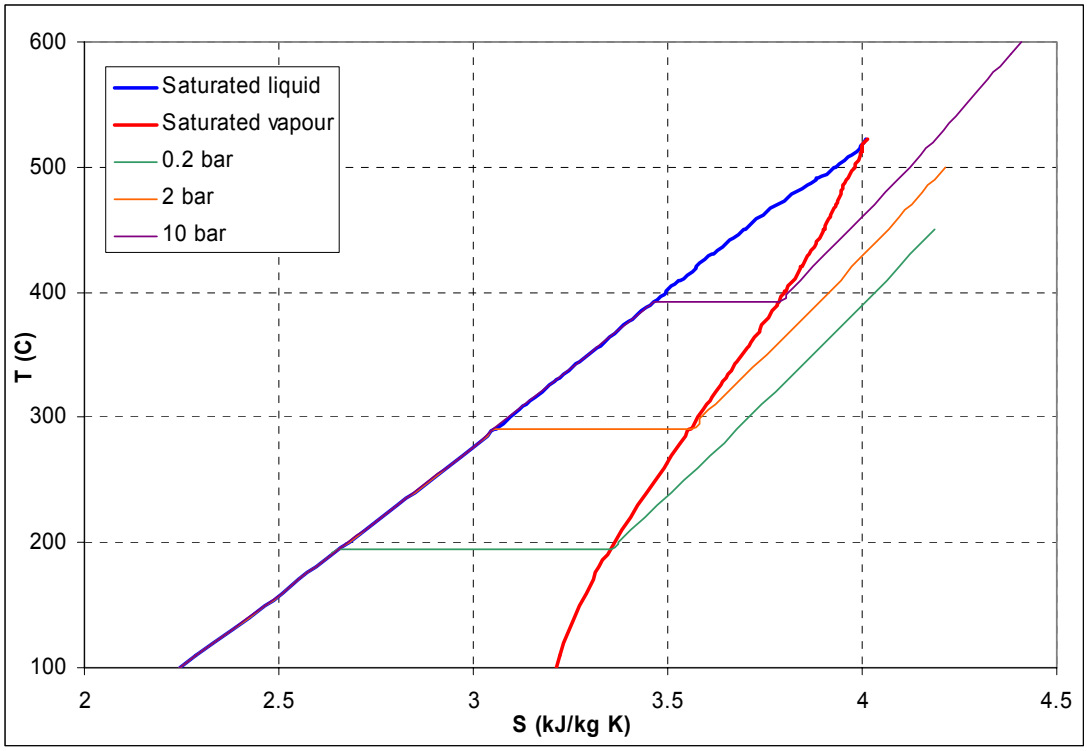

Figure 38. T,s -diagram of the organic working medium, which contains curves of saturated liquid and saturated vapour and three isobars (0.2 bar, 2 bar and 10 bar).

At first it is useful to analyze the most important thermodynamical charasteristics from the extensive calculation data. In Figure 38 the T,s -diagram, i.e. the temperatures of saturated liquid and saturated vapour as functions of entropy, is presented. Furthermore, there are three different isobars illustrated in the figure. The curve of the saturated vapour is quite peculiar, because in the T,s -diagram of water the corresponding curve is of different form: temperature decreases as entropy rises.

The T,s -diagram of Figure 38 is of special character also from the turbine expansion point of view. Traditionally water being the working medium, the superheated steam expands in the turbine, steam pressure decreases and steam becomes moist. If the expansion is isentropic, i.e. entropy remains unchanged during the expansion, the turbine expansion phase can be illustrated as vertical descent from the higher isobar to the lower. It can be observed from the T,s -diagram that the expansion of the superheated vapour cannot end up in the moist steam area, since a downward oriented vertical line cannot intersect the saturated vapour curve. It is difficult to say whether this kind of property is charasteristic of organic working mediums.

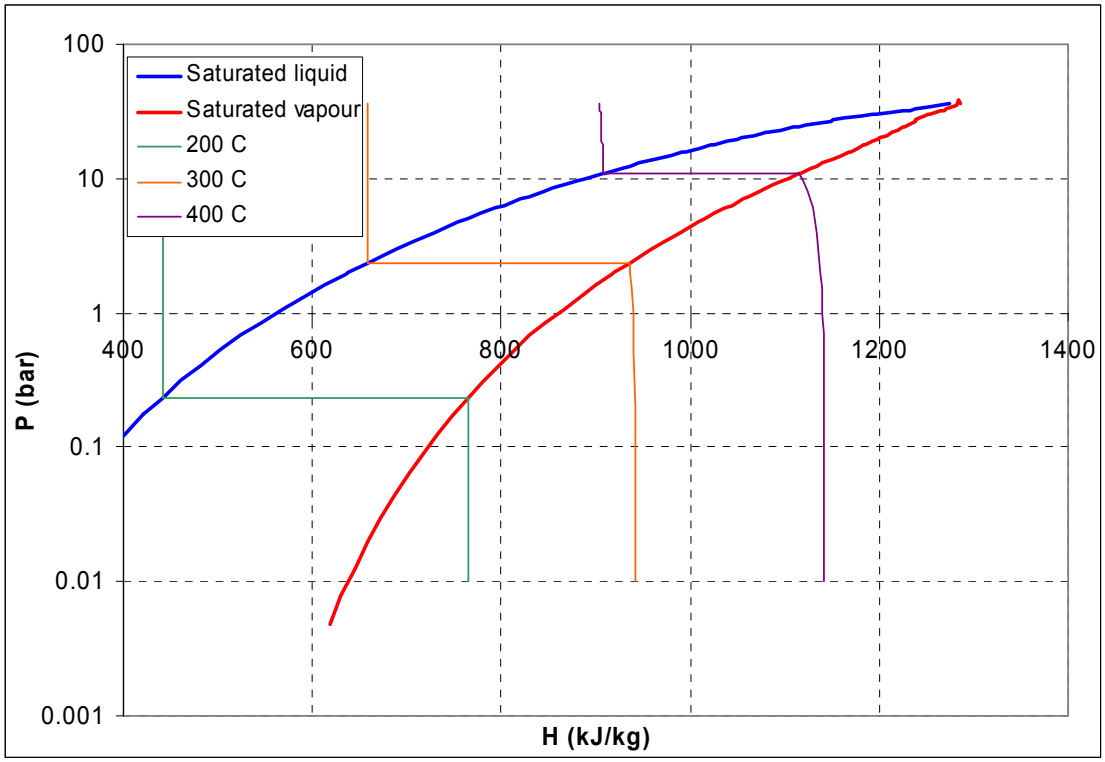

Figure 39. PH diagram of the organic working medium, which contains curves of saturated liquid and saturated vapour and three isotherms (200 °C, 300 °C and 400 °C).

Also, the PH diagram of Figure 39, which illustrates the pressure of saturated liquid and saturated vapour as functions of enthalpy, is different from the case of water. The behaviour of isotherms is quite similar, but the curve of saturated vapour bends slightly differently as compared to the corresponding curve of water.

5.1.2 Formation of property functions

The grid given to the ASPEN software consisted of values of pressure, temperature and steam quality within certain steps. As a result from the calculation corresponding values of enthalpy, entropy etc. were obtained. When an organic substance is used as working medium in SOLVO simulation, it is required e.g. in the dry steam area a proper value of enthalpy for any given pressure and temperature. Therefore, by using the grid points a method must be formed, by which the correct values can be calculated in any point occuring in simulation. There are two different methods.

The first method is based on using the grid of calculation points as such and applying the up-and-down method for the grid and then calculating the correct values for required quantities by linearisation. The problem of this method lies in the assumption that

values of variables between the grid points alter linearly and therefore calculation can be erroneus. Furthermore, the borders of the thermodynamical areas can be intangible, if the areas are defined only based on the grid points on the saturation curves.

Another feasible method is forming fitting functions based on grid points. This method searches for the best possible functions which describe the interdependencies of the variables. In this project the method of fitting functions was used, since functions describe better the changes between the grid points and programming of the functions in Fortran language is much more convenient than managing all the grid points programmatically.

The functions required by SOLVO define the interdependencies of the different variables. In simulation not all the dependencies are necessary, but in total 15 functions must be fitted:

H(P,T,X): enthalpy as function of pressure and temperature or steam quality

C(P,T,X): specific heat capacity as function of pressure and temperature or steam quality

M(P,T,X): dynamic viscosity as function of pressure and temperature or steam quality

K(P,T,X): thermal conductivity as function of pressure and temperature or steam quality

V(P,T,X): specific volume as function of pressure and temperature or steam quality

H(P,S): enthalpy as function of pressure and entropy

S(P,H): entropy as function of pressure and enthalpy

T(P,H): temperature as function of pressure and enthalpy

V(P,H): specific volume as function of pressure and enthalpy

X(P,H): steam quality as function of pressure and enthalpy

P(T,H): pressure as function of temperature and enthalpy

P0(T): pressure of saturated steam as function of temperature

T0(P): temperature of saturated steam as function of pressure

T0(H): temperature of saturated liquid as function of enthalpy

H1(S): enthalpy of saturated vapour as function of entropy.

There are functions of three, two and one variables listed above. However, the functions of three variables are in fact functions of two variables, since in the liquid and dry steam areas the variables are pressure and temperature whereas in the moist steam area the variables are pressure and steam quality. The functions of one variable are used to define the area of moist steam.

Forming the functions of one variable is quite simply curve-fitting of the calculation data, and this can be performed by several softwares. However, the forming of the two variable functions is a bit more challenging, since it is based on surface-fitting of the calculation data. The shapes of surfaces are difficult to fit with simple functions, and therefore more complex surface functions are required.

In order to fit functions of two variables, in this project a TableCurve 3D software was used. This program finds from its database the best fitting surface function to describe the grid points. The program is useful due to the high quality and quantity of these surface functions and e.g. fractional functions are included in the database. The program evaluates the optimal parameters for all the functions and sorts these functions by the coefficient of determination. It is then easy to choose the perfect function by e.g. observing the residuals of the data points.

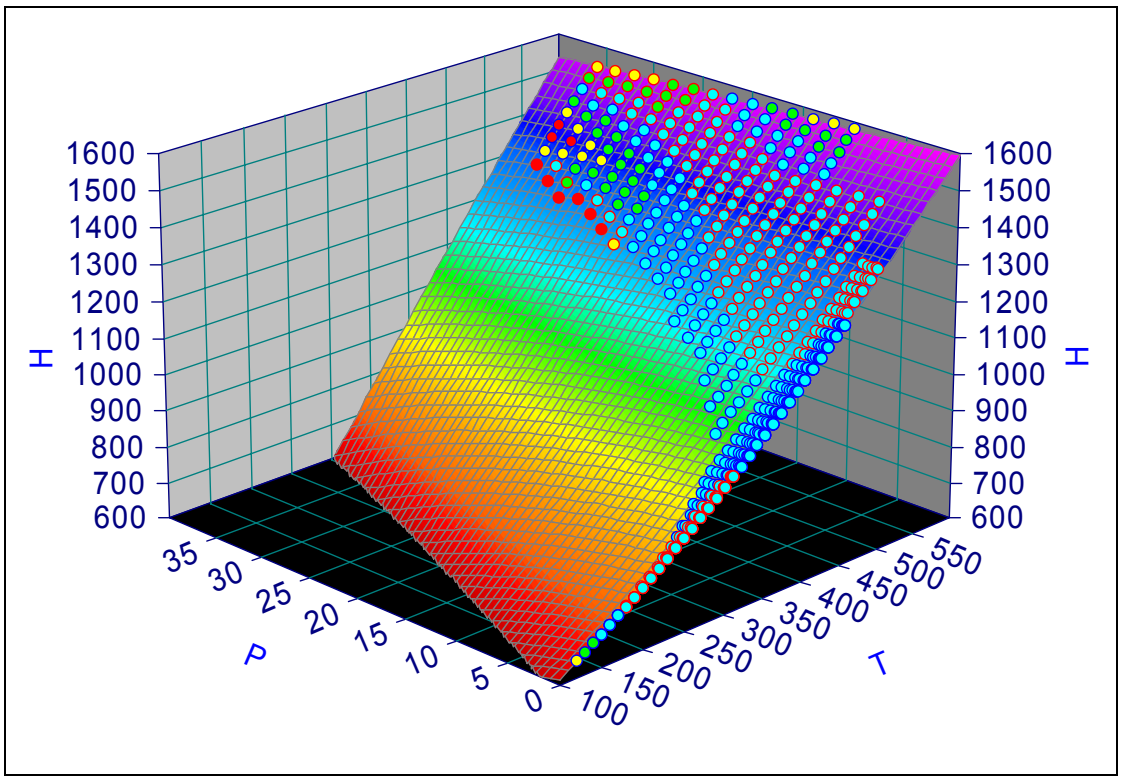

Figure 40. Enthalpy as a function of pressure and temperature in the dry steam area. The points represent the actual data values and the surface represents the fitted function.

In Figure 40 an example of a fitting function is illustrated. In the figure enthalpy as a function of pressure and temperature in the dry steam area is fitted as a surface and the points illustrate the actul data values. The colour of the point indicates the goodness of the fit, i.e. a blue point is better fitted than a red point. The function of the Figure 40 is of form:

$$H(P,T) = a + bT + cP + dT^2 + eP^2 + fTP + gT^3 + hP^3 + iTP^2 + jT^2P \qquad (45).$$

The goodnes of the fit can be analysed in several ways. The coefficient of determination describes how well the function defines the data points overall. The coefficient of determination in Figure 39 is 0.9999862212 which is quite high for this kind of case.

Another way to measure the goodness of fit is to analyse the residual values which are the difference between the actual data points and points calculated by the function. In Figure 41 the residual values of the surface function of Figure 40 as a function of pressure and temperature are illustrated.

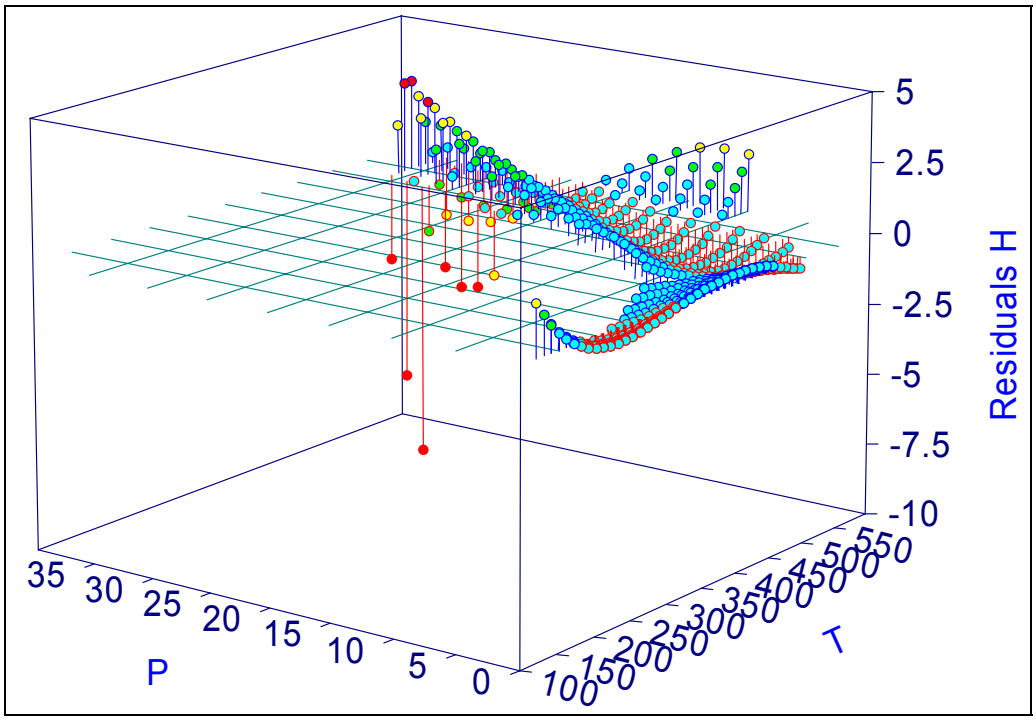

Figure 41. The residual values of the surface function H(P,T) in the data points.

The residuals seem to be within tolerance, since at their highest they are 10 and these high residuals of over 5 are just a few and those mainly in the high pressure area. It can be seen in Figure 41 that in the low pressure zone the residuals are moderately low when proportioned to the absolute values of the enthalpy, 600–1600 kJ/kg, in the dry steam area.

It is advisable that residual values are as low as possible at the borders of the thermodynamical areas so that there would not be any major discontinuity between the areas affecting possibly the SOLVO simulation. This is not though always possible, because in some cases the good fitting of the border zones may cause major residuals in other data points.

Surface-fitting of some functions is quite straightforward, as is illustrated in Figure 42. In this case the dynamic viscosity as a function of pressure and temperature in the liquid area is fitted. In this area the effect of pressure on other thermodynamical quantities is minimal, and so the fitted function in Figure 42 is merely a simple function of one variable, namely temperature. The residuals are also at their highest only of rank 0.5%.

On the other hand fitting of some functions is extremely difficult. Especially the cases where the magnitudes of values vary greatly, are difficult to fit. E.g. the magnitude of specific volume increases vastly as pressure decreases. In the moist steam area speciic volume can be of magnitude 10 m^3/kg at low pressures ($P < 0.05$ bar), whereas at higher pressures ($P > 1$ bar) it can be of rank 0.001 m^3/kg. However, specific volume should be calculated as accurately at low pressures as at high pressures.

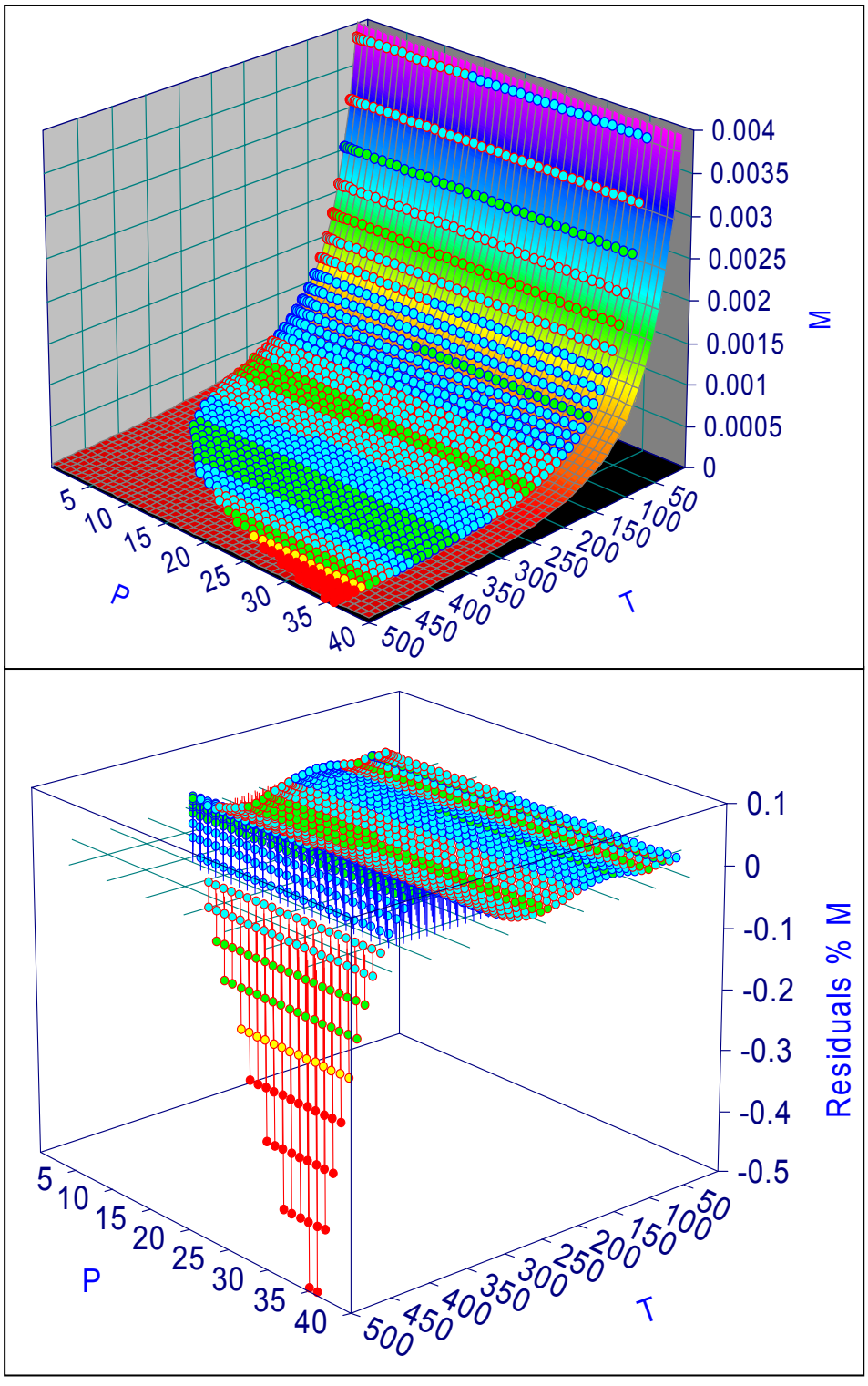

Figure 42. Dynamic viscosity as a function of pressure and temperature in liquid area. Above are the data points and the surface function. Below are the percentual residual values i.e. the proportional values of the difference between the actual and the calculated data points.

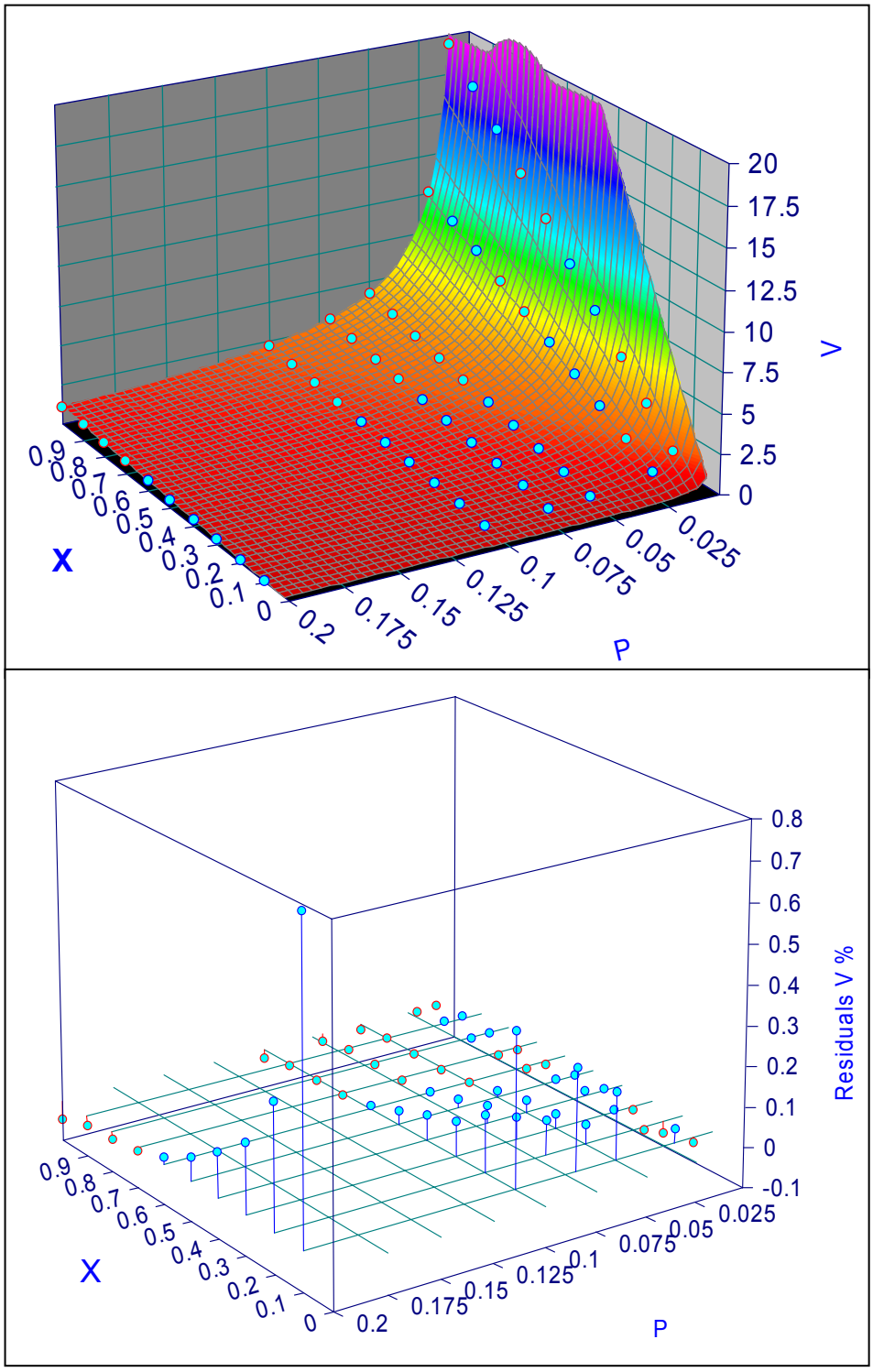

Figure 43. Specific volume as a function of pressure and steam quality in the moist steam area (pressure 0.01–0.2 bar). Above the surface function and below the percentual residuals.

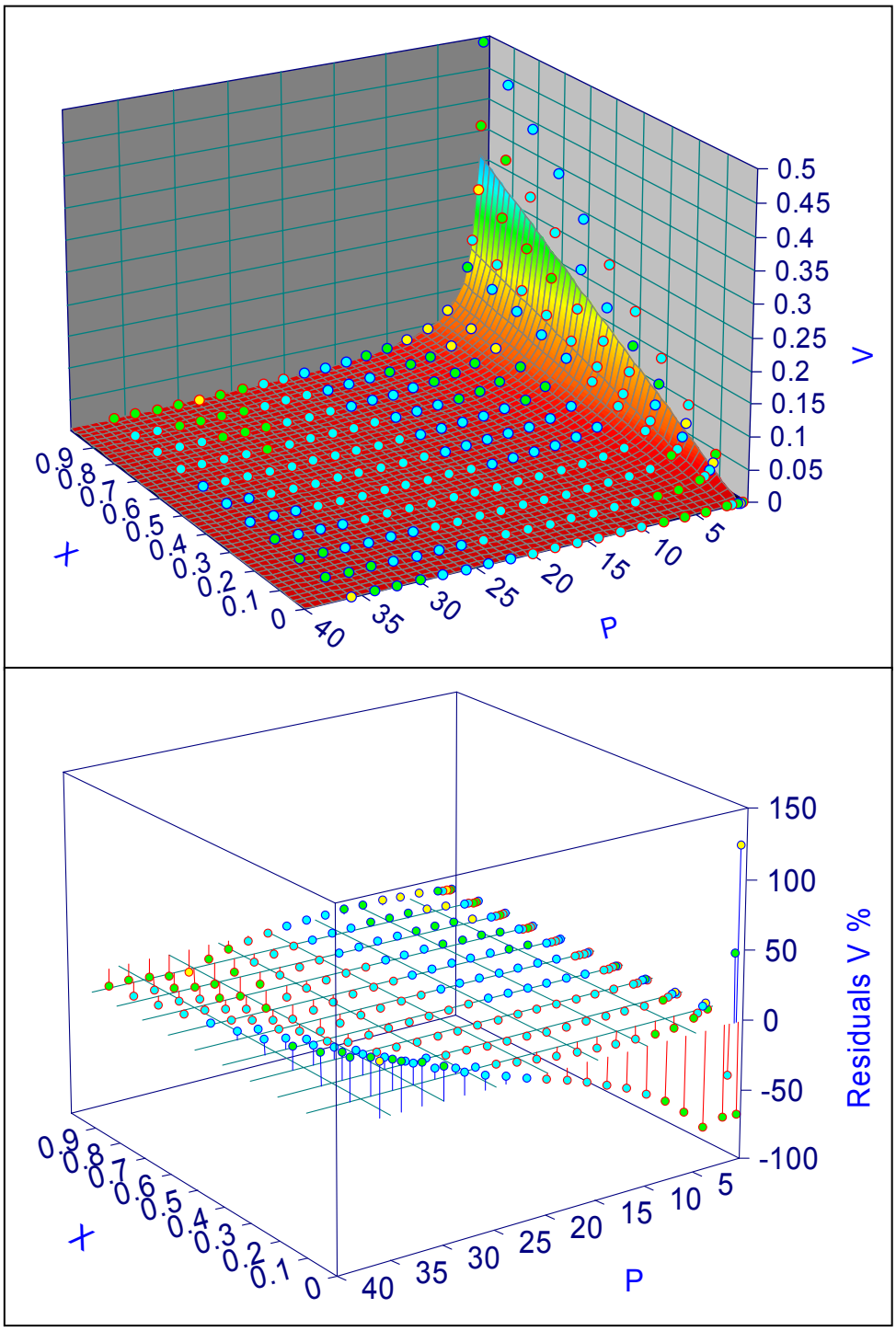

Figure 44. Specific volume as a function of pressure and steam quality in the moist steam area (pressure 0.5–36 bar). Above the surface function and below the percentual residuals.

The problems of the specific volume can be handled e.g. by dividing the data points by pressure to two parts: pressures between 0.01 bar and 0.2 bar and pressures between 0.5 bar and 36 bar. The ”empty” area (0.2 bar–0.5 bar) between these two parts is intentional, so that discontinuity would be avoided in the connection of these parts. Two separate fitting functions can thus be connected via linearising values between pressures 0.2 bar and 0.5 bar.

The surface function for specific volume in moist steam area represented in Figure 43 contains low pressures (0.01 bar–0.2 bar) and the corresponding percentual residuals. It can be noticed that the fit is successful despite the altering magnitudes. On the other hand, in Figure 44 the corresponding graphs are illustrated in the higher pressure case (0.5 bar–36 bar). In this fit the percentual residuals are higher, probably due to the greater sample, but the highest residuals are mostly located at the border of the liquid area. Since the significance of specific volume in liquid area in SOLVO simulation is small, these high residuals (10–100%) can be tolerated.

5.1.3 Property functions in Fortran language

When all the necessary property functions are evaluated by surface-fitting software, these functions must be adapted to the requirements of SOLVO. Obviously, there are more fitted functions than Fortran functions, since in one Fortran function the property functions of liquid area, moist steam area and dry steam area are used. In Figure 45 a graphic illustration of the method to form Fortran function for SOLVO from the property functions is presented.

From the graph above the molds of two Fortran functions become clear. Both functions have pressure as variable, and so the minimum and maximum pressure values are common restrictions for them. Other restrictions are minimum and maximum values subject to temperature or enthalpy. In liquid area and dry steam area both examples are quite similar, but in the moist steam area the procedures differ greatly. The functions of pressure and temperature require steam quality to be included in the moist steam area, whereas in the case of functions of pressure and enthalpy steam quality variable is not necessary, since pressure and enthalpy define quantities explicitly in the moist steam area too. For the sake of clarity, it is better in the following to go through in detail the structure of the Fortran function forming procedures of these two examples.

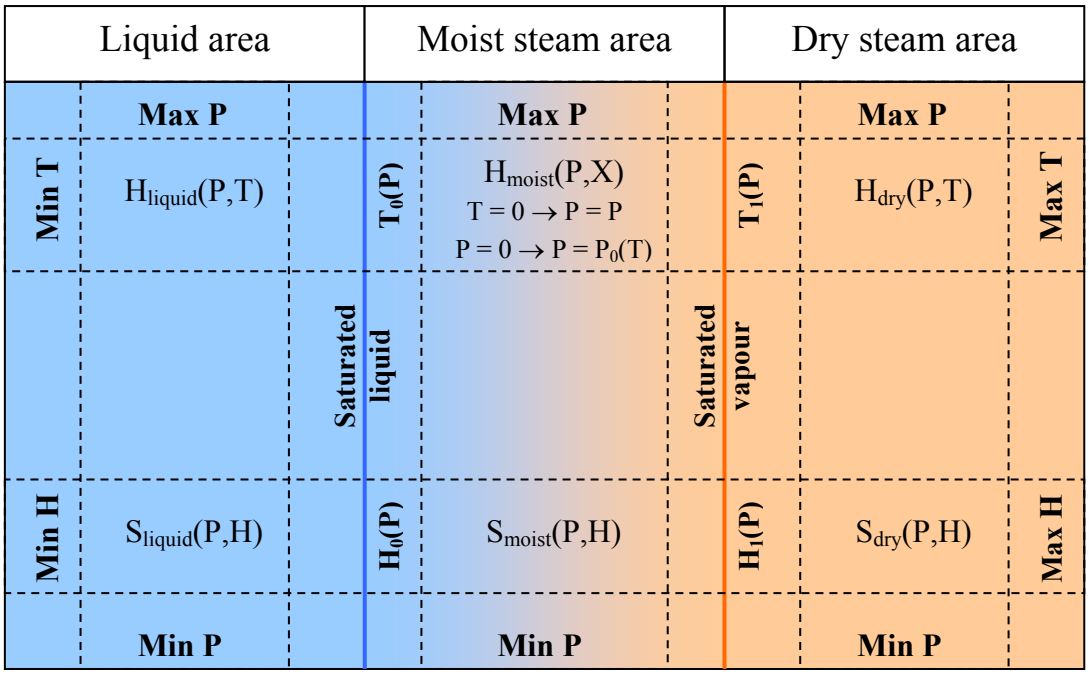

Figure 45. A chart of forming the Fortran functions by using property functions and restrictions. Examples are enthalpy as a function of pressure, temperature and steam quality, and entropy as a function of pressure and enthalpy.

The first example is enthalpy as a function of pressure, temperature and steam quality, and its label is OR1HPT. This identifying label consists of the code of the organic substance (OR1) and the symbols of the variables (HPT) used in the function. The structure is as follows:

1. The variables in the function OR1HPT(P,T,X,cn,cc) are pressure (P), temperature (T), steam quality (X) and numbers of components in SOLVO (cn, cc).

2. At first in the agenda is the special case of moist steam in which either the given pressure or temperature is of value zero. In the moist steam area temperature depends on pressure and therefore one of the other is obsolete and gets the value zero.

3. If temperature is zero, then pressure is checked whether it is in the feasible area. If pressure is over the maximum value, then it gets maximum as a new value and error message is performed. In the case of minimum value the procedure is corresponding.

4. If pressure is zero, then the pressure of saturated steam for the given temperature is calculated by using the function OR1PT0. The feasibility subject to pressure or temperature restrictions are not performed, since the function OR1PT0 calculating pressure does that.

5. For the given pressure and steam quality, enthalpy is calculated by using the fitting function $H_{moist}(P,X)$ of the moist steam area.

6. In the other case neither pressure nor temperature is zero. In this case the feasibility of pressure and temperature is checked subject to the restrictions.

7. Next it is analysed in which area is the combination of pressure and temperature located. This is performed by calculating temperature of saturated steam from the given pressure by using the function OR1TP0. The given temperature is then compared to this value.

8. If temperature is below the temperature of saturated steam, enthalpy is calculated by using the fitting function $H_{liquid}(P,T)$ of the liquid area.

9. If the difference from temperature of saturated steam is small (e.g. 0.01 ^{o}C), for the sake of certainty, the fitting function $H_{moist}(P,X)$ of the moist steam area is used and the given steam quality is used in that function as a variable.

10. If temperature is above the temperature of saturated steam, enthalpy is calculated by using the fitting function $H_{dry}(P,T)$ of the dry steam area.

Another example, entropy as a function of pressure and enthalpy has a label OR1SPH. This Fortran function is not as complex as the function above, since pressure and enthalpy define explicitly entropy in all the thermodynamical areas and therefore steam quality is not necessary as a variable. The structure is as follows:

1. The variables in the function OR1SPH(P,H,cn,cc) are pressure (P), enthalpy (H), and numbers of components in SOLVO (cn, cc).

2. At first it is checked whether pressure or enthalpy is outside of the restrictions. If they are, minimum or maximum values are used.

3. Enthalpy values of saturated liquid and saturated vapour for the given pressure are calculated by using functions OR1HP0 and OR1HP1.

4. If enthalpy is below the enthalpy of saturated liquid, entropy is calculated by using the fitting function $S_{liquid}(P,H)$ of the liquid area.

5. If enthalpy is above the enthalpy of saturated liquid and below the enthalpy of saturated vapour, entropy is calculated by using the fitting function $S_{moist}(P,H)$ of the moist steam area.

6. If enthalpy is above the enthalpy of saturated vapour, entropy is calculated by using the fitting function $S_{dry}(P,H)$ of the dry steam area.

All the Fortran functions in which pressure, temperature and steam quality are given as variables, are based on the structure of the first example above. The exception is the specific volume function OR1VPT, in which moist steam consists of two separate functions.

Other functions are modifications of the latter example. OR1HPS is similar to OR1SPH, but variables are opposite. In OR1XPH there is just the moist steam area, since steam quality is otherwise 0 or 1. In the case of specific volume the function OR1VPH is similarly divided in the moist steam area into two parts as in OR1VPT.

OR1PTH and OR1TPH are special cases, since pressure and temperature are interdependent in the moist steam area. Therefore enthalpy as a variable is irrelevant in that area, and only the liquid area and the dry steam area are significant. Furthermore, OR1PTH does not include the liquid area, because it is quite impossible to fit any function in this area which would describe pressure as a function of enthalpy and temperature. The reason is the minimal effect of pressure on quantities in the liquid area.

5.2 Construction of the SOLVO model

Now that the organic working medium has been modelled for the simulation purposes and the Fortran functions have been attached to the SOLVO software, the simulation model of an ORC plant has to be constructed by using these new features of SOLVO. The purpose of the simulation is firstly to model the Admont ORC plant with Diphenyl-DiphenylEther as a working medium and secondly to explore possibilities of improvements by adding some new properties to the current Admont plant model.

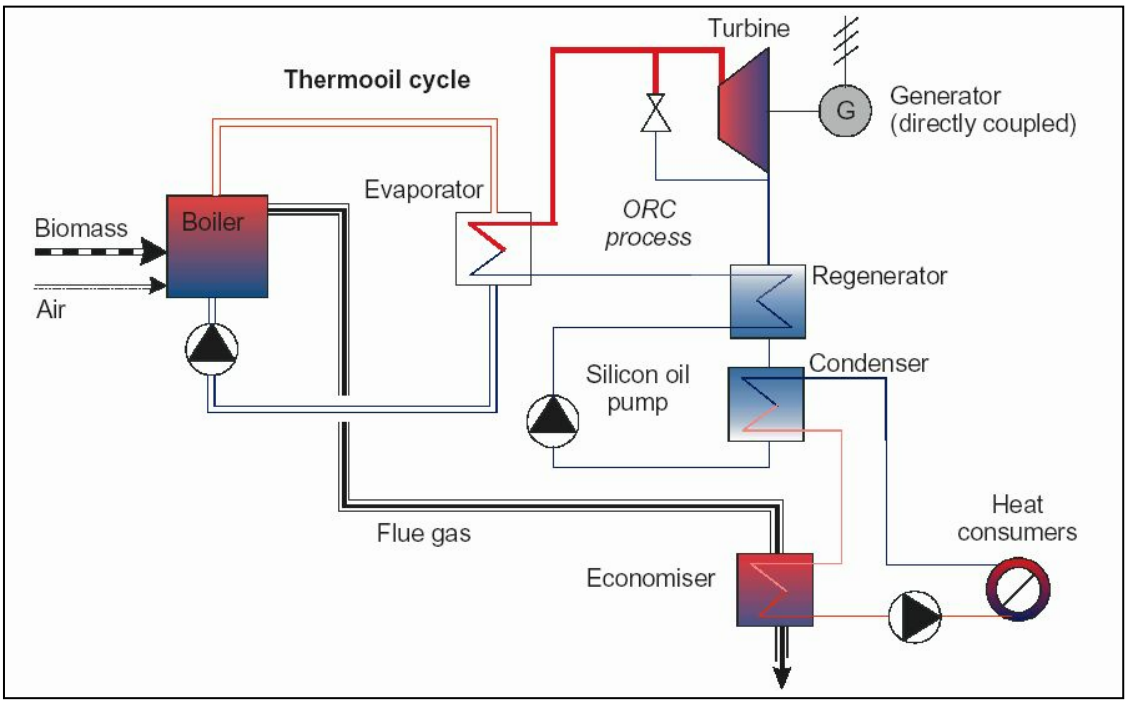

Figure 46. Working principle of the Admont ORC plant (Admont, 2001).

With the SOLVO simulation model the Admont ORC process represented in Figure 46 is reproduced as accurately as possible. There are though some changes to the process model: the pressure reducing device in parallel with the turbine is abandoned and there will be a combustion air pre-heater to be attached to the flue gas flow. Otherwise, within the limits of few restrictions of SOLVO, the process of Figure 46 is the target of the simulation.

5.2.1 Total process model

In SOLVO the simulation model is constructed by adding components such as turbines, condensers etc., and connecting these components by lines representing the flow of the working medium, may it be organic substance or water. For example, in the process of Figure 46 there are in fact four different working mediums: organic substance, thermooil of the boiler, water of the district heat and flue gas from the thermooil boiler. In the simulation model all these substance must be in their own cycles and mixing of substances is prohibited. The thermodynamical interaction between these different working mediums is handled by heat exchangers, condensers, economisers etc.

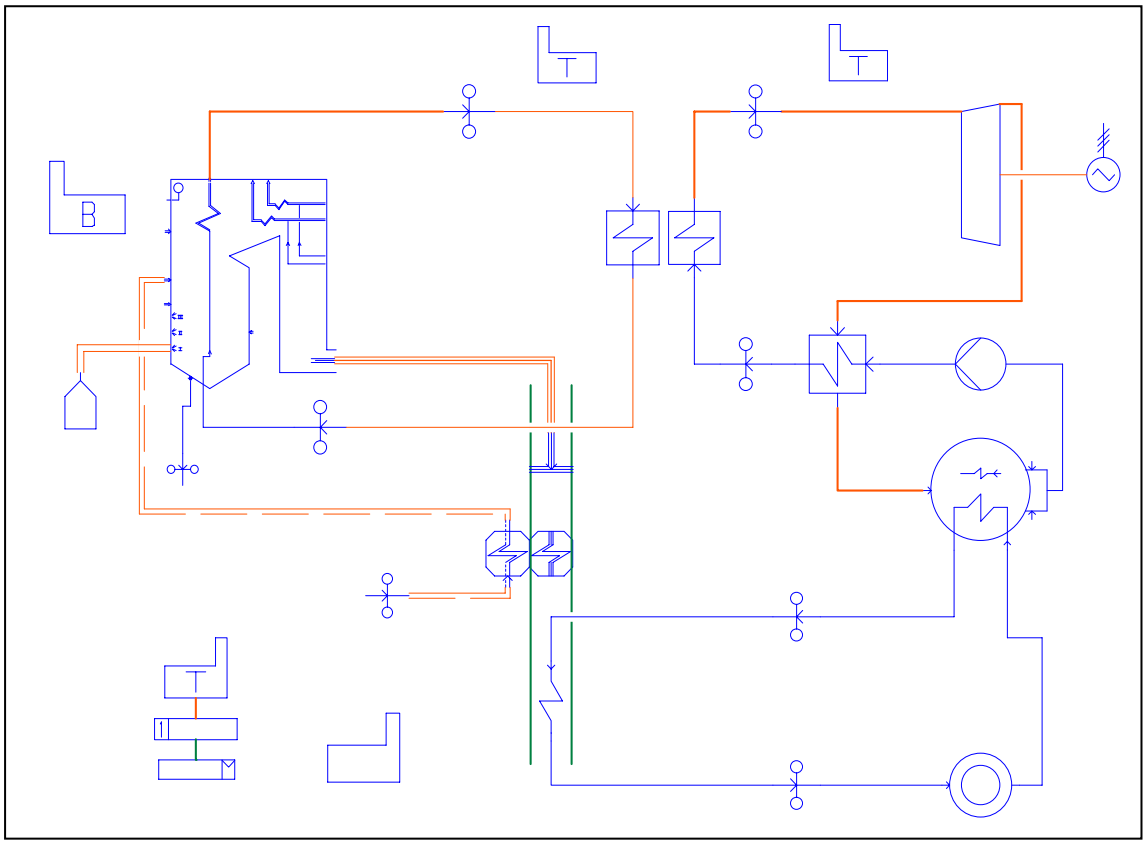

Figure 47. The basic ORC process model constructed with SOLVO software.

In Figure 47 the foundation of the SOLVO simulation model is illustrated. The characteristics of the process described in Figure 46 can be observed quite easily from this figure. The details of the model will be explained in the following subchapters, but some matters concerning the total process model must be discussed here.

In SOLVO the total plant must be divided into subplants in order to maintain balance and calculate total efficiencies etc. These plants can be seen in Figure 47 as separate plant-like components labeled with T or B as turbine or boiler. The plants are divided with limit components. It can be noticed that there are two main plants: the ORC turbine system with district heating, and the thermooil boiler system with fuel gas system. In order to achieve thermodynamical balance these plants are interlinked with each other so that parts of their systems are defined to be in other plants. For example, the economiser warming the district heat water is actually in the boiler plant, because the boiler flue gas goes through the economiser. There are also two additional turbine plants in order to maintain heat balance between the ORC cycle and the thermooil cycle but this will be explained later. Finally, the summary plant adds up the information from all the plants and calculates total efficiency, power-to-heat ratio etc.

The SOLVO simulation model consists of three subsystems: the thermooil boiler which is the heat source for the plant, the ORC system which generates electricity and finally the district heating system which warms the water required for heating purposes. In the following subchapters these elements are examined in more detail.

5.2.2 Thermo-oil boiler

In the ORC plant the thermo-oil boiler is responsible for transferring the heat energy from the fuel to the ORC cycle. Organic working medium is not heated in the boiler due to the properties of the organic substance, e.g. it can be dangerously flammable as vapour in boiler circumstances. Therefore, in the boiler thermal oil is used as heat-transfer medium. The advantage of thermo-oil boiler is that in the temperatures required by the organic medium to evaporate thermal oil is in liquid state. Also, there is no need for high pressures in the boiler due to the liquid state of the heat-transfer medium.

In Admont ORC plant the temperature of thermal oil coming from the boiler is 300 ^{o}C and after the cycle 250 ^{o}C (Admont, 2001). Since the thermal oil transfers heat from the boiler to the ORC cycle, this 300 ^{o}C would be in Admont case the maximum temperature for the evaporated organic substance due to the rules of thermodynamics. However, there are thermo-oil boilers which are capable of heating the thermal oil up to 350 ^{o}C temperature. The corresponding pressure of saturated steam for the Diphenyl-DiphenylEther is about 5 bar. Therefore, the highest theoretical pressure and temperature in the ORC cycle would be 5 bar and 350 ^{o}C.

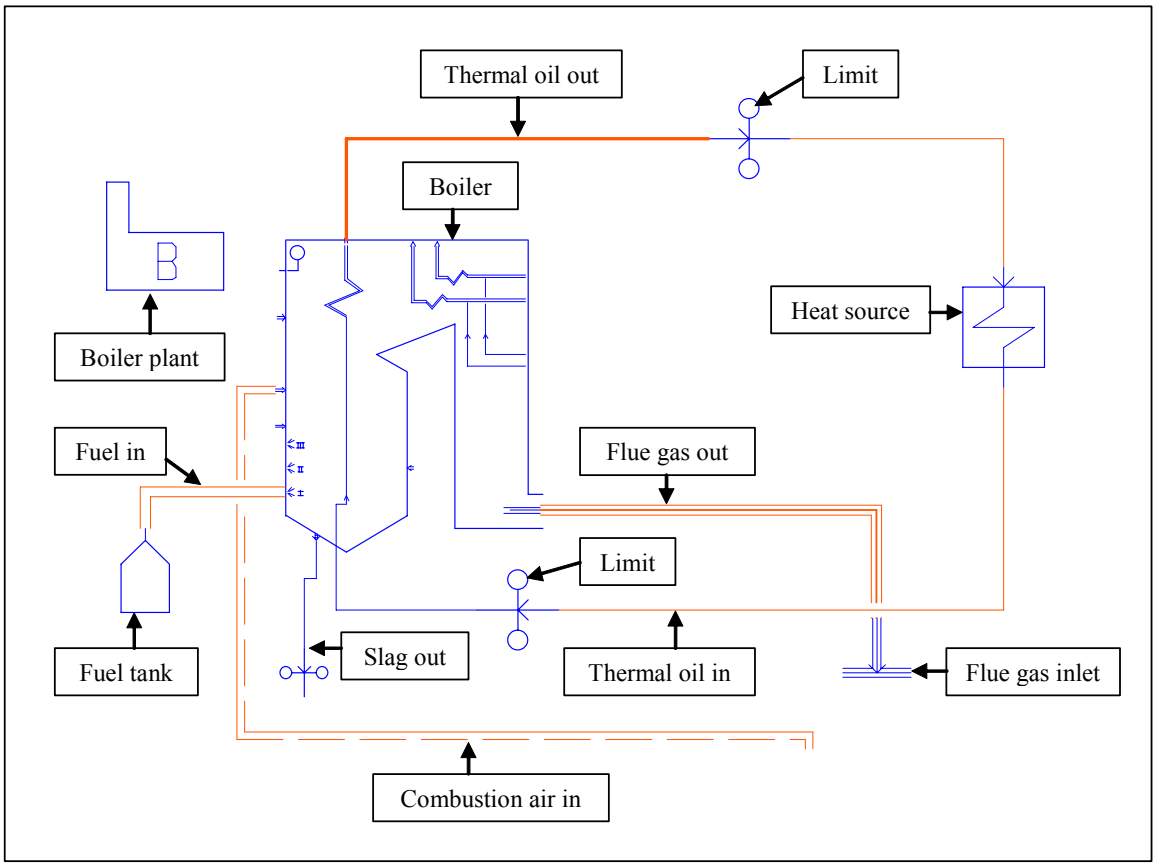

Figure 48. Thermooil boiler part of the SOLVO simulation model with components and substance flows labeled.

In Figure 48 the structure of the thermooil cycle is illustrated. The central part of the system is the boiler itself. In SOLVO this boiler is modelled according to DIN 1942 standard. The boiler is in this case given the mass flow of the thermal oil, temperatures of the outgoing and incoming oil and temperature of the outgoing flue gas. The boiler calculates in simulation the power of boiler, mass flow of the fuel, fuel power, combustion air flow and flue gas flow. The slag from the boiler illustrated in Figure 48 is irrelevant in this simulation.

The fuel tank feeds fuel, which is wood in this case, to the boiler with room pressure and temperature. The temperature of the combustion air supplied to the boiler affects fuel efficiency, but this is discussed later in this chapter. The flue gas from the boiler is directed to the gas inlet which is necessary in order to capitalise the flue gas heat in district heating.

The limits in the thermooil cycle divide the boiler plant and the turbine plant used in transferring the heat of thermal oil to the ORC cycle. Thermal oil cools down to e.g.

300 °C in the heat source and surrenders the heat power from that cooling to the heat source component. This heat power is negative in SOLVO. The heat source in the ORC cycle gets this power and uses it to evaporate organic substance. This procedure of two separate heat sources and turbine plants is necessary, since there are not at the moment any general heat exchanger which could transfer heat between thermal oil and organic substance. The temperature of thermal oil going from the boiler is fixed in the boiler component but the temperature of oil coming to the boiler is fixed in the heat source component.

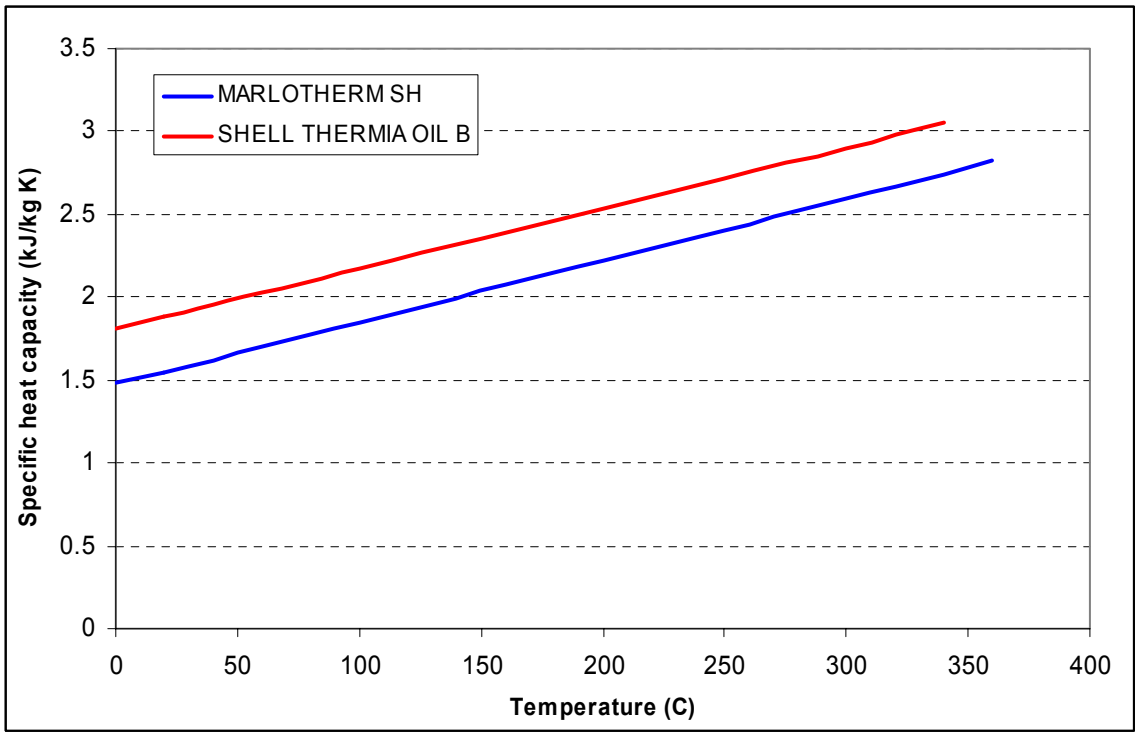

Figure 49. Specific heat capacities of two types of thermal oils as a function of temperature.

In SOLVO there is not a selection of thermal oils which can be used in simulation. Therefore thermal oil properties must be attached to the software. Since, thermal oil is in liquid state in the cycle there is not necessity to model as comrehensive functions as in the case of organic substance. Actually, only the specific heat capacity is required in the boiler model. In Figure 49 heat capacities of two different thermal oils are represented.

MARLOTHERM SH is a synthetic heat-transfer medium produced by SASOL company (SASOL, 2004) and it is used in the thermooil boiler of Lienz ORC plant (Lienz, 2003). Therefore, it is used as the thermal oil in the SOLVO simulation. MARLOTHERM SH can be used in thermal cycle up to temperatures of 350 °C, and

therefore this is the upper limit of the ORC system too. For a reference, there is also the heat capacity of another thermal oil illustrated in Figure 48. SHELL THERMIA OIL B is also a synthetitc heat-transfer oil produced by Shell. Heat capacity of this thermal oil is a bit higher than MARLOTHERM SH and it has a maximum operational temperature of 320 ^{o}C (Shell, 2001). Hereby, since MARLOTHERM SH has higher operational temperature limit and it is already used in an ORC plant, it is a reasonable choice for the simulation purposes. Properties of the thermal oil boiler were added to SOLVO by Fortum.

5.2.3 ORC cycle

Electricity from an ORC plant is obviously produced by the ORC cycle. This is the part of the model where all the property functions described in the previous chapter are used. The ORC cycle of the SOLVO simulation model is illustrated in Figure 50.

The ORC cycle is interlinked with thermooil boiler via a heat source which represents the evaporator of Figure 46. In thermooil cycle temperature of oil decreases in a heat source and transfers heat power to the ORC cycle. In the heat source of Figure 50 that heat power is used to evaporate organic working medium. There is a function in SOLVO which takes care that powers of the heat sources are equal. It must be noted that the high pressure of the ORC cycle must be set so that temperature of saturated steam in that pressure does not exceed the high temperature of the outgoing thermal oil. For example, if thermal oil from the boiler is at 350 ^{o}C temperature, then the pressure before the turbine in the ORC cycle can be approximately 5 bar at maximum.

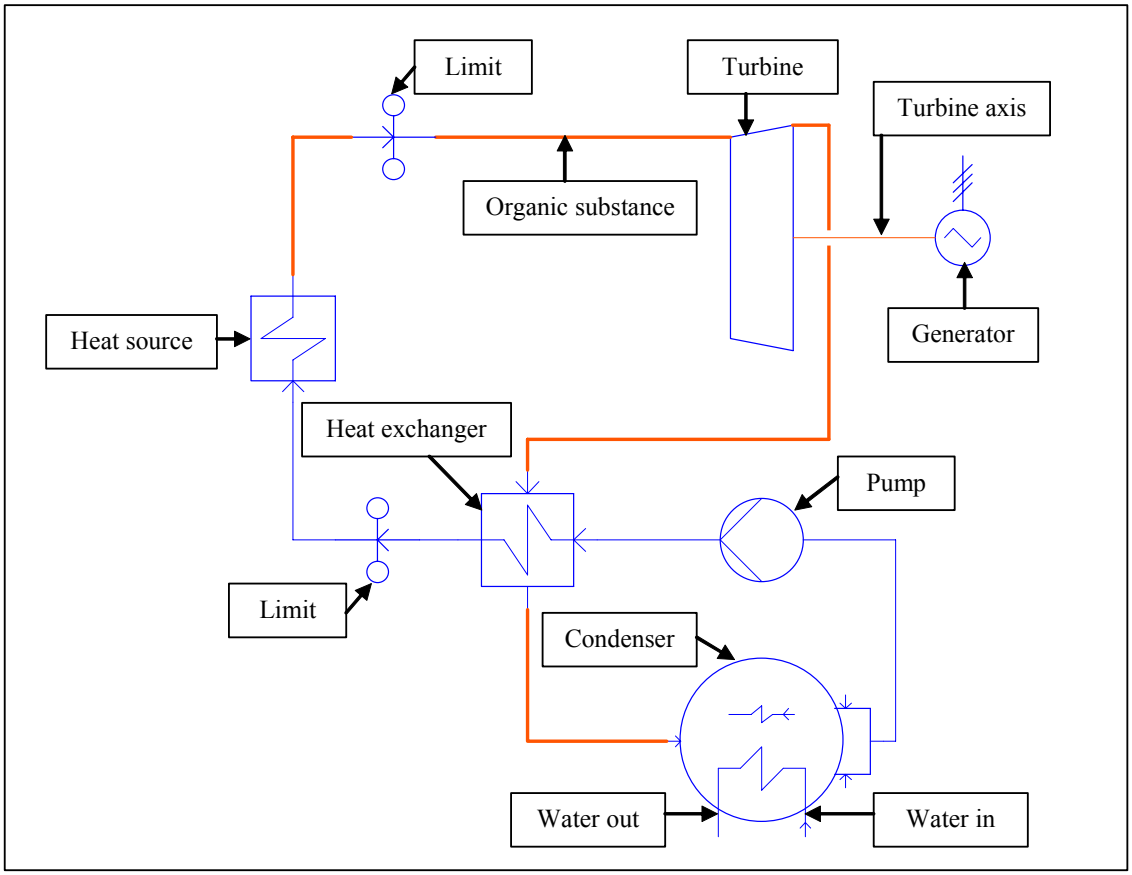

Figure 50. ORC cycle part of the SOLVO simulation model with components and substance flows labeled.

Since the evaporator of the ORC cycle is modeled in this SOLVO simulation by matching the heat powers of the two heat sources, the rules of thermodynamics must be taken care of by the user. SOLVO just takes the heat power of thermo-oil heat source and heats up the organic substance without considering temperatures. However, the end temperature of the organic substance cannot exceed the starting temperature of the thermal oil. Therefore, there is a separate controller in the SOLVO model in order to manage the temperatures. This controller sets the mass flow of the ORC cycle so that the ORC end temperature stays below the thermo-oil starting temperature.

Hereby, pressure, temperature and mass flow of the organic substance before the turbine are defined by the characteristics of the thermo-oil cycle. In turbine organic steam expands to lower condensing pressure with isentropic efficiency of the turbine defining end enthalpy. Electricity is generated by multiplying enthalpy difference of the turbine expansion and mass flow.

After the turbine, organic substance is still superheated steam at the condensing pressure due to the thermodynamical charasteristics of the organic working medium. Temperature of superheated steam is higher than the temperature of saturated steam at condensing pressure. In Figure 50 it is illustrated that superheated steam is cooled down in a heat exchanger which heats up the high pressure organic working medium before the evaporator i.e. the heatsource. In order to perform this cooling of the superheated steam, the heat exchanger in SOLVO must be set to desuperheater mode. It is reasonable to cool the superheated steam near the temperature of saturated steam. Therefore, the end temperature of the low pressure steam in heat exchanger is set to few degrees above the temperature of saturated steam.

In the condenser organic substance is condensed to liquid and the transferred heat power is used to heat the water in the district heating cycle. After the condenser organic liquid is pumped to higher pressure which is defined by thermo-oil cycle. This high pressure liquid is then heated up in the heat exchanger and finally evaporated in the heat source. It must be noted that condensing pressure should be so low that the terminal temperature difference, i.e. the difference between the condensed organic substance temperature and heated water temperature, does not exceed the maximum value of 60 C° defined in SOLVO.

5.2.4 District heating cycle

Since the simulated ORC plant is a CHP plant, the heat power transferred from the ORC condenser is used to heat water required by the district heating system. In Figure 46 it can be seen that district heating water is warmed in series in a condenser and in an economiser. From Figure 47 it can be noticed that subject to SOLVO topology condenser is in the ORC turbine plant whereas the economiser is in the boiler plant.

The usual specification of district heating system is as follows: water is in constant pressure of 6 bar, going water temperature is 50 ^{o}C and coming water temperature is 115 ^{o}C. It depends on the simulation how much condenser or economiser heat up water. If thermooil boiler produces constant heat power to the ORC cycle, the mass flow of organic working medium is set by the end temperature of the ORC heat source. Furthermore, the fixed mass flow defines the condensing power transferred to the district heating cycle. Therefore, it depends on the mass flow of heated water how high a temperature the water has after the condenser and how much is left to the economiser to be heated. The heat power of the economiser depends on flue gases of the boiler, but this will be discussed in the next subchapter.

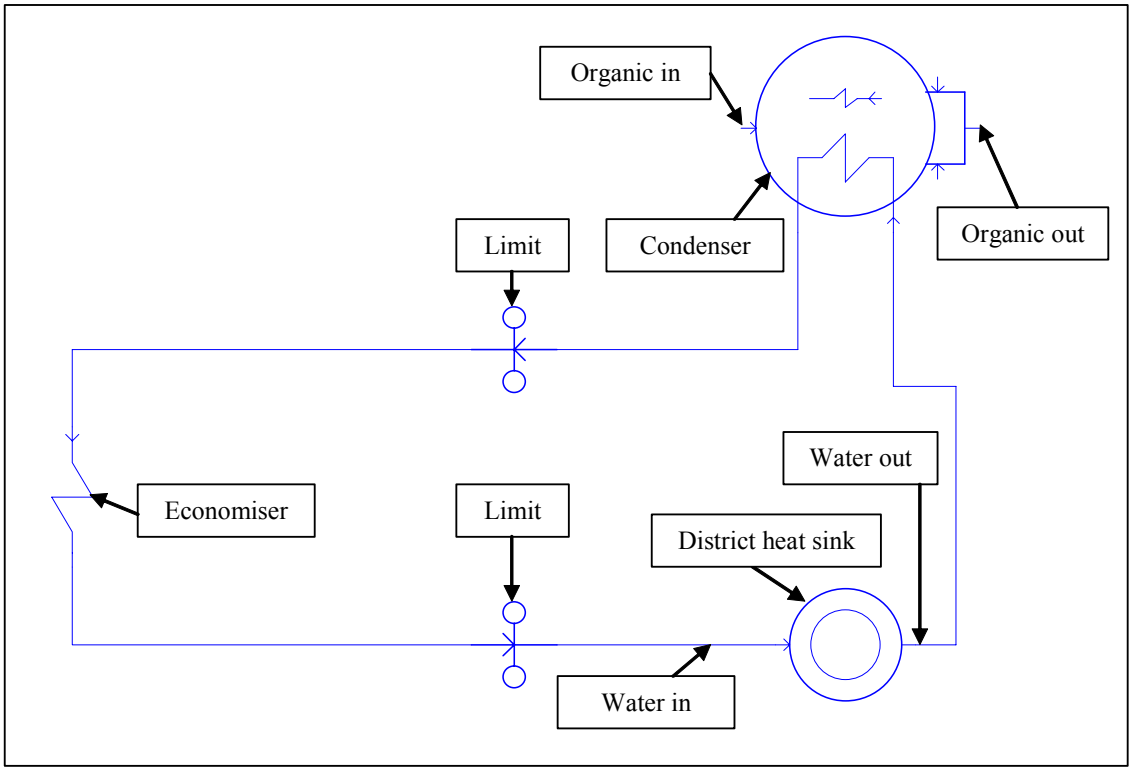

Figure 51. District heat cycle part of the SOLVO simulation model with components and substance flows labeled.

In the cycle illustrated in Figure 51 the district heat sink represents heating power used. In this sink the district heat pressure, starting and end temperatures are set. Although the end temperature can be fixed in the economiser too, it has to be set also in the sink so that water mass flow can be altered in simulation. After the sink the district heat cycle is quite straightforward. Water is heated in condenser and then further in economiser.

Obviously, the district heat mass flow is optimised in SOLVO in such a manner that the condenser preheats water and then the economiser uses as much as possible of flue gas power to heat water to required temperature of 115 °C. Therefore, it is not easy to simulate cases of part load subject to district heat due to the fluctuation of water mass flow. The part load cases are rather simulated by setting the thermal oil mass flow to part load and then observing the district heating power.

5.2.5 Flue gas system

The final part of model illustrated in Figure 47 to be described here in detail is the flue gas system linked to the boiler. The heat power of flue gases can be fully utilised, since there are no constraints for these emitted gases. In Admont ORC plant of Figure 46

there is just an economiser to take advantage of the flue gas heat. However, in this project a combustion air pre-heater is added to the simulation model in order to improve the process. The combustion air pre-heater uses flue gases to heat the air used in the boiler from room temperature to e.g. 300 °C and thereby improving the boiler efficiency and decreasing the fuel power.

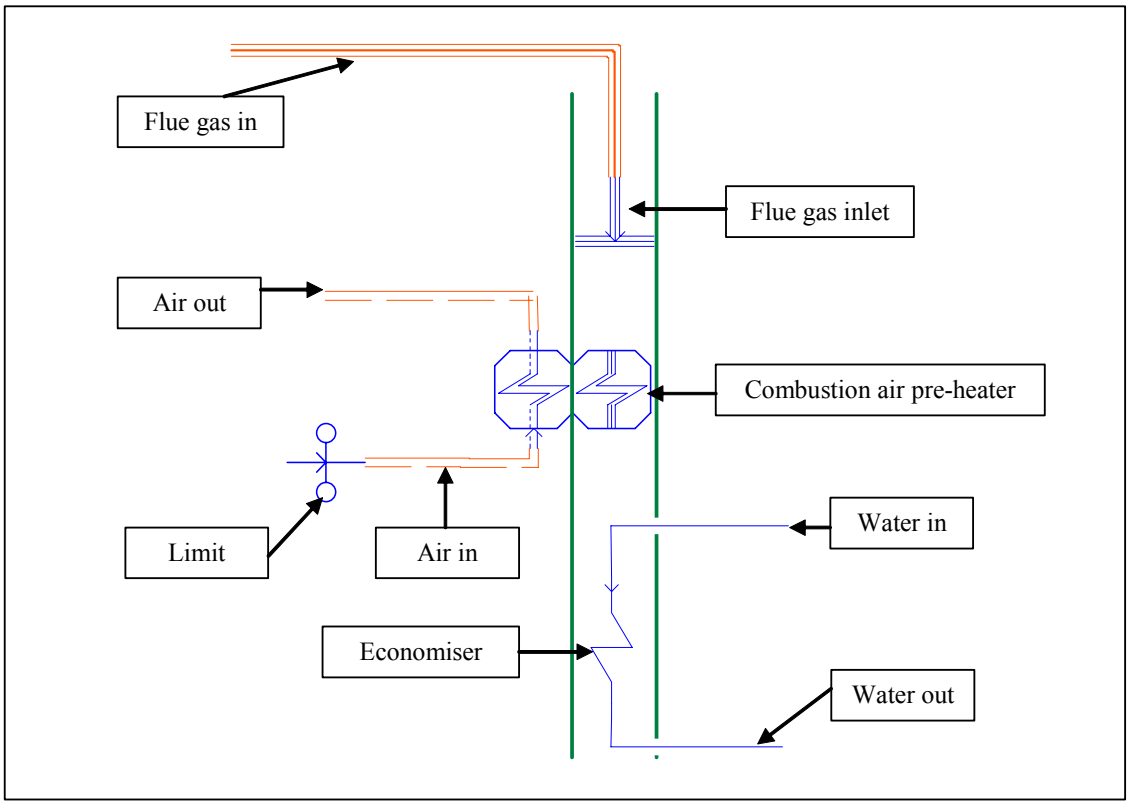

Figure 52. Flue gas part of the SOLVO simulation model with components and substance flows labeled.

In Figure 52 the flue gas system of the SOLVO model is illustrated. First of all flue gas temperature must be set in the boiler. The flue gas is then transferred to the flue gas inlet which defines the start of the flue gas channel described in Figure 52 with green lines. In SOLVO components using flue gases must be set to zones which define in which order the components use flue gases. In this case the inlet gets the zone number 1, air pre-heater gets number 2 and economiser number 3.

The air going to the combustion air pre-heater is set to room pressure and temperature in the limit component, and then the end temperature is set in the pre-heater. When setting the end temperature of air, also the flue gas end temperature must be considered. Flue gas going to the economiser must be hot enough to be able to heat the water up to 115 °C.

As was stated above the end temperature of the flue gas from the combustion air pre-heater must be above the end temperature of district heat water. Furthermore, according to the rules of thermodynamics, the starting end temperature of flue gases from the economiser must be above the starting temperature of water coming to the economiser. It must be noticed that in Figure 52 the direction of the economiser subject to the flue gas channel does not imply that the economiser would be a parallel-flow model. Instead, in this model counter-current economiser was assumed, and therefore the assumptions on the starting and end temperatures hold true.

5.3 Simulation and results

In the previous chapter the structure of the SOLVO simulation model was presented. The purpose of this project is to use that model based on Admont ORC plant in order to analyse the characteristics of an ORC process using Diphenyl-DiphenylEther as a working medium. Furthermore, by tuning and expanding the basic model illustrated in Figure 10 the possibilities of improving the ORC process can be studied.

The main measurements of CHP plants are total efficiency and power-to-heat ratio. Total efficiency of a CHP plant is calculated by dividing the sum of produced electricity and heat power by power of used fuel. In SOLVO these values can be read from the powers of generator, district heat sink and fuel tank. Power-to-heat ratio is calculated by dividing produced electricity power by produced heat power. Another measurement of the process is electricity efficiency i.e. the ratio between produced electricity and consumed fuel.

Usually, in this kind of thermodynamical process the load of the boiler defines the total efficiency. However, the end temperature of the flue gases leaving the system affects total efficiency too, but in smaller scale than boiler load. On the other hand, power-to-heat ratio cannot be affected as easily by altering boiler load, but structural and inner changes of the process are required. In the SOLVO simulations performed in this project both structural and load based alterations were examined and results are presented in this chapter.

5.3.1 Simulation cases and parameters

There were numerous simulation cases performed with SOLVO model in this project. Mostly, these cases differ by the thermodynamical parameters, since tuning the model described in the previous chapter is the first priority. However, there is also a need for changing the structure of this model in order to examine possibilities of improving the power-to-heat ratio. In the following several simulation cases are described for two

different SOLVO models: basic model presented in the previous chapter and double model as the improved process model with double organic cycle.

5.3.1.1 Basic model

The basic model is the case from which all the other cases are modified. These modifications are mostly alterations in thermodynamical parameters, such as mass flow, pressure and temperature. In the case definitions abbreviations are used and the first case is obviously basic model:

BM: basic model

Most of the simulation cases are based on the basic model with slight parameter changes. Therefore, it is reasonable to firstly represent all the necessary parameters of the basic model. It must be noted that the technical parameters of the simulation model are default values of SOLVO and they represent accustomed values for the corresponding components. It is not reasonable to define as accurate technical parameters as possible for the process components, because there is not data available of the components used in the existing ORC plants. Also, there are components in the SOLVO model such as the evaporator for which no technical parameters can be set, since it is merely a combination of heat sources. However, some technical parameters should be mentioned. The isentropic efficiency of the turbine in the organic cycle is 85% and for the pump this parameter value is 75%. Furthermore, the surface of the heat exchanger in the organic cycle is 300 m^2. All these are default values in SOLVO.

Thermodynamical parameters of the basic model are far more important than technical parameteres, since they define the process and affect greatly electricity and heat production. In the previous chapter the properties of thermal oil were examined and the upper limit of the thermooil temperature is considered to be 350 ^oC. Therefore, temperature of thermal oil leaving the boiler is set to 350 ^oC.

In the Lienz ORC plant the temperature drop in the evaporator is 50 ^oC, and therefore the temperature of thermal oil coming back to the boiler is set to 300 ^oC. Furthermore, pressure of the thermooil cycle is 6 bar and mass flow is 14 kg/s. Actually, since thermal oil is modelled in SOLVO to be in liquid form in the boiler and in the cycle, pressure is an irrelevant factor.

Other boiler related parameters define values of fuel, combustion air and flue gases. Fuel used in the boiler is wood and contents of wood fuel are default values of SOLVO. Fuel is supplied to the boiler in 1 bar pressure and 10 ^oC temperature. The initial state of

combustion air is 1 bar pressure and 20 °C temperature, but air temperature is increased by the pre-heater to 300 °C. Flue gas emitted from the boiler is set to 400 °C temperature.

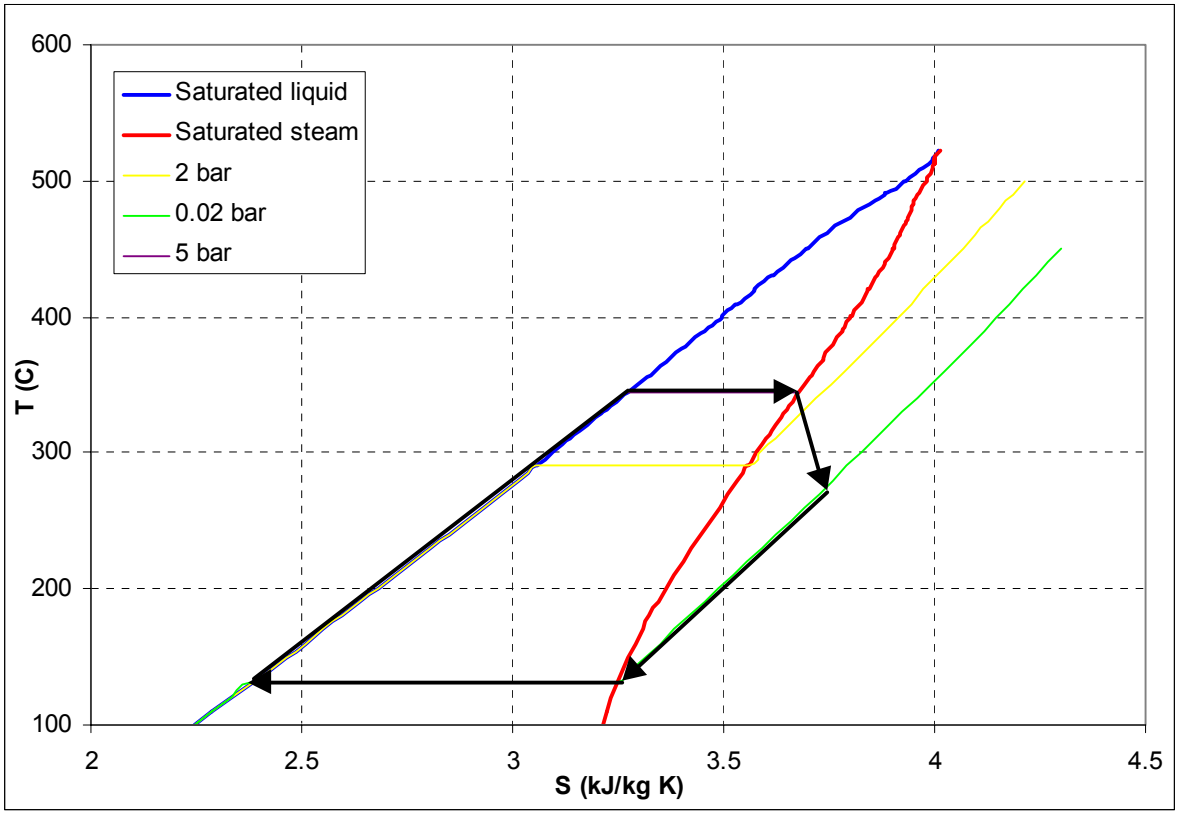

Figure 53. Process cycle of the basic model case in the T,s -diagram of the organic substance.

In the organic cycle the high pressure is set to 5 bar and temperature after the heat source to 348 °C. This is an optimal state subject to thermal oil temperature, and in this temperature and pressure organic working medium is only just in the vapour form i.e. superheating is minimal. Lower pressure is set to 0.02 bar which is as low as possible in order to obtain sufficiently low condensing temperature. The end temperature of the heat exchanger operating as desuperheater is set to 132 °C which is just above the temperature of saturated steam at 0.02 bar pressure. Mass flow of the organic cycle is set by SOLVO such that the heat source gives an end temperature of 348 °C. The T,s -diagram of the organic cycle in the basic model case is illustrated in Figure 53.

Thermodynamical parameters of the district heating cycle are quite simple. Start temperature of water is 50 °C and end temperature 115 °C. Pressure of the district heat water is set to 6 bar. Mass flow is determined by SOLVO so that end temperature of the flue gas from the economiser is as low as thermodynamically possible.

The first alteration from the basic model is the case of part load. Generally, using part load in the process decreases total efficiency and in this case part load is examined by setting the thermooil mass flow to 7 kg/s. Usually, part load analysis in CHP process is performed by setting district heat load to smaller level. However, in this SOLVO model district heat mass flow is determined by the combination of organic cycle and flue gas channel. Therefore, part load is analysed subject to thermooil cycle. Identifier of the part load case is the following:

BM PL: basic model with part load

Temperature of flue gas leaving the boiler is set to 400 ^{o}C in the basic model. This temperature affects naturally district heating via the economiser, but flue gas temperature has also an effect on boiler efficiency. Thus, higher flue gas temperature increases consumed fuel power but increases heating power of the economiser too. The effect of flue gas temperature was examined by increasing this temperature from the basic model to value 500 ^{o}C. The case of flue gas analysis is labeled as follows:

BM FG 500: basic model with flue gas temperature at 500 ^{o}C

Other temperature related cases concern combustion air pre-heating. In the basic model combustion air heated to 300 ^{o}C before going to the boiler. Pre-heating improves boiler efficiency, but decreases heating power of the economiser. Three different cases of air pre-heating were examined with air end temperatures of 200 ^{o}C, 100 ^{o}C and with pre-heater switched off. These cases are labeled as follows:

BM PH 200: basic model with combustion air pre-heated to 200 ^{o}C

BM PH 100: basic model with combustion air pre-heated to 100 ^{o}C

BM PH OFF: basic model with combustion air pre-heater switched off.

The previous simulation cases concerned the boiler cycle and the flue gas channel. However, it is highly important to make alterations to the organic cycle too in an attempt to improve power-to-heat ratio. One way to analyse the organic cycle is to alter the high pressure which is 5 bar before the turbine in the basic model case. If high pressure decreases, temperature of thermal oil can be lowered too.

In Lienz ORC plant thermal oil is heated in the boiler from 250 ^{o}C to 300 ^{o}C. This upper limit of 300 ^{o}C temperature equals approximately 2 bar of pressure in the organic cycle since temperature of saturated steam at 2 bar pressure is 296 ^{o}C. This lower presssure case is labeled as follows:

BM 2B: basic model with organic cycle pressure 2 bar and thermal oil temperature 300 ^{o}C

Another interesting case is examining the effect of superheating in the organic cycle. In the basic model there is no possibility to superheat organic medium before the turbine, since temperature after the evaporation is already 348 °C and thermal oil temperature of 350 °C sets the upper limit. However, if the thermal oil temperatures remain unchanged from the basic model case and pressure in the organic cycle is set to 2 bar, superheating of organic medium from 296 °C to 348 °C is possible. This case is shaped by setting the high pressure to 2 bar and end temperature of the organic heat source to 348 °C. The case of superheating changes the organic cycle in such a way that an analysis of part load as in the basic model case should be performed. Labels of these two cases are the following:

BM 2B SH: basic model with superheating in organic cycle

BM 2B SH PL: basic model with superheating in organic cycle and part load.

There are still two cases of modifications from the basic model. However, they are represented in the next subchapter, because these cases are in the context of double cycle model in which the basic model structure is altered.

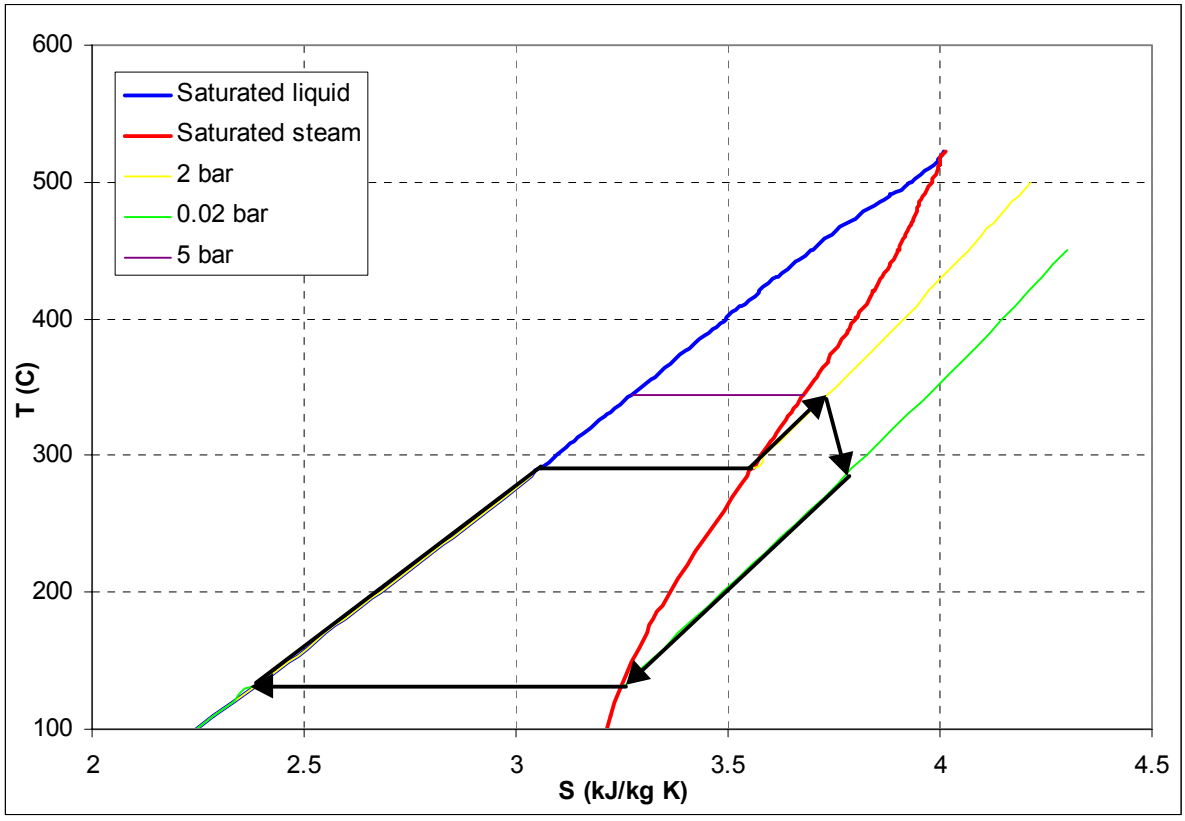

Figure 54. Process cycle of the superheated case in the T,s -diagram.

5.3.1.2 Double model

The SOLVO model illustrated in Figure 47 is based in Admont ORC plant of Figure 46 and its structure is quite straightforward. However, there are possibilities to expand the organic cycle in an attempt to improve the process. In regular power plants steam can make several cycles through different turbines and thereby improve efficiency or power-to-heat ratio. Double cycle model is the case in which this idea is applied to the organic cycle. This double case and the part load variation are labeled as follows:

DM: double cycle model

DM PL: double cycle model with part load.

In Figure 55 the organic cycle part of the double cycle model is illustrated. In the end of the cycle after the turbine #2 condensing pressure is 0.02 bar as in the basic model. Organic medium goes through the heat exchanger #1, condenser #1 and pump #1 as normally. After the pump #1 organic medium is at pressure 5 bar and it is warmed by heat exchanger #1 and in addition by heat exchanger #2.

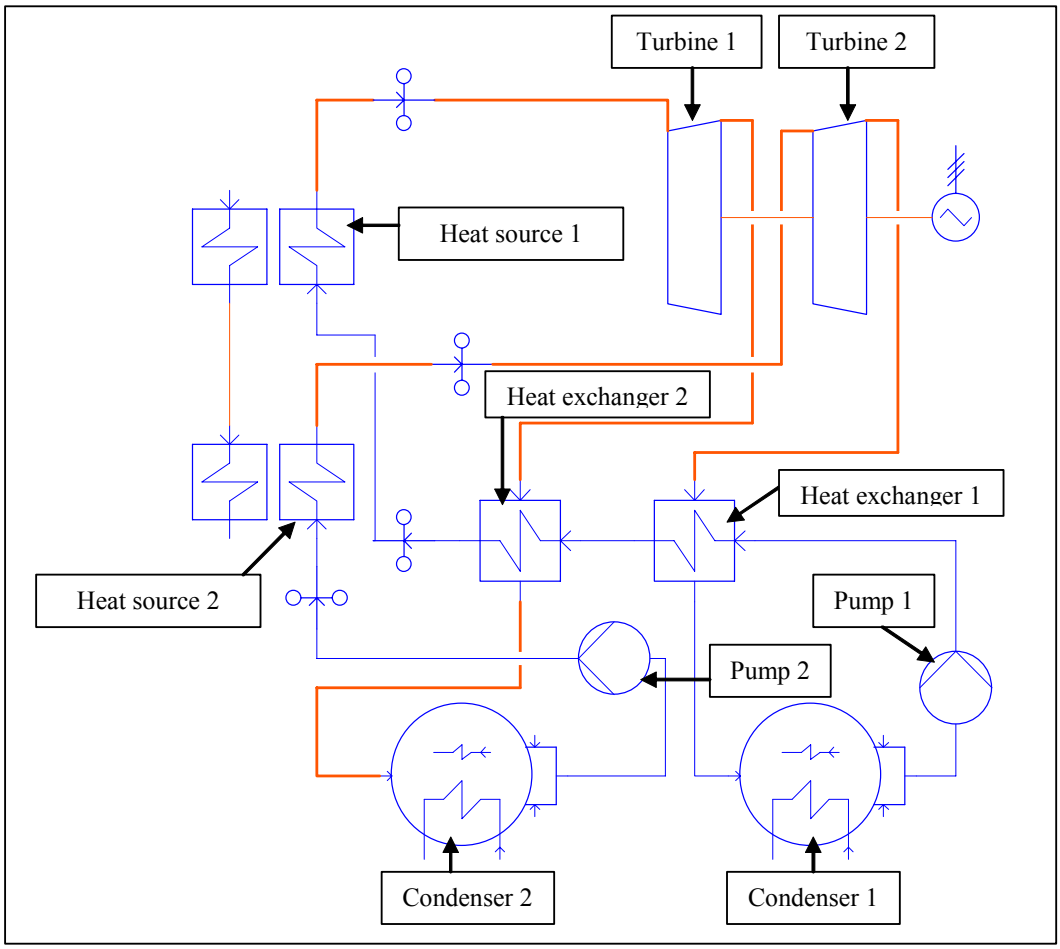

Figure 55. Structure of the organic cycle in the double cycle model case.

In the heat source #1 organic medium is evaporated to temperature 348 °C and in the corresponding heat source thermal oil cools down from 350 °C to 300 °C. By setting the end temperature of 348 °C in the organic heat source #1, mass flow of the organic cycle is determined. In turbine #1 organic medium expands to pressure of 0.08 bar and transfers heat to the first cycle. Condensing pressure of 0.08 bar is chosen by testing so that temperature difference between outgoing water and outgoing organic medium does not exceed 60 °C limit.

In the pump #2 pressure of organic medium is increased to 2 bar which equals the end temperature 296 °C of heat source #2. This temperature is defined obviously by the corresponding heat source in the thermooil cycle which has starting temperature set to 300 °C. Since organic mass flow is determined by the heat source #1 and end temperature of heat source #2 is set to 296 °C, end temperature of the thermooil cycle has to be altered by SOLVO in order to attain balance. The thermodynamic principle of the double cycle model is presented in the T,s -diagram of Figure 56.

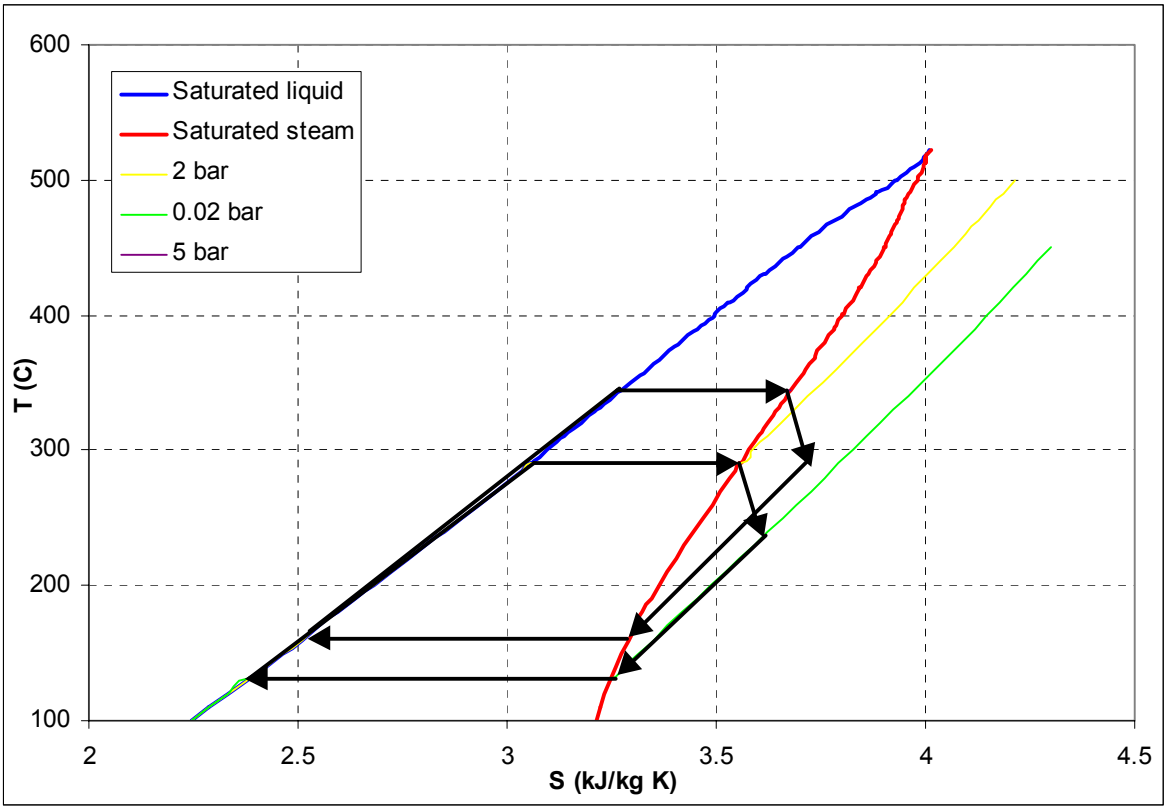

Figure 56. Process cycle of the double cycle model case in the T,s -diagram.

In all cases presented in the previous subchapter temperature drop in the thermooil heat source is 50 °C, mostly from 350 °C to 300 °C and from 300 °C to 250 °C in the DM 2B case. As stated before, in the double cycle model the end temperature of the thermal

oil is determined by SOLVO to balance the heat sources. Therefore it would be reasonable to examine the basic model with thermal oil end temperature which equals the value determined by SOLVO in the double cycle model. For example, if the double cycle model gives an end temperature of 250 °C for thermal oil, then in the modified basic model thermal oil would cool down in the heat source from 350 °C to 250 °C. This way double cycle model and basic model can be compared with identical boiler powers. These cases are labeled as:

BM DMT: basic model with double cycle model end temperature

BM DMT PL: basic model with double cycle model end temperature and part load.

As usual part load means also in all these cases mass flow of 7 kg/s in the thermooil cycle. It should be noted that in the part load case the thermal oil end temperature is set to equal the end temperature of the double model part load case.

5.3.2 Results

All of the cases described in the previous subchapter were simulated by SOLVO and result data was documented. In SOLVO the calculation results are presented on top of the model graph such as presented in Figure 48, so that different process values in any part of the process can be viewed by user. In SOLVO calculation graphs there is a standard matrix form of presenting process data. In the process value matrix top left corner is mass flow (kg/s), top right corner is pressure (bar), bottom left corner is temperature (°C) and bottom right corner is enthalpy (kJ/kg). In flue gas channel there are single values labeled with t which means flue gas temperature. Also, the single values with bold font attached to the SOLVO components stand for component powers. One important component in the SOLVO process graph is the summary plant labeled with sigma, by which are total process values: total efficiency, electricity efficiency and power-to-heat ratio.

5.3.2.1 Detailed results of BM and DM

It would be impractical and too voluminous to present in this report SOLVO process graphs from all the simulated cases. Therefore, only the basic model case and double cycle model case are illustrated here in detail. Basic model is presented in Figure 58 and double cycle model in Figure 59. Summarised results from other cases are presented later in this subchapter.

First case examined in detail is the basic model case from Figure 58. Gross total efficiency is 84.4%, electricity efficiency is 21.9% and power-to-heat ratio is 0.35. It must be noted that gross total efficiency is used due to the behaviour of the pump which is the only component consuming electricity. From Figure 58 it can be observed that during the increase of pressure from 0.02 bar to 5 bar, temperature decreases marginally instead of a thermodynamically correct increase. This defect is based on the error marginals of the property functions. It is difficult to estimate how much this error affects the difference between enthalpy values and thus the pump power, but overall power of pumping pressure from 0.02 bar to 5 bar is relatively small and it can be ignored. Therefore, gross total efficiency can be used instead of net efficiency.

In the organic cycle desuperheating of low pressure steam heats up high pressure organic liquid to 246 °C and therefore there remains approximately 100 °C of temperature difference to be heated by the thermal oil before evaporation. Effect of flue gases on district heating is quite small, since 94% of heating power comes through ORC condenser. Also, temperature rise of district heating water after the condenser is merely 3.6 °C. With flue gas temperature of 400 °C efficiency of the boiler is 73%.

Second case examined here is the double cycle model illustrated in detail in Figure 59. Total efficiency is 88.8%, electricity efficiency 17.7% and power-to-heat ratio is 0.25. It can be seen that the end temperature of thermal oil is set by SOLVO to 225 °C in order to obtain balance. Therefore, boiler power is greater than in the basic model case and boiler efficiency of 77% is higher. Hereby, the end temperature of thermal oil in the BM DMT case was set to 225 °C.

Although boiler power is 2.3 times as great as in the basic model, the corresponding factor for generated electricity power is only 1.8 and for district heat 2.5. Since the effect of flue gases is as minimal as in the basic model case, reason for low power-to-heat ratio must be found from the double cycle structure. It can be observed that condenser #2 gets steam nearly 50 °C hotter than condensing temperature, since end temperature of cooling steam cannot go below starting temperature of heated liquid in the heat exchanger #2. Although it remains merely 70 °C to be heated by the heat source #1 and therefore organic mass flow can be increased to 6.5 kg/s compared to 5.6 kg/s of basic model case, heating of 110 °C temperature difference before evaporation is left to responsibility of heat source #2. This temperature difference and greater organic mass flow cause the low end temperature of thermo-oil cycle.

It seems as if there was no real advantage of the double cycle structure, on the contrary power-to-heat ratio decreases by these changes. Since the condensers in the organic cycle get superheated steam, they transfer extra heat energy to district heating and no significant extra electricity is gained. Furthermore, double cycle structure means also raising costs in infrastructure. However, final judgement of double cycle model can be obtained by comparing it to basic model with similar boiler parameters i.e. case BM DMT.

5.3.2.2 Results from all cases

Basic model and double cycle model cases were examined above in detail, but the remaining cases must be analysed too. Total efficiencies, electricity efficiencies and power-to-heat-ratios were gathered from all the simulations. In Table 13 these values are represented.

Table 13. Gross total efficiencies, electricity efficiencies and power-to-heat ratios of all the simulated cases.

Case	Total efficiency	Electricity efficiency	Power-to-heat ratio
BM	84.4%	21.9%	0.350
BM PL	77.7%	20.1%	0.348
BM FG 500	85.0%	20.7%	0.322
BM PH 200	84.8%	21.0%	0.329
BM PH 100	85.1%	20.1%	0.310
BM PH OFF	85.7%	19.5%	0.294
BM 2B	83.6%	18.0%	0.274
BM 2B SH	84.3%	19.5%	0.300
BM 2B SH PL	77.7%	17.9%	0.299
DM	88.8%	17.7%	0.248
DM PL	85.4%	17.0%	0.248
BM DMT	88.8%	23.1%	0.351
BM DMT PL	85.3%	22.1%	0.351

The effect of part load in thermo-oil boiler on basic model case is visible subject to total efficiency but power-to-heat ratio does not change much. Apparently, only the boiler efficiency is affected significantly by part load of boiler. In the part load case mass flow of district heat water approximately half of the full load case, and therefore choice of setting part load subject to thermal oil mass flow can be justified.

Higher flue gas temperature has an obvious effect on the process: Heat power from economiser increases by 185 kW, whereas consumed fuel power increases by 195 kW. Total efficiency rises slightly, but power-to-heat ratio decreases, since district heat power increases while generated electricity remains unchanged. Alterations in end temperature of pre-heated combustion air cause decline in power-to-heat ratio too. Since

more heat energy of flue gases after the pre-heater is available to economiser, power-to-heat ratio decreases from 0.350 of basic model case to 0.294 when pre-heater is switched off. There is also a visible increasing trend in total efficiency when combustion air is heated less. This can be explained by the temperatures of flue gases leaving the process. When district heat water gets more power from the flue gases, mass flow of water can be higher and consequently temperature of water coming to the economiser lower. Therefore, temperature of flue gases leaving the economiser can be lower and this increases total efficiency.

When pressure in the organic cycle is changed to 2 bar, total efficiency and power-to-heat ratio decrease. Electricity generated by the turbine decreases due to smaller enthalpy difference of expansion from 2 bar to 0.02 bar. Since thermal oil cools down from 300 C° to 250 C° in 2 bar case, boiler power and thereby fuel power is on lower level. However, characteristics of basic model provide much better electricity efficiency. When pressure of organic cycle remains at 2 bar but thermal oil is heated to 350 C°, organic working medium can be superheated to 348 C°. This superheating has slightly better power-to-heat ratio of 0.300, but basic model has still higher value. Although in the superheated case organic mass flow is greater than in the basic model case, generated power is lower due to the smaller enthalpy difference in the expansion.

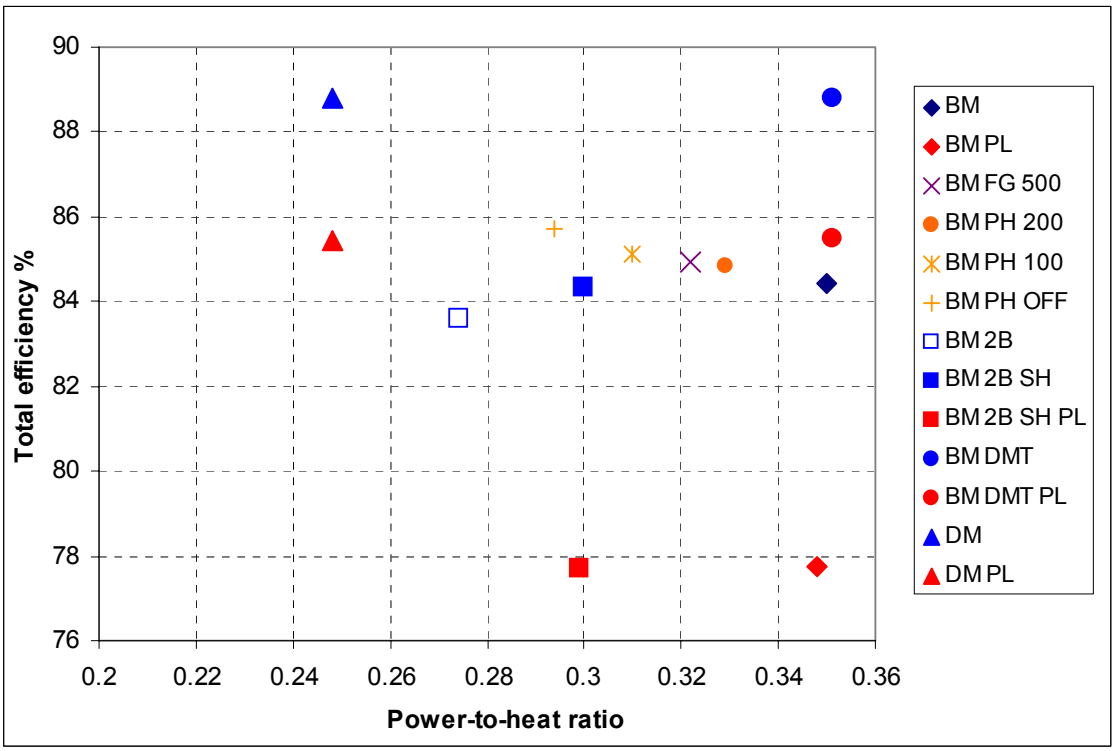

Figure 57. Total efficiencies and power-to-heat ratios of the simulated cases.

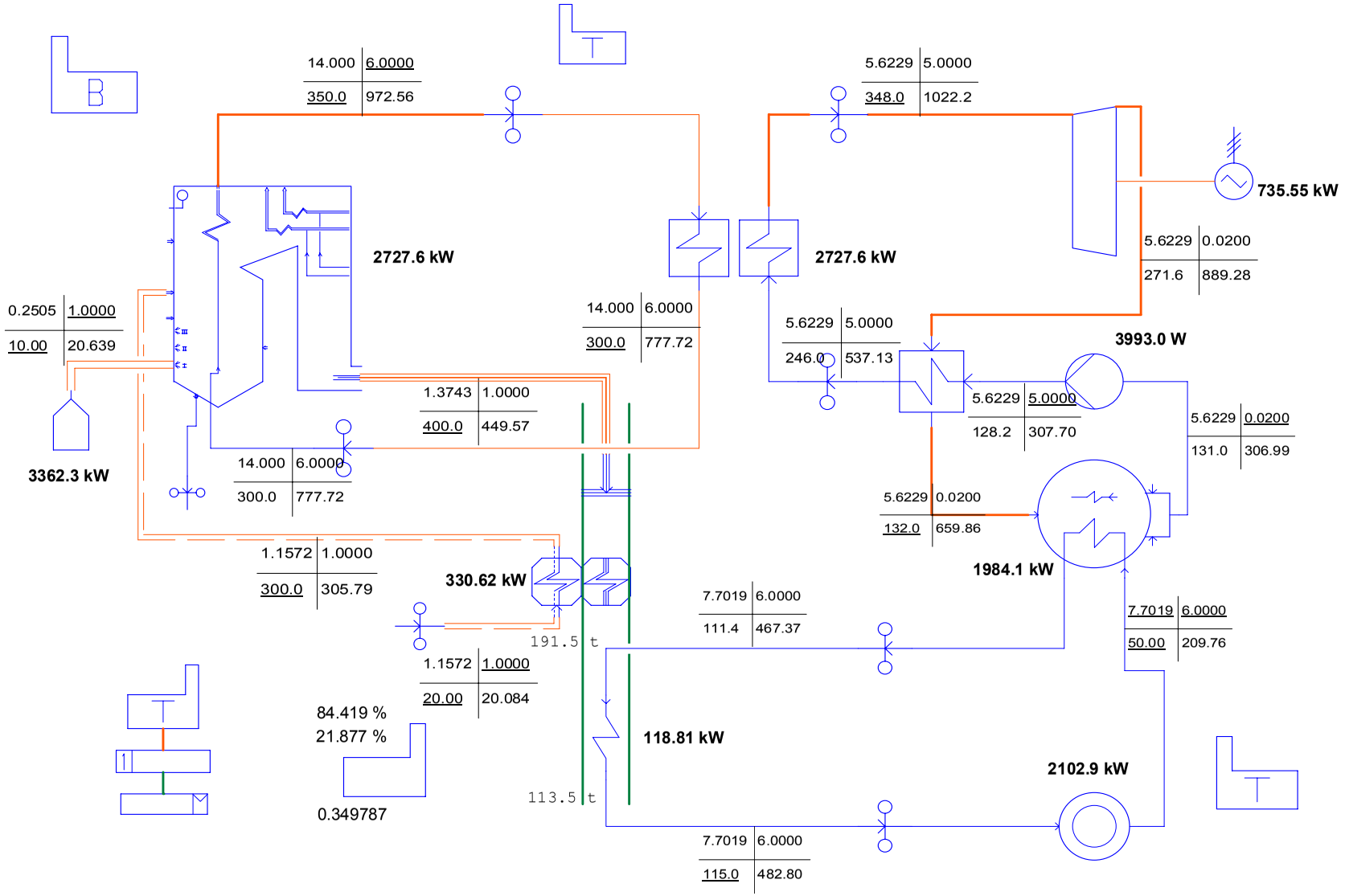

Figure 58. Simulation results of the basic model case.

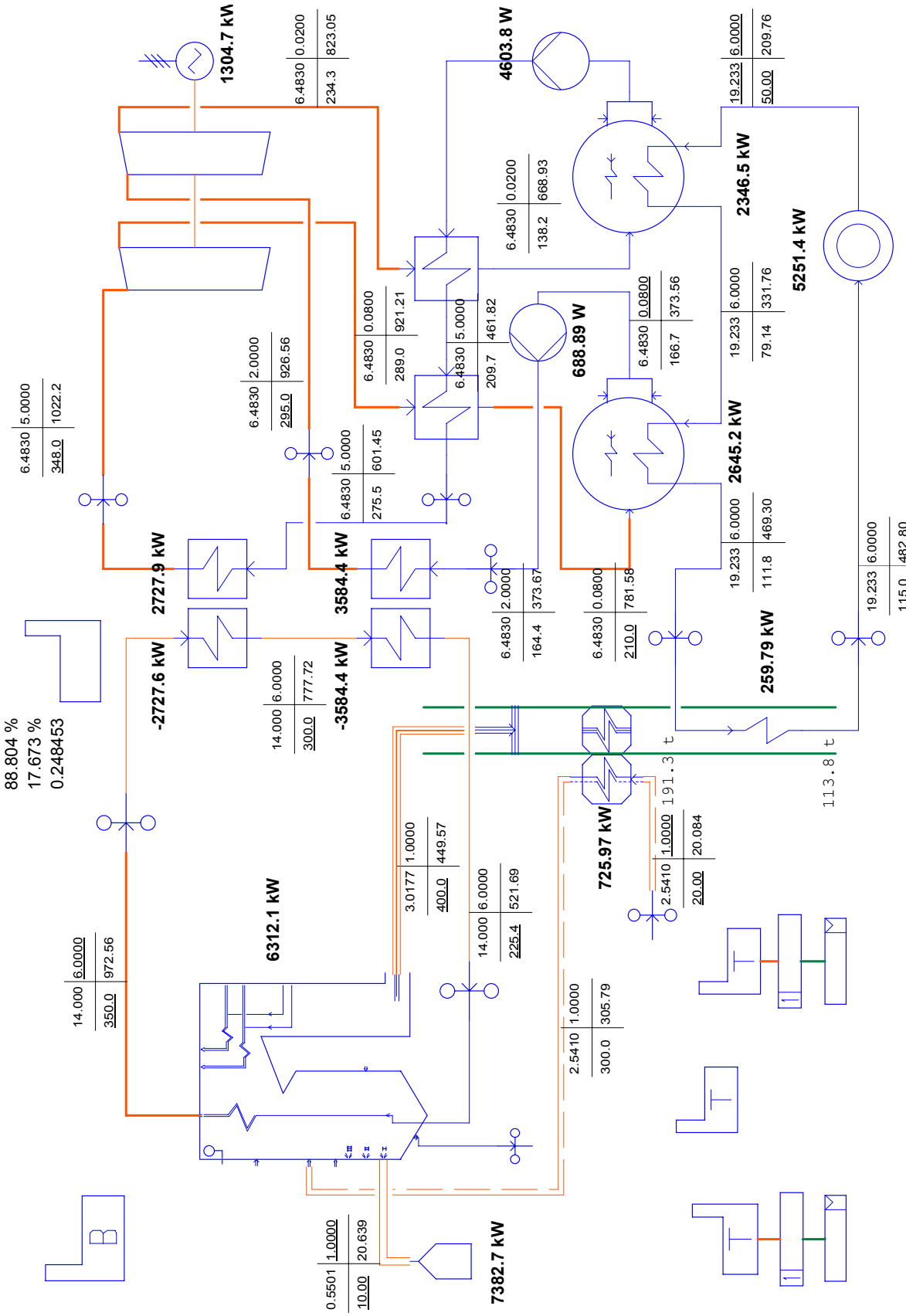

Figure 59. Simulation results of the double cycle model case.

From Figure 57 it can be seen that all the full load cases of the basic model have total efficiencies on similar level. However, double cycle model case has clearly higher total efficiency, since thermo-oil cycle has different parametrisation: End temperature of thermal oil depends on the organic cycle. Regardless of high total efficiency based on greater boiler power, power-to-heat ratio is lowest of all cases.

However, when setting end temperature of thermal oil in the basic model to 225 °C as in double cycle model, highest electricity efficiency value is achieved. It seems that broader temperature scale of thermo-oil cycle increases electricity production effectively. This result indicates that double cycle structure has no positive effect on ORC plant, on the contrary, it decreases power-to-heat ratio and increases costs.

The extra investment cost of the ORC plant has not been evaluated in the project, because those extra features require special constructions. It is difficult to have reliable cost offers from producers to those fabricated extra parts of ORC plant.

5.4 Conclusions

In this project properties of an organic substance were examined and attached to SOLVO simulation program in order to simulate an ORC plant and thereby evaluate possibilities of improvements to power-to-heat ratio of the plant. The organic substance modelled for the simulation purposes was Diphenyl-DiphenylEther and it proved to be a potential working medium for an ORC plant. It would be reasonable to examine other organic substances and use them in simulations. However, it is a highly laborious way from substance properties to simulations and therefore only Diphenyl-DiphenylEther was analysed. From the substance property point of view the original pressure scale of 0.01 bar–36 bar proved to be unnecessarily large, since temperature limit of thermal oil set the pressure upper limit to 5 bar. Probably the fitted property functions would have been more accurate with smaller pressure span and tighter grid of calculation points.

Simulation results indicate that the most simple structure is the best choice for ORC plant subject to power-to-heat ratio. Only the combustion pre-heater has a positive effect on electricity efficiency when compared to the Admont ORC plant of Figure 46, although pre-heater does not affect electricity production at all but it improves boiler efficiency. Any changes in the organic cycle, superheating or double cycle structure, only lower power-to-heat ratio. It seems that turbine expansion from the saturated steam temperature is optimal for the ORC plant. Since one of the reasons behind choosing organic substance for working medium is avoiding moist steam in the turbine, it is not reasonable to examine whether starting turbine expansion from the moist steam area were worthwhile.

6. Summary

The CHP potential in Finland has been evaluated to be 80 MW of electricity and 214 MW of heat. The annual peak load time was 6000 hours based on district heat energy production in biofuelled CHP in 2000 plants. The total amount of possible CHP units is 51. 90% of the potential CHP plants are smaller than 10 MW in thermal effect. The range 1–5 MW covers the most part of the CHP amount with the proportion of 53%.

The profitability of an investment in a small biofuel-fired CHP plant was also studied. An optimisation model describing production, distribution and consumption of the heat was constructed. This model combines characteristics from operational and design models, which have previously been used separately. The energy production from the CHP plants is based on simulations done for three different plants, thus giving a wider perspective on the behaviour of such plant.

The results indicate, that the economically feasible scale for biofuel-fired CHP plants remains relatively large; when a biofuel-fired boiler is among the options for heat production, no investment is made in the smallest of three CHP plants. Specific investment costs for the two larger plants could be only slightly higher until no investment in them would be made either. This means, that if these plants were scaled down, their specific investment cost should not rise considerably. A rise of 3 percent in the discount rate causes again the same effect. When it is taken into account, that the future electricity prices are not deterministic in the real world and therefore a higher rate of return is required, the competitiveness of the biofuel-fired boiler increases even more. This competitive edge of the heat-only boiler has been noted before. Emission trading and the resulting rise in the price of electricity or increased subsidies could tip the scales in favor of CHP plant in the future. More research is needed to estimate the effects of short and long term uncertainties on investment decisions.

In this work possibilities to increase the power production and the power-to-heat ratio of 1–20 MW_e CHP plants using biomass fuels were studied with simulation and optimisation tools. The basis for the simulations and optimisations was the data collected from Finnish and Swedish small-scale CHP plants between 2002 and 2004. In order to test the considered changes four existing CHP plants from Finland and Sweden were selected to represent the different size CHP processes. The results showed that the addition of a feed water preheater, a steam reheater, and a two-stage district heat exchanger to the selected CHP plant cases was profitable with the current electricity price of 30 €/MWh. This increased the power-to-heat ratios from 0.23–0.50 to 0.45–0.50 depending on the case plant. The considered integration of a gas engine needed electricity prices over 42–45 €/MWh but increased the power-to-heat ratios to 0.59–0.78.

The integration of a gas turbine to the case plants was not profitable in the analysed electricity price range. The ratio of electricity price to natural gas price should have been at least 3.5–4.0 before the gas turbine integration to these cases would have become profitable.

Overall, the addition of a feed water preheater, a steam reheater, and a two-stage district heat exchanger seemed to be the most promising alternatives for increasing the power production in all the case plant sizes between 1–20 MW_e. When the simulation results and the optimisation results were compared, higher profits were gained with the process change combinations suggested by the optimisation model than with the separate process changes evaluated one-by-one with the simulation models. Thus, when applied to the existing CHP plants, the constructed MINLP model showed its capability to handle the trade-offs between power production, efficiency, costs, and the complexity of the process.

ORC process plant is evaluated as one possibility for a small scale biofuelled CHP power plant. The organic substance to be used is Diphenyl-DiphenylEther, which is a mixture of two substances. In order to calculate the substance properties, ASPENPlus-software was used. This software evaluates by using given parameters, quantities of chemical thermodynamics for the chosen substance. There are three thermodynamical areas: liquid, moist steam and dry steam. Based on the organic substance properties the property functions have been developed in Fortran code for SOLVO calculation software. The functions required by SOLVO define the interdependencies of the different variables. In simulation not all the dependencies are necessary, but in total 15 functions must be fitted. ORC-plant process was simulated with SOLVO software.

Simulation is first modelled for the Admont ORC plant in Austria with Diphenyl-DiphenylEther as a working medium and secondly to explore possibilities of improvements by adding some new properties to the current Admont plant model. Possibilities to improve the basic process were to make the process starting point (pressure and temperature) higher after the boiler, to change the temperature of the preheated air and to use double circle organic process.

In this project properties of an organic substance were examined and attached to SOLVO simulation program in order to simulate an ORC plant and thereby evaluate possibilities of improvements to power-to-heat ratio of the plant. The organic substance modelled for the simulation purposes was Diphenyl-DiphenylEther and it proved to be a potential working medium for an ORC plant. It would be reasonable to examine other organic substances and use them in simulations. However, it is a highly laborious way from substance properties to simulations and therefore only Diphenyl-DiphenylEther was analysed. From the substance property point of view the original pressure scale of

0.01 bar–36 bar proved to be unnecessarily large, since temperature limit of thermal oil set the pressure upper limit to 5 bar. Probably the fitted property functions would have been more accurate with smaller pressure span and tighter grid of calculation points.

Simulation results indicate that the most simple structure is the best choice for ORC plant subject to power-to-heat ratio. Only the combustion pre-heater has a positive effect on electricity efficiency when compared to the Admont ORC plant of Figure 9, although pre-heater does not affect electricity production at all but it improves boiler efficiency. Any changes in the organic cycle, superheating or double cycle structure, only lower power-to-heat ratio. It seems that turbine expansion from the saturated steam temperature is optimal for the ORC plant. Since one of the reasons behind choosing organic substance for working medium is avoiding moist steam in the turbine, it is not reasonable to examine whether starting turbine expansion from the moist steam area were worthwhile.

References

Alakangas, E. 2000. Properties of fuels used in Finland. VTT Research Notes 2045. Espoo: Technical Research Centre of Finland. 172 p. + app. 17 p. (In Finnish.). ISBN 951-38-5699-2; 951-38-5740-9. http://www.vtt.fi/inf/pdf/tiedotteet/2000/T2045.pdf

Alakangas,E. & Flyktman, M. 2001. Biomass CHP technologies. VTT Energy Reports 7/2001. 54 p. + app. 8 p.

Ambiente Italia srl, Kraftwärmeanlagen GmbH, Eicher + Pauli AG & CIT Energy Management AB. 2001. Risks and changes for small scale combined heat and power in the liberalized energy market. Final project report, European Commission SAVE contract XVII/4.1031/Z/99-063. Brussels, Belgium. [Available in http://www.cogen.org, last visited July 17th, 2002.]

Benonysson, A., Bøhm B. & Ravn, H. F. 1995. Operational optimization in a district heating system. Energy Conversion and Management 36(5), pp. 297–314.

Brammer, J. G. & Bridgewater, A. V. 1999. Drying technologies for an integrated gasification bio-energy plant. Renewable and Sustainable Energy Review 3(4), pp. 243–289.

Bruno, J. C., Fernandez,F., Castells, F. & Grossmann, I. E. 1999. A rigorous MINLP model for the optimal synthesis and operation of utility plants. Transactions of the Institute of Chemical Engineers, Part A 76(A3), pp. 246–258.

Carcasci, C. & Colitto Cormacchione, N. A. 2001. Part load operating strategies for gas turbines in district heating CHP applications. Proceedings of the Institution of Mechanical Engineers, Part A: Journal of Power and Energy 215(5). Pp. 529–544.

Chou, C. C. & Shih, Y. S. 1987. A thermodynamic approach to the design and synthesis of plant utility systems. Industrial & Engineering Chemical Research 26(6), pp. 1100–1108.

Cogen Europe, Energy for Sustainable Development Ltd, ETSU – AEA Technology plc, KAPE S.A., VTT & Sigma Elektroteknisk. 2001. The future of CHP in the European market – The European cogeneration study. European Commission SAVE XVII/4.1031/P/99-169: Brussels, Belgium. [Available at http://www.cogen.org, last visited February 10th, 2005.]

Directive 2004/8/EC of the European Parliament and of the Council of 11 February 2004 on the promotion of cogeneration based on a useful heat demand in the internal energy market and amending Directive 92/42/EEC. Official Journal of the European Union L 52, 21.2.2004, pp. 50–60.

Elomatic Oy. 2002. Design principles of biofuel-fired heating stations of <10 MW. OPET Finland report 7. Jyväskylä: Elomatic Oy.

Energy-Economic Society. 1989. Kaukolämmityksen käsikirja. Raportti 23/1989. [The handbook of district heating. Report 23/1989.] Helsinki: Energy-Economic Society.

Finergy. 2002. Electricity and district heating 2002 yearbook. Helsinki: Adato Energia Oy. [Available at http://www.energia.fi, last visited January 20th, 2005.]

Floudas, C. A. 1999. Deterministic Global Optimization: Theory, Methods and Applications. Vol. 37 of Nonconvex Optimization and its Applications. Boston: Kluwer Academic Publishers.

Fridh, J. 2001. Efficient steam turbines for small-scale energy conversion plants. Technical report KTH/HPT 01-14. Department of Energy Technology, Royal Institute of Technology, Sweden. [Available at http://www.energy.kth.se/, last visited September 27th, 2004.]

GAMS. 2004. GAMS – The Solver Manuals. GAMS Development Corporation.

GTW. 2003. Gas Turbine World 2003 GTW Handbook. Fairfield, CT: Pequot Publishing Inc.

Gustavsson, L. 1997. Energy efficiency and competitiveness of biomass-based energy systems. Energy 22(10), pp. 959–967.

Harvey, S., Carcasci, C. & Berntsson, T. 2000. Gas turbines in district heating combined heat and power systems: influence of performance on heating costs and emissions. Applied Thermal Engineering 20(12), pp. 1075–1103.

Helynen, S., Flyktman, M., Mäkinen, T., Sipilä, K. & Vesterinen, P. 2002. Bioenergian mahdollisuudet kasvihuonekaasupäästöjen vähentämisessä. [The possibilities of bioenergy in reducing greenhouse gases.] VTT Research Notes 2145. Espoo: Technical Research Centre of Finland. 110 p. + app. 2 p. (In Finnish.). ISBN 951-38-6054-X; 951-38-6055-8. http://www.vtt.fi/inf/pdf/tiedotteet/2002/T2145.pdf

Henning, D. 1997. MODEST – An energy-system optimisation model applicable to local utilities and countries. Energy 22(12), pp. 1135–1150.

Kirjavainen, M., Sipilä, K., Savola, T., Salomón, M. & Alakangas, E. 2004. Small-scale biomass CHP technologies: Situation in Finland, Denmark and Sweden. OPET Report 12, VTT Processes and Finnish District Heating Association. [Available at http://www.opet-chp.net, last visited September 21, 2004.]

Kocis, G. R. & Grossmann, I. E. 1987. Relaxation strategy for the structural optimization of process flow sheets. Industrial & Engineering Chemical Research 26(9), pp. 1869–1880.

Manninen, J. & Zhu, X. X. 1999. Optimal gas turbine integration to the process industries. Industrial Engineering and Chemical Research 38(11), pp. 4317–4329.

Marbe, Å., Harvey, S. & Berntsson, T. 2004. Biofuel gasification combined heat and power – new implementation opportunities resulting from combined supply of process steam and district heating. Energy 29(8), pp. 1117–1137.

Marlotherm® SH Heat Transfer Fluid. 2004. Product information Rev: 09/04. Sasol Olefins & Surfactants GmbH. 6 p.

Neuer Helmut. 2001, Biomass fired CHP plant based on an ORC cycle, project: ORC-STIA-Admont, EU-Thermie-A-project, contract BM/120/98/AT/IT, final report, STIA – Holzindutrie GES.m.b.H. 12 p.

Orispää, Y. 2000. Manual for calculating CHP electricity and heat. Finnish District Heating Association. Helsinki: Protermo Oy.

Pörn, R. 2000. Mixed integer non-linear programming: Convexification of different classes of non-convex MINLP problems. PhD Thesis. Åbo Akademi University.

Reisinger, H. & Pointer, G. 2003. Fuzzy logic controlled CHP plant for biomass fuels based on highly efficient ORC process. EU-project NNE5/2000/475, EES-part B, Final report, Stadtwaerme Lienz. 35 p.

Rolfsman, B. 2004. Optimal supply and demand investments in municipal energy systems. Energy Conversion and Management 45(4), pp. 595–611.

Salomón, M., Savola, T., Kirjavainen, M., Martin, A. R. & Fogelholm, C. J. 2002. Distributed combined heat and power generation with small-scale biomass plants – state of the art review. Proceedings of The Second International Symposium on Distributed Generation: Power System and Market Aspects. Stockholm, Sweden.

Savola, T. 2005. Simulation and optimisation of power production in biomass-fuelled small-scale CHP plants. Licentiate's thesis. Helsinki University of Technology.

Savola, T. & Fogelholm, C. J. 2005a. Increasing the power-to-heat ratios of small-scale CHP plants using biomass and natural gas. Energy Conversion and Management. (Submitted.)

Savola, T. & Fogelholm, C. J. 2005b. MINLP optimisation model for increased power production in small-scale CHP plants. Applied Thermal Engineering. (Submitted.)

Savola, T. & Keppo, I. 2005. Off-design simulation and mathematical modeling of small-scale CHP plants at part loads. Applied Thermal Engineering 25(8–9), pp. 1219–1232.

Shell Thermia oil proceedings. 2001. Oy Shell Ab. 2 p.

Soini, I. 1982. Ilmastolliset taulukot Helsingin lentoasemalta – Aeronautical climatological tables at Helsinki airport. Helsinki: Finnish Meteorological Institute.

STEM (Swedish Energy Administration). 2001. Electricity market 2001. [Available at http://www.stem.se, last visited January 20th, 2005.]

STEM (Swedish Energy Administration). 2004. Energy in Sweden, Facts and figures 2004. [Available at http://www.stem.se, last visited January 20th, 2005.]

Sundberg, G. & Henning, D. 2002. Investments in combined heat and power plants: influence of fuel price on cost minimised operation. Energy Conversion and Management 43(5), pp. 639–650.

Sundberg, G. & Karlsson, B. G. 2000. Interaction effects in optimising a municipal energy system. Energy 25(9), pp. 877–891.

Traupel, W. 2001. Thermische Turbomaschinen. Zweiter Band. 4. Auflage. Heidelberg: Springer.

Turunen, T. (editor). 2003. Energy Review 1/2003. Helsinki: Finnish Ministry of Trade and Industry.

Wagner, W. & Kruse, A. 1998. Properties of water and steam. The industrial standard IAPWS-IF97 for the thermodynamic properties and supplementary equations for other properties. Germany: Springer.

Wahlund, B., Yan, J. & Westermark, M. 2000. Comparative assessment of biofuel-based combined heat and power generation plants in Sweden. In: Kyritsis, S., Beenackers, A., Helm, P., Grassi, A. & Chiaramonti, D. (eds). Proceedings of 1st World Conference on Biomass for Energy and Industry, Seville, Spain. Pp. 1852–1855.

Wahlund, B., Yan, J. & Westermark, M. 2002. A total energy system of fuel upgrading by drying biomass feedstock for cogeneration: a case study of Skellefteå bioenergy combine. Biomass and Bioenergy 23(4), pp. 271–281.

Wimmerstedt, R. 1999. Recent advances in biofuel drying. Chemical Engineering Processes 38(4-6), pp. 441–447.

Zhao H., Holst J. & Arvastson L. 1998. Optimal operation with storage. Energy 23(10), pp. 859–866.

Appendix A

Mathematical formulation of the MINLP model

A MINLP model has the general form presented e.g. by Kocis and Grossmann (1987):

$$\begin{aligned} &\min z = c^T y + f(x) \\ &\text{s.t. } Ay + h(x) = 0 \\ &By + g(x) \le 0 \\ &Cy + Dx \le 0 \qquad (1). \\ &Ey \le 0 \\ &x \in X = \{ x \in R^n;\ x^L \le x \le x^U \} \\ &y \in Y = \{ 0, 1 \}^m \end{aligned}$$

The minimisation problem can be transformed to a maximisation one by using the rule that min $z = -\max z$. In this case the objective function is a sum of incomes and costs resulting from the process changes. The constraints for the MINLP model were constructed by creating the mass and energy balances for the process modules and by connecting the binary variables to the selection of modules with Big-M constraints. The streams were directed to different modules depending on which one is included into the model by using selection nodes and Big-M constraints. The linear regression functions for steam and water enthalpies and entropies were calculated with a separate optimisation program for fixed pressures and for the needed temperature ranges on the basis of the equations in Wagner and Kruse (1998). Linear regression functions of the temperature and pressure dependence of the saturated steam were also constructed.

Mass balance. Mass balances for the process modules are calculated according to

$$\sum m_j = \sum m_k , \qquad \forall\, i \in UNITS,\ j \in IN(i, j),\ k \in OUT(i, k) \qquad (2)$$

where m is the mass of the incoming or outgoing flow. The *UNITS* is the set of process modules that can be included in the model, the *IN* and *OUT* are the sets of incoming and outgoing streams, respectively, to and from the modules.

Energy balance. Energy balances are calculated according to

$$\sum m_j \cdot h_j = \sum m_k \cdot h_k + W_i \,, \quad \forall\, i \in UNITS \cap \{HEAT\ EXCHANGERS, \tag{3}$$

$$FEED\ WATER\ TANK,\ TURBINES,\ SPLITTERS,\ FUEL\ DRYER\ \},\ j \in IN(i, j),\ k \in OUT\ (i, k)$$

where h_j is enthalpy of the steam j and W_i is the work done by the unit i. For the heat exchangers, the feed water tank, and the splitters $W_i = 0$. The burner, the pumps, and the blower are excluded from this energy balance, as their properties are calculated with Eqs. (5), (12), and (13). In addition, the gas engines and gas turbines are excluded from the Eq. (3), as the fuel input and electrical efficiency of the different size engines and turbines are given as an input parameter.

Burner. The air flow to the burner is calculated using the air-to-fuel ratio, AF_{ratio}

$$\sum m_j = AF_{ratio} \cdot m_k \quad \forall\, i \in BURNERS,\ j \in IN(i, j) \cap AIR(j),\ k \in IN(i, k) \cap FUEL(k) \tag{4}.$$

The energy balance of the burner was defined as

$$m_j \cdot LHV_j + \sum m_k \cdot c_{p,k} \cdot (T_k - T_{ref}) = \sum m_l \cdot c_{p,l} \cdot (T_l - T_{ref}) \,, \quad \forall\, i \in BURNERS, \tag{5}$$

$$j \in IN(i, j) \cap FUEL(j),\ k \in IN(i, k) \cap (AIR(k) \cup EXHGAS(k)),\ l \in OUT(i, l) \cap FLUEGAS(l)$$

where LHV_j is the lower heating value of the fuel in [kJ/kg], $c_{p,k}$ is the specific heat capacity of the flow k in constant pressure, T_k is the temperature of the flow k, and T_{ref} is the reference temperature.

Steam turbine. The temperatures and the enthalpies after each steam turbine stage are calculated using the entropies, s_j, isentropic entropies, $s_{isentropic,\ k}$, and the isentropic efficiencies, $\eta_{isentropic,i}$,

$$s_j = s_{isentropic,\,k} \qquad \forall\, i \in TURBINES,\, j \in IN(i,\, j),\, k \in OUT(i,\, k) \tag{6}$$

$$h_j - h_k = \eta_{isentropic,I} \cdot (h_j - h_{isentropic,\,k}) \tag{7}.$$

The steam content x_i in the moist steam after the turbine stages with steam extraction to DH exchangers is calculated using the entropies

$$x_i \cdot (s_k - s_l) \geq (s_j - s_l), \quad \forall\, i \in TURBINES,\, j \in IN(i,\, j),\, k \in OUT(i,\, k) \cap STEAM(k), \tag{8}.$$

$$l \in OUT(i,\, l) \cap WATER(l)$$

The steam and moisture mass flows are then defined with

$$x_i \cdot (m_k - m_l) = m_k, \quad \forall\, i \in TURBINES,\, k \in OUT(i,\, k) \cap STEAM(k),\, l \in OUT(i,\, l) \cap WATER(l) \tag{9}.$$

Heat exchangers. Additional mass balances for the hot and cold sides of the heat exchangers are calculated on the basis of the Eq. (2). This is done to ensure that the hot and cold streams are not mixed in the heat exchangers. Heat exchanger temperatures are limited so that the temperature differences between hot and cold streams are always higher than or equal to a fixed minimum temperature difference ΔT. The load of the two-stage DH exchanger is divided so that the temperature increase of the DH water is same in both exchangers. The investment costs for heat exchangers, c_{hex} , including the reheater, the high pressure feed water preheater, and the DH exchanger are calculated according to Eqs. (10) and (11):

$$c_{hex} = 8000\ €/\text{unit} + 100\ €/\text{m}^2 \cdot A_{hex} \tag{10}.$$

The heat exchanger area A_{hex} is defined as

$$Q_i = A_{hex} \cdot U_i \cdot \Delta T_{lm}\ , \quad \forall\, i \in PREHEATER,\, REHEATER,\, 2^{ND}\ STAGE\ DH\ EXCHANGER \tag{11}$$

where Q_i is the transferred heat and ΔT_{lm} is the logarithmic mean temperature difference. U_i is the overall heat transfer coefficient and is here given the values of 4 kW/m^{2}K for the feedwater preheater and the DH exchanger and 0.1 kW/m^{2}K for the reheater.

Pumps and blower. The work required by a pump and a blower, $-W_i$, are calculated with Eqs. (12) and (13):

$$-W_i \cdot \eta_i = \nu \cdot (m_k \cdot p_k - mj \cdot pj) , \quad \forall i \in PUMPS, j \in IN(i, j), k \in OUT(i, k) \qquad (12)$$

$$-W_i \cdot \eta_i = (m_k \cdot p_k - m_j \cdot p_j) , \quad \forall i \in BLOWER, j \in IN(i, j), k \in OUT(i, k) \qquad (13)$$

where η_i is the efficiency of a pump or a blower, ν is the specific volume of water, and p_j is the pressure of the flow j. Temperatures in the pumps are fixed.

Fuel dryer. The fuel drying is calculated by using a regression model for the dependence between the lower heating value LHV_j [MJ/kg] of the biomass fuel and the fuel moisture content f_{H20} [weight-%]

$$LHV_j = -0.221 \cdot f_{H20} + 19.8, \quad \forall i \in BURNER, j \in IN(i, j) \cap FUEL(j) \qquad (14)$$

where the coefficients are calculated according to the data reported in Alakangas (2000). The heat transferred in the fuel dryer is calculated according to Eq. (3) and an additional equation is included in the model for defining the mass balance of the fuel moisture going through the fuel dryer and exiting as condensate. The fuel dryer investment cost is evaluated on the basis of an unpublished Finnish research on the economical feasibility of the dryers and a cost of 300 k€ for the fuel dryer in a small-scale CHP plant is used.

Gas turbines and engines. The gas turbines and engines are defined by giving their fuel and air input and the electrical efficiency as parameters to the model. The gas turbine price data is adopted from GTW (2003) and the gas engine price data is based on the manufacturer information. In both cost equations (15) and (16) the price of the gas turbine and gas engine has been multiplied by a factor of 1.7 to include the additional installation etc. costs of the gas turbine and gas engine integration:

$$c_{gt} = 1251.1 \cdot P_{gt}^{-0.3925}, \quad \text{for } 0.5 \text{ MW}_e \le P_{gt} \le 20 \text{ MW}_e \qquad (15)$$

$$c_{ge} = 514.2 \cdot P_{ge}^{-0.0760}, \quad \text{for } 0.5 \text{ MW}_e \le P_{ge} \le 20 \text{ MW}_e \qquad (16)$$

where c_{gt} and c_{ge} are the specific gas turbine and engine costs, respectively, in €/kW$_e$ and P_{gt} and P_{ge} are the sizes of the gas turbine and engine, respectively, in MW$_e$.

Selection nodes. The mass balances of the selection nodes are calculated similarly to the Eq (2). The logic for setting the right temperatures over the selection nodes are modelled with binary variables.

Binary variables. The binary variables y_i are used in the selection of the process modules. For a selection of a turbine, the same binary variable is used for all turbine stages and for a possible reheater or a feed water preheater connected to the turbine. So there are altogether four binary variables used for the selection of the turbines. Since only one of them can be selected at a time, this is modelled as

$$\sum y_i = 1 \qquad y \in \{0,1\} \qquad \forall\, i \in TURBINES \tag{17}$$

Only one gas turbine or engine can be integrated to the process, but it is also possible not to include them to the process:

$$\sum y_i \leq 1 \qquad y \in \{0,1\} \qquad \forall\, i \in GAS\ TURBINES\ or\ ENGINES \tag{18}$$

Separate binary variables are used for the selection of a fuel dryer, an air preheater, and a two-stage district heat exchanger. Big-M constraints are used for limiting the mass flows only to the selected modules

$$m_j \leq y_i \cdot M_j, \qquad y \in \{0,1\} \qquad \forall\, i \in UNITS,\ j \in IN(i,j) \tag{19}$$

where M_j is a large number (e.g. M_j = upper bound of the variable j). In an air preheater and in a fuel dryer the mass flows of the air and fuel remain always the same and the heat flow to the air and the fuel is limited by

$$T_j - T_k \leq y_i \cdot M_j, \quad y \in \{0,1\} \qquad \forall\, i \in UNITS,\ j \in IN(i,j),\ k \in OUT(i,k) \tag{20}$$

Power and heat production. The net power P_{net} and the district heat Q_{dh} produced by the process are calculated with Eqs. (21) and (22), where η_i is the efficiency of the generator for the turbines and engines:

$$P_{net} = \sum \eta_i \cdot W_i - \sum W_j, \quad \forall\, i \in TURBINES,\ GAS\ TURBINES\ and\ ENGINES \tag{21}$$

$$j \in PUMPS,\ BLOWERS$$

$$Q_{dh} = \Sigma Q_i \qquad \forall i \in DH\ EXCHANGERS \qquad (22).$$

Efficiencies. The total fuel input Q_{fuel} to the process, the electrical efficiency η_e, the power-to-heat ratio α, and the total efficiency η_{tot} are calculated with Eqs. (23)–(26):

$$Q_{fuel} = \Sigma Q_{fuel,i} + \Sigma y_j \cdot Q_{fuel,j} \quad \forall i \in BURNER,\ j \in GAS\ TURBINE\ and\ ENGINE \qquad (23)$$

$$Q_{fuel} \cdot \eta_e = P_{net} \qquad (24)$$

$$Q_{dh} \cdot \alpha = P_{net} \qquad (25)$$

$$Q_{fuel} \cdot \eta_{tot} = Q_{dh} + P_{net} \qquad (26).$$

CO_2 emissions. The CO_2 emissions are included in the model by calculating how much fossil CO_2 would be saved in comparison to the situation where the additional electricity production resulting from the changes were to be produced in a coal-fired condensing power plant, which is marginal production in the Nordic energy systems.

$$m_{CO2} = (P_{net} - P_{base\ case}) \cdot t_{annual} \cdot e_{coal} / \eta_{coal\text{-}fired\ cond} - m_j \cdot e_{ng}, \qquad (27)$$

$$\forall i \in GAS\ TURBINE\ and\ ENGINE,\ j \in IN(i, j) \cap FUEL(j)$$

where m_{CO2} is the annual mass flow of saved CO_2 emissions, $P_{base\ case}$ is the net power production of the base case process, t_{annual} is the annual operation time of the plant, e_{coal} and e_{ng} are the specific CO_2 emissions of coal and natural gas combustion, respectively, and $\eta_{coal\text{-}fired\ cond}$ is the electrical efficiency of a coal-fired condensing power plant.

Income and costs. The annual income I_e from the additional electricity production gained with the process changes is calculated as

$$I_e = c_e \cdot (P_{net} - P_{base\ case}) \cdot t_{annual}, \qquad (28)$$

where c_e is the price of electricity. Operation costs C_{oper} include the natural gas cost, c_{ng}.

$$C_{oper} = c_{ng} \cdot (\Sigma y_i \cdot Q_{fuel,i}) \cdot t_{annual}, \quad \forall i \in GAS\ TURBINE\ and\ ENGINE \qquad (29).$$

Investment costs C_{inv} contain the annuity factor, a:

$$C_{inv} = a \cdot c_i \cdot \Sigma y_i \quad \forall i \in \text{REHEATER, PREHEATER, } 2^{ND} \text{ STAGE OF DH EXCHANGER, FUEL DRYER, and GAS TURBINE and ENGINE} \quad (30).$$

Objective function. The objective function z calculates the additional profit gained with the process changes

$$max\ z = I_e - C_{oper} - C_{inv} \quad (31).$$

Published by

Series title, number and report code of publication

VTT Research Notes 2301
VTT–TIED–2301

Author(s)
Sipilä, Kari, Pursiheimo, Esa, Savola, Tuula, Keppo, Ilkka, Fogelholm, Carl-Johan & Ahtila, Pekka

Title

Small-Scale Biomass CHP Plant and District Heating

Abstract

CHP potential in Finland has been evaluated to be 80 MW of electricity and 214 MW of heat with 6000 hours of annual peak load time based on the district heat production in biofuelled CHP plants in the year 2000. Part of this capacity is already built when this report has been written. The total amount of possible CHP units is 51. 90% of the CHP would be smaller than 10 MW in thermal effect. Most of the potential CHP plants (53%) would be 1–5 MW in thermal effect.

An optimisation model was constructed describing production, distribution and consumption of heat. The energy production in CHP plants is based on simulations done for three different size plants, thus giving a wider perspective on the behaviour of such a plant. The results indicate, that the economically feasible scale for biofuel-fired CHP plants remains relatively large; when a biofuel-fired boiler is among the options for heat production, no investment is made in the smallest of three CHP plants. Specific investment costs for the two larger plants could be only slightly higher until no investment in them would be made either.

Possibilities to increase the power production and the power-to-heat ratio of 1–20 MW_e steam process CHP plants using biomass fuels were studied with simulation and optimisation tools. The basis for the simulations and optimisations was the data collected from Finnish and Swedish small-scale CHP plants between 2002 and 2004. Four existing CHP plants from Finland and Sweden were selected to represent a BAT technology in the different sizes of CHP processes. The results showed that the addition of a feed water preheater, a steam reheater, and a two-stage district heat exchanger is profitable with the current electricity price of 30 €/MWh. This increases the power-to-heat ratios from 0.23–0.50 to 0.45–0.50 depending on the case plant. The considered integration of a gas engine needs electricity prices over 42–45 €/MWh but increases the power-to-heat ratios to 0.59–0.78. The addition of a fuel dryer was connected to the integration of gas engine and gas turbine, as this provided extra heat to the flue gases that could be used for fuel drying.

ORC process plant is evaluated as one possibility for small-scale biofuelled CHP power plant. Simulation is first modelled for a BAT technology ORC plant and secondly to explore possibilities of improvements by adding some new properties to the basic plant model. Possibilities to improve the basic process are to make the process starting point (pressure and temperature) higher after the boiler, to change the temperature of the preheated air and to use double circle organic process. Simulation results indicate that the most simple structure is the best choice for an ORC plant subjected to power-to-heat ratio. Only the combustion pre-heater has a positive effect on electricity efficiency when compared to the basic ORC plant, although pre-heater does not affect electricity production at all but it improves boiler efficiency. Any changes in the organic cycle, superheating or double cycle structure, only decrease the power-to-heat ratio.

Keywords
combined heat and power generation, biomass, district heating plants, small-scale co-generation, steam Rankine cycle, organic Rankine cycle, optimisation, modelling, simulation

Activity unit
VTT Processes, Lämpömiehenkuja 3, P.O.Box 1606, FI–02044 VTT, Finland

ISBN			Project number
951–38–6722–6 (soft back ed.) 951–38–6723–4 (URL: http://www.vtt.fi/inf/pdf/)			C2SU00106
Date June 2005	Language English	Pages 129 p. + 7 p. app.	Price C
Name of project		Commissioned by Technology Agency of Finland (Tekes), 10 companies	
Series title and ISSN VTT Tiedotteita – Research Notes 1235–0605 (soft back edition) 1455–0865 (URL: http://www.vtt.fi/inf/pdf/)		Sold by VTT Information Service P.O.Box 2000, FI–02044 VTT, Finland Phone internat. +358 20 722 4404 Fax +358 20 722 4374	

CHP potential in Finland has been evaluated to be 80 MW of electricity and 214 MW of heat with 6000 hours of annual peak load time based on the district heat production in biofuelled CHP plants.

The economically feasible scale for biofuel-fired steam process CHP plants remains relatively large. Addition of a feed water preheater, a steam reheater, and a two-stage district heat exchanger is profitable with the current electricity price of 30 euro/MWh. This increases the power-to-heat ratios from 0.23–0.50 to 0.45–0.50. Integration of a gas engine needs electricity prices over 42–45 euro/MWh but increases the power-to-heat ratios to 0.59–0.78.

Possibilities to improve the basic ORC-process are to make the process starting point (pressure and temperature) higher after the boiler, to change the temperature of the preheated air and to use double circle organic process. Simulation results indicate that the most simple structure is the best choice for an ORC plant subjected to power-to-heat ratio.

Tätä julkaisua myy

VTT TIETOPALVELU
PL 2000
02044 VTT
Puh. 020 722 4404
Faksi 020 722 4374

Denna publikation säljs av

VTT INFORMATIONSTJÄNST
PB 2000
02044 VTT
Tel. 020 722 4404
Fax 020 722 4374

This publication is available from

VTT INFORMATION SERVICE
P.O.Box 2000
FI–02044 VTT, Finland
Phone internat. + 358 20 722 4404
Fax + 358 20 7226 4374

ISBN 951–38–6722–6 (soft back ed.)
ISSN 1235–0605 (soft back ed.)

ISBN 951–38–6723–4 (URL: http://www.vtt.fi/inf/pdf/)
ISSN 1455–0865 (URL: http://www.vtt.fi/inf/pdf/)